Eindhoven University of Technology

MASTER

Measuring the temporal contrast sensitivity function for isoluminant chromatic flicker stimuli

a heterochromatic flicker photometry approach

Bueno Perez, M.R.

Award date:
2017

Link to publication

Measuring the Temporal Contrast Sensitivity Function for Isoluminant Chromatic Flicker Stimuli

An Heterochromatic Flicker Photometry Approach

Master's thesis in Master Program of Human-Technology Interaction

Mijael R. Bueno Pérez

Department of Industrial Engineering & Innovation Sciences
Eindhoven University of Technology
Eindhoven, North Brabant, Netherlands 2017

Measuring the Temporal Contrast Sensitivity Function for Isoluminant Chromatic Flicker Stimuli

An Heterochromatic Flicker Photometry Approach

Mijael R. Bueno Perez
Student ID 0976414

Supervised by

Dr. I.M.L.C. (Ingrid) Vogels
X. Kong BSc
Dr. Ir. R.H. (Raymond) Cuijpers
Dr. Sekulovski, D.

in partial fulfillment of the requirements for the degree of
Master of Science
in Human-Technology Interaction

TU/e

Department of Industrial Engineering & Innovation Sciences
Human-Technology Interaction Group
Eindhoven University of Technology
Eindhoven, North Brabant, Netherlands 2017

Measuring the Temporal Contrast Sensitivity Function for Isoluminant Chromatic Flicker Stimuli

An Heterochromatic Flicker Photometry Approach

M. R. Bueno Pérez

Supervisors:

Dr. I.M.L.C. (Ingrid) Vogels	Industrial Engineering & Innovation Sciences, TU/e
X. Kong BSc	Industrial Engineering & Innovation Sciences, TU/e
Dr. Ir. R.H. (Raymond) Cuijpers	Industrial Engineering & Innovation Sciences, TU/e
Dr. Sekulovski, D.	Philips Research

Cover: CIE 1976 $u'v'$ chromatic diagram and gamut used during the experiments

Typeset in LaTeX

Eindhoven, Netherlands 2017

Abstract

In this study, two experiments were carried to measure the temporal contrast sensitivity functions (tCSFs) of chromatic flicker with a mean luminance of 37.5 cd/m^2 for 9 base colors (in CIE 1976 $u'v'$ chromatic coordinates), 4 directions of the chromatic modulation and 7 frequencies. In the first experiment, to stimulate only color-sensitive perceptual mechanisms and not luminance-sensitive mechanisms of the visual system, luminance flicker was minimized with heterochromatic flicker photometry (HFP) by adjusting the luminance ratio of the two extreme colors of the modulation. It was found that for most conditions of equal perceived luminance, the luminance ratios differed from 1. Subsequently, these luminance ratios are mostly adjusting the S-cones responses between the two extreme colors (ΔS), more than for the L- and M-cones and especially for base colors with components at short wavelengths. Thus, the implications are that the standard luminosity function $V(\lambda)$ used to make photometric measurements underestimates the spectral characteristics of individual observers, especially at short wavelengths. In the second experiment, participants had to adjust the amplitude (i.e. distance between the two extreme colors) of the chromatic modulation until they did not perceive flicker. The visibility thresholds were converted to contrast sensitivities and plotted as a function of the frequency in order to obtain tCSFs. An exponential model (linear fit on log scale) resulted in high goodness of fit R^2 of the tCSFs of around 96%, 87% and 94% for participant MIJ, ANN and KON, respectively. There was not a large difference between the goodness of fit of the tCSFs with thresholds expressed in the CIE 1976 as $\Delta u'v'$, cone space as ΔLMS and normalized cone space as Δlms. For the slopes and intercepts of the fits, main effects of participant, direction, base color and interactions effects (base color and direction) were found significant (p < 0.05). The effect of base color, direction and frequency was illustrated with the color points of respective thresholds fitted with ellipses on the chromaticity diagram $u'v'$. It was found that the ellipses are close to have a vertical orientation, thus, in the y-axis the sensitivity is lower (larger threshold) and in the x-axis the sensitivity is higher (lower threshold). The shape of the ellipses are similar for each frequencies (in some cases different for low frequencies), but their size is dependent of the frequency. These findings have shown that the sensitivity of the human visual system to chromatic flicker cannot be described by a simple function but is a complex function of the chromaticity, modulation direction and frequency.

Contents

Contents

List of Figures

List of Tables

Chapter I

Introduction

"The whole world, as we experience it visually, comes to us through the mystic realm of color."

– Hans Hofmann

Human vision is complex in nature and it is not hard to understand why evolution has made us with this sensitivity. Color is the consequence of the eyes converting light rays of different wavelengths into neural signals that are interpreted by the brain to construct images. This outcome of processing produces visual experiences that form a significant aspect of our consciousness. We rely on these visual experiences to understand the world and the complexity of events that happen around us. But colors are not simply cues for discriminating objects; like music they also produce emotional sensations, for example, like when we stare at a piece of art of our favorite painter, or when we enjoy the colorful lights of our Christmas tree. As an analogy with taste, beautiful arrangements of color can be known as the cheese cake for our vision.

Nowadays, light is not just a simple and natural phenomenon like the light from the sun or fire. Humans have developed new ways of creating light, for example from the light bulb to the most modern mechanism of artificial light; the light-emitting diode (LED). LEDs offer extensive opportunities for visual perception research. The controllability of the spectral power distribution, spatial distribution, color temperature, temporal modulation and polarization properties enable the design of easily adaptable experimental settings. Thanks to this technology, we have a great support to work towards a better understanding of the temporal chromatic characteristics of the human visual system.

When light rays come from a temporally modulated light source, the human visual system has different abilities in resolving them. For example, when the light varies in luminance it gives sensation of luminance flicker and when it varies in color, observers perceive what is known as chromatic flicker. The word chromatic is defined as something that is produced by or related to color. The Greeks were the first to use this word as chrōmatikos that comes from chrōmat-, chrōma that means skin, color and modified tone.

In research, a typical way to understand and explore the spatial and temporal chromatic characteristics of the human visual system is through measurements of the contrast sensitivity functions (CSFs). A temporal chromatic contrast sensitivity function (tCSFs) describes the relation between the temporal frequency of a sinusoidal light wave that varies

in chromaticity and the sensitivity of a human observer to the temporal modulation. The concept of chromatic contrast is used in opposition to luminance (achromatic) contrast, where differences only occur in grey level. Several studies have provided evidence that for luminance and chromatic flicker the human visual system acts like two separate band-pass filters that peak around 8 Hz and 4 Hz, respectively (Shady, MacLeod, and Fisher, 2004; Green, 1968). Other studies have reported low pass characteristics of the tCSFs for chromatic flicker (Granger and Heurtley, 1973; Van der Horst and Bouman, 1969; Swanson, Ueno, Smith, and Pokorny, 1987). In addition, studies have shown that for chromatic flicker, a frequency of 25Hz or higher produces only one fused color and for luminance flicker, 50Hz or higher can cause flicker fusion (Jiang, Zhou, and He, 2007), this frequency depends of different variables like the light level and stimulus size (De Valois, 2000; Bodrogi and Khan, 2012; de Lange, 1958).

Luminance flicker has been well studied by researchers, but limited research has been done on chromatic flicker. Among the few studies, most of them only studied red-green chromatic flicker due to technical limitations, resulting in inconclusive results for a large range of colors and directions in which the color can change. On the other hand, several color models have been put forward to describe how two colors match in appearance to the human vision and to enable us to calculate color attributes. However, these models were developed based on the perception of spatial properties of color and appear not to be valid to describe the perception of temporal properties. Moreover, there is evidence that the attractiveness of dynamic colored light depends on the path and the speed of color transitions in a color space (Vogels, Sekulovski, and Rijs, 2007; Murdoch, Sekulovski, and Seuntiëns, 2011). In order to determine the distance between colors that produce an appealing and smooth dynamic color transition at a desired speed, a temporal model of human color perception should be developed. It is therefore necessary to further investigate the temporal behavior of the human visual system to chromatic flicker.

In the current study the tCSFs for chromatic flicker were measured and modelled for several base colors and directions of the chromatic modulation. In order to measure the tCSFs, two experiments were designed. First, it is known that lights of different color and equal in luminance are not always perceived as equally bright (Kaiser and Comerford, 1975). In consequence, an initial experiment was designed as in the study by Swanson et al. (1987) to investigate how to stimulate only color-sensitive perceptual mechanisms and not luminance-sensitive mechanisms. In this experiment, the method of heterochromatic flicker photometry (HFP) was used. This method enabled participants to adjust the luminance ratio between the two extreme colors of the chromatic modulation until the sensation of flicker was minimized. In this way, we found the subjective point where both colors are perceived with equal luminance (called: isoluminance) for each participant, base color and direction. In the second experiment, participants had to adjust the amplitude (distance between the two extreme colors) of the chromatic modulation until they did not

perceive flicker. The luminance ratios that were measured in the first experiment were used in the second experiment to obtain the tCSFs of the chromatic mechanisms of our visual system. In previous studies where the HFP experiment was left behind (Shady et al., 2004; Green, 1968) the final result was a contrast sensitivity function of chromatic flicker with a band-pass shape that is typical for luminance flicker. Other studies managed to obtain subjective isoluminant conditions and the result was a contrast sensitivity function with a low-pass shape (Van der Horst and Bouman, 1969; Kim, Mantiuk, and Lee, 2013). After analyzing the data, we were able to answer the following questions: *Are the luminance ratios that minimize brightness flicker different from 1? What is the shape of the tCSFs?* and *What is the goodness of fit of the model?*.

In this report, the following chapters are included to provide descriptive and analytic information of the study presented. *Chapter 2* provides the theoretical concepts that were thoroughly used in this study. Topics like spectral power distribution, additive mixing, color attributes, color models are presented in this chapter. The physiology behind color perception is briefly discussed and just aspects that were of great interest for our study are included. In addition, the concepts to understand the temporal characteristics of our visual system are explained. Furthermore, practical information about HFP and the method of adjustment are described. *Chapter 3* is dedicated for describing all the practical things related to the equipment used, laboratory settings and participants. In addition, the two experiments are detailed. *Chapter 4* provides the results of the two experiments and explorative insights are included. *Chapter 5* is dedicated to summarize the results, provide points for further investigation and give recommendations that might improve follow-up experiments.

Chapter II

Theoretical Background

"If one says 'red' - the name of color - and there are fifty people listening, it can be expected that there will be fifty reds in their minds. And one can be sure that all these reds will be very different."

– Josef Albers

2.1 Composition of a Color Stimuli

Color belongs to the realm of phenomena that is interpreted in our brain. It consists of a combination of chromatic (color) and achromatic (luminance) information. This package of information is primarily contained by the physical entity that reaches our eyes, known as light. Light is a kind of electromagnetic radiation that, once captured by the eye, is transformed to neural signals, the kind of signals that our brain can deal with. Light can be produced by many kinds of light sources like the sun and fire. Though time ago, humans found a way to produce their own light sources from incandescent lamps and fluorescent tubes to the most modern and efficient way: the light-emitting diode (LED). Nowadays, LEDs can be manufactured with almost any desired color (see Figure 2.1) with a relatively narrow spectrum located in the visible range and even in the ultraviolet range. In addition, the combination of red, green and blue LEDs can be used to generate any color, including white. Furthermore, the controllability of the spectral power distribution, spatial distribution, color temperature, temporal modulation and polarization properties enables improved studies of color perception. For example, LEDs can be turned on and off or pulsed with very high frequency, and they have long useful lives (around 50,000 hours). We expect that LED technology will keep progressing and in a few years it will replace almost every light source that we use now.

2.1.1 Light

Humans have been profoundly interested in the nature of light for centuries. The concept of light rays was first introduced by Euclid in the year 300 BC and the concept of the wave nature of light is attributed to Christiaan Huygens (1629-1695). On the other hand, Isaac Newton (1642-1727) was more in favor of a particle theory of light. Nowadays, theories

Figure 2.1: LEDs that produce different colored light.

use either the particle or the wave analogy depending of which suits best the phenomenon being studied.

Light is known as visible radiation; a narrow range of the spectrum of electromagnetic radiation. Electromagnetic waves can have many different wavelengths as illustrated in Figure 2.2. Isaac Newton (1660) was the first to use the word "spectrum" when he demonstrated that a white light could be split up into an array of colors that differ in wavelength like the ones in a rainbow.

The concept of wavelength λ measured in nanometers helps to physically describe an electromagnetic wave. Lights that differ in wavelength can produce different perceptions of color. For example, a long wavelength in the visible spectrum can produce the perception of red (625-750nm), while the shorter ones can produce the perception of violet (380-450nm). Outside of this range we have the ultraviolet light (UV) that is located below 380nm down to 100nm and the infrared light (IR) that is located above 750nm up to 1mm.
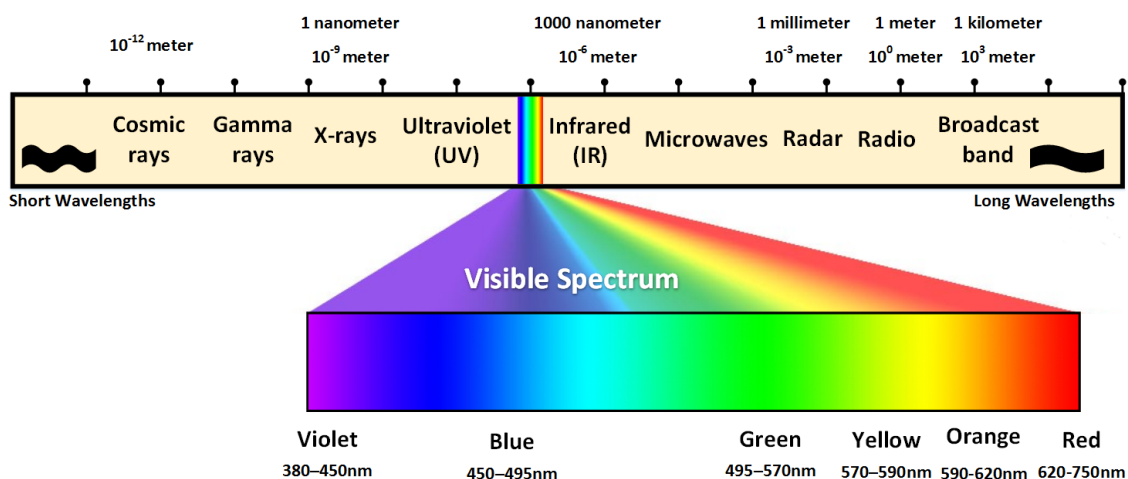
Figure 2.2: Electromagnetic waves of different wavelengths from short wavelengths to long wavelengths (10^{-12}-10^3nm). The visible spectrum is located in a narrow range (380-750nm) and lights that differ in wavelength at this range can produce different perception of color.

2.1.2 Spectral Power Distribution

Every light source can be physically characterized by its spectral composition. This characterization normally is shown as a spectral power distribution (SPD) as illustrated in Figure 2.3. An SPD is the total amount of power P that a light source emits in a small unit interval $\Delta\lambda$ as a function of wavelength.

$$P(\lambda) = \Delta P/\Delta\lambda \quad \text{W/nm} \tag{2.1}$$
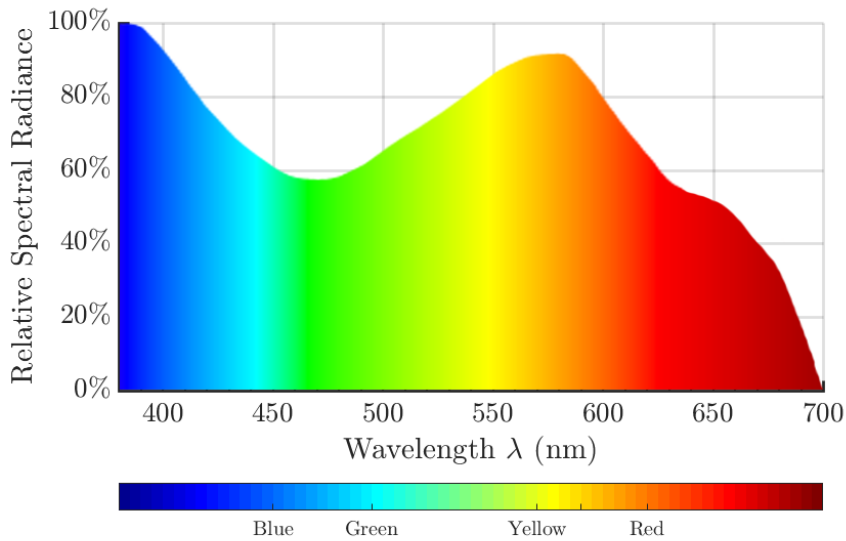
Figure 2.3: An example of a relative spectral power distribution containing power information in almost every wavelength of the visible range. This example is not associated to any kind of light source.

There are different ways to express the power or energy of a light source, but the most frequently used is the power that is emitted per unit of time (expressed in Joules per second or watts). An absolute distribution of power P_λ is typically expressed as Radiance $(\text{W/(sr} \cdot \text{m}^2))$, radiant energy in a direction reflected from a surface. The physical radiometric descriptions of a spectral distribution are: Radiant flux $\phi_e(\text{W})$, Radian Intensity (W/sr), Irradiance $E_e(\text{W/m}^2)$ and Radiance $L_e(\text{W/(sr} \cdot \text{m}^2))$. The letter 'e' as an index means that these magnitudes are based on energy units. The power of this radiometric spectral energy distributions weighted by a luminosity function (function that models human brightness sensitivity) are called photometric units and corresponds to: luminous flux $\phi_v(\text{lumen,lm})$, luminance intensity (lm/sr), illuminance $E_v(\text{lm/m}^2$ or lx$)$ and luminance $L_v(\text{cd/m}^2)$. The letter 'v' of visual, means that the units corresponds to photometric magnitudes.

Light perceived through our eyes can be originated in different ways, i.e., when viewing directly to a light source, but most commonly when viewing to an object being

illuminated. In this case, the SPD of the light that reaches our eyes is the product of the SPD of the light source and the spectral reflectance of the object. In addition, the power of light can change smoothly throughout the spectrum and there are infinite number of SPDs that can produce the same perception of color (Raghavachary, Pharr, Luebke, and Strothotte, 2008).

2.1.3 Color Additive Mixing

When three lights, a red, a blue and a green light are overlapped on a white background as shown in Figure 2.4, they are also superimposed on our eyes (i.e. when the light is reflected towards the eyes). This additive color mixture results in white where the three lights overlap, in yellow where the red and green light overlap, in magenta where red and blue light overlap, and in cyan where the blue and green light overlap. Experiments have shown that observers with normal vision can match a given color with the mixture of these three colors (tristimulus values), often called primary colors (Valberg, 2007). The law of additive mixture of color is illustrated with equation 2.2, that states that any color C can be matched by certain amounts r, g and b of the red R, green G and blue B lights.

$$C = R(r) + G(g) + B(b) \tag{2.2}$$
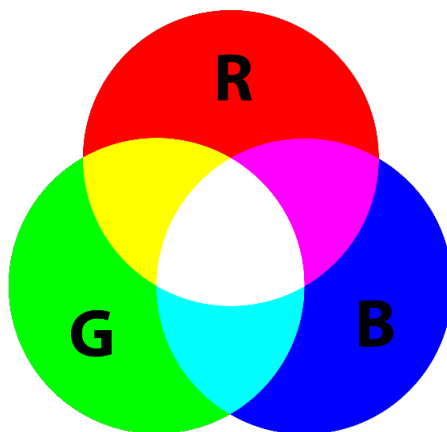
Figure 2.4: Additive color mixture of the three primary light colors (red, green and blue).

Though this phenomena is not exclusive for these three primaries, it happens for any combination of lights with different spectral composition, but colors that have the same appearance will always show the same additive mixture color (Valberg, 2007). Nowadays, is possible to make different spectral power distributions thanks to the combination of LEDs of different spectral compositions as shown in Figure 2.5.
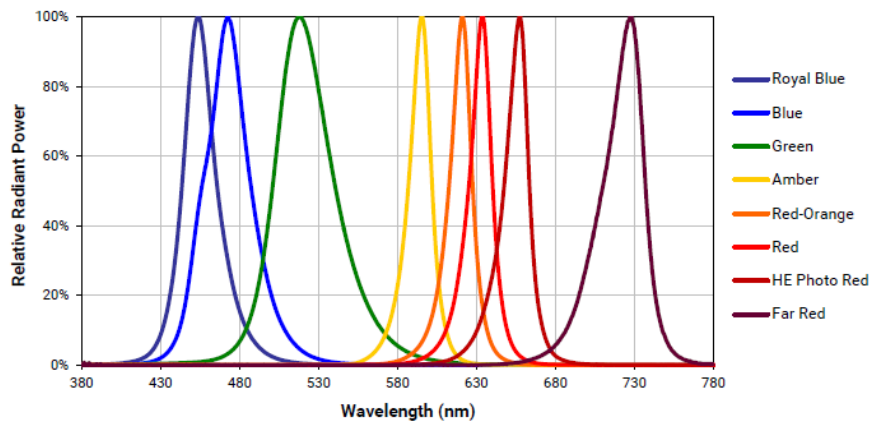
Figure 2.5: Relative spectral power distribution of Cree XP-E LEDs with different dominant wavelengths. Different light colors can be produced from the additive mixture of LEDs with different dominant wavelengths.

2.1.4 Color Attributes

In practical situations, it might be useful to refer to color with psychological descriptions rather than just physical descriptions like the spectral power distribution or wavelength. The three psychological Munsell attributes have become widely accepted; hue, brightness and saturation. These attributes are illustrated in Figure 2.6.
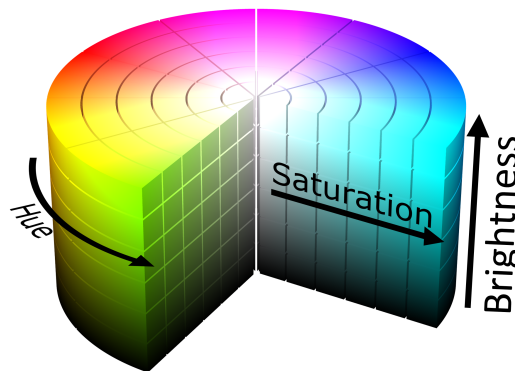
Figure 2.6: Color system which describes colors by hue, saturation, and brightness (or lightness)

Hue

The term hue is defined as "attribute of visual perception according to which an area appears to be similar to one of the colors red, yellow, green, and blue or to a combination of adjacent pairs of colors considered in a closed ring" (CIE, 1987). An example of hue can be seen in the variation of color observed in a projected visible spectrum or a rainbow (Kuehni, 2003; Fairchild, 2013).

Brightness, Lightness

The term brightness is defined as "attribute of a visual perception according to which an area appears to emit, or reflect, more or less light" (CIE, 1987). In addition, the term lightness is "the brightness judged relative to the brightness of a similarly illuminated area that appears to be white or highly transmitting" (CIE, 1987). A distinction is that brightness refers to the absolute perceived amount of light, and lightness to the relative perceived amount of light (Kuehni, 2003; Fairchild, 2013). For example, brightness is when judging the intensity of a light source, it might appear very bright or dim. Lightness refers to the brightness of a non-white object (or an illuminated area) compared to a perfect white object (or highly transmitting area).

Saturation, Chroma

The term saturation is defined as "attribute of a visual sensation that permits a judgment to be made of the proportion of pure chromatic color in the total sensation" (CIE, 1987). Chroma can be related to the attribute "colorfulness" as lightness is related to brightness. The definition for chroma is: "attribute of visual sensation that permits a judgment to be made of the amount of pure chromatic color present, regardless of the amount of achromatic color" (Kuehni, 2003; Fairchild, 2013). For example, a transition from a non-saturated to a saturated color would be when a metal burns until it produces an intense saturated red color. This color would be also perceived as a high-chroma red.

2.2 The Physiology of Color Perception

Color perception is not an exclusive capability of human beings. Color enables primates and other animals to discriminate suitable food and sexual partners (Conway, 2002). Humans are capable of recognizing around 200 levels of gray, but the recognition of visual cues increases with color vision (Malacara, 2011). In this section, the background knowledge of the physiology of human vision is presented. Afterwards, we will be able to understand how our eyes are able to retrieve visual information from the world around us. Additionally, spectral characteristics of our vision are explained in this section.

As mentioned before, the first part in the process of a visual experience is the light that travels through space to reach our eyes as illustrated in Figure 2.7. The first layer that light has to go through is called cornea, a transparent tissue with an ideal spherical shape. If it takes a different shape it can produce different kinds of refractive errors, and cause problems like corneal astigmatism and keratoconus. Afterwards, light passes through a circular opening in front of the eye called pupil. This mechanism controls the amount of light entering the eyes by increasing or decreasing its diameter. Examination of the pupil from the side for different angles shows that light can enter from about 105° field-of-view

and the other side is limited to 60° due the combination of the nose and the extend of the retina. A total of 210° is the extend of the field-of-view in the horizontal plane with 120° of overlap between the vision of both eyes (Atchison and Smith, 2000). After the pupil, some light rays will be transmitted and others absorbed at the surrounding structure called iris. A flexible lens called the crystalline lens is a mechanism that can tense to focus on near objects and relax to focus on distant objects. When light reaches the interior of our eye ball, light rays will be absorbed by our retina. This is the light-sensitive surface of less than half a millimeter thick, formed by several layers. The last layer in the back has the light-sensitive cells, the photoreceptors, i.e. the rods and cones. These cells are capable of absorbing the light and transforming the light into chemical and electrical signals that are transmitted to our brains through nerve cells.
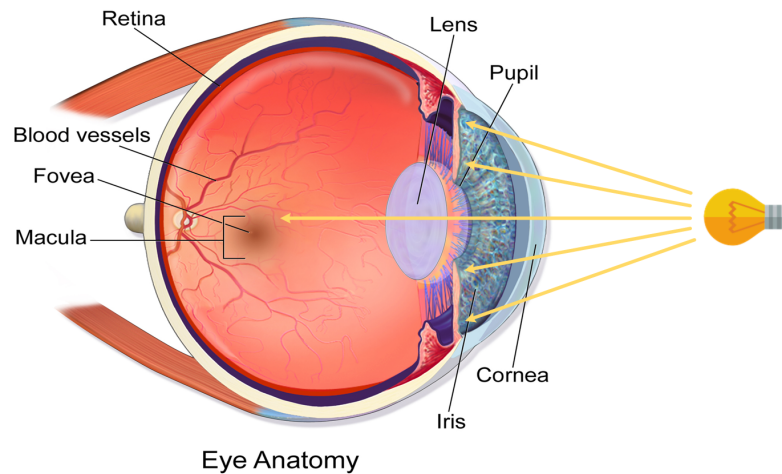
Figure 2.7: Illustration of light rays entering the human eye

The rods and cones are two different classes of photoreceptors in the human retina as illustrated in Figure 2.8. In the human retina 95 percent of our 130 million photoreceptors are rods (120×10^6 rods and 6×10^6 cones). The rest of the photoreceptors are cones of three types properly referred to as L (long-wavelength), M (medium-wavelength), and S (short-wavelength) cones. These three types of cones serve for color vision, in contrast with the one type of rod that is incapable of color coding.
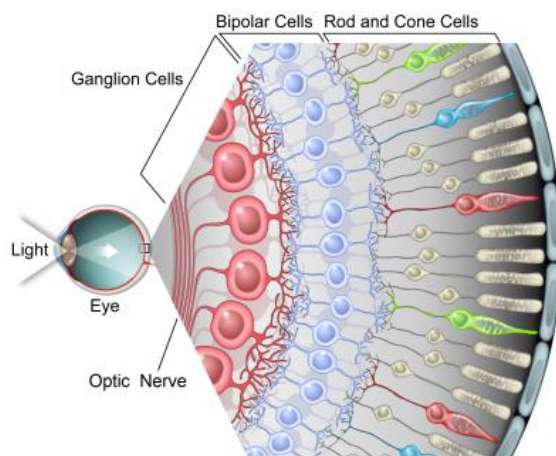
Figure 2.8: Illustration of the location of rods and cones in the optic pathway.

The different photosensitive pigments of the cones differ in spectral sensitivities as shown in Figure 2.9.
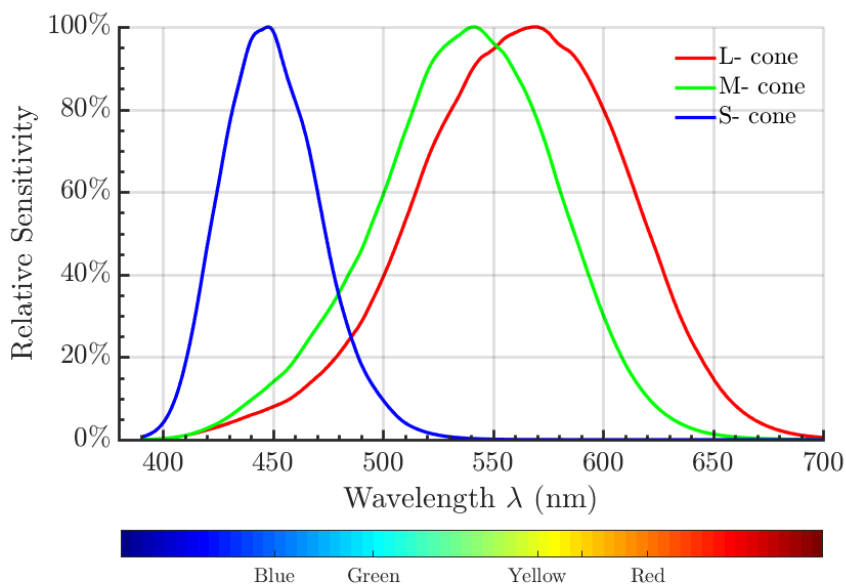
Figure 2.9: Spectral sensitivities of the three types of cones properly referred to as L- (long-wavelength), M- (medium-wavelength), and S- (short-wavelength) cones. These where found from a 10° viewing angle derived from the Stiles & Burch 10° color-matching functions (Stockman and Sharpe, 2000).

The mayor concentration of cones occurs in a zone called fovea that corresponds to a 5.2° field-of-view. This is where a higher visual spatial resolution is achieved. A retinal layer with a yellow pigment that is in front of the cone layer of the fovea is called the macula lutea (or yellow spot) which corresponds to 17° field-of-view (larger than the fovea). The spectral absorbance for the eye lens pigment and macular pigment is shown in Figure 2.10. The macular pigment absorbs mainly light with short wavelengths in order

to protect the nerve tissue from damage, but it is compensated with the greater sensitivity to blue light of the cones on the macula.
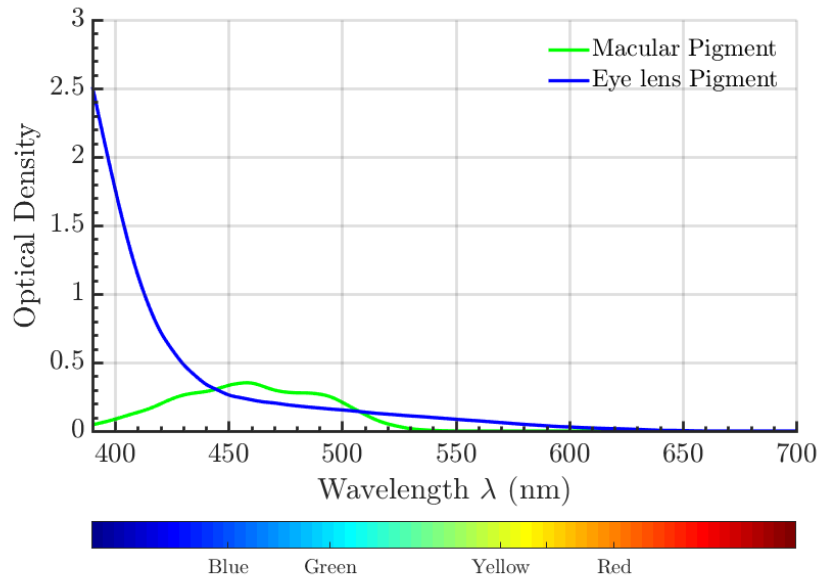
Figure 2.10: The spectral absorbance of the eye lens and macular pigments.

The cones are less sensitive to illumination levels, thus, they respond to higher levels of illumination, responsible of photopic or daylight color vision. The rods are more sensitive, and can respond to lower levels of illumination, responsible for scotopic or night vision. A german phyiologist J. von Kries came up with this theory, called the duplicity theory. Rods are designed for scotopic vision (less than 0.03 cd/m^2), and cones for photopic vision (more than 10 cd/m^2) vision (Valberg, 2007). Mesopic vision (between 0.03 cd/m^2 and 10 cd/m^2) is where both rods and cones are partially active, for example, most night-time outdoor scenarios with street lighting are in the mesopic range. At scotopic light levels the spectral sensitivity of the visual system has a maximum at 507nm, whereas at photopic light levels the sensitivity has a maximum at 555nm. These sensitivities are represented by the luminous efficiency curves (luminosity functions) as shown in Figure 2.11. These functions are the overall sensitivity of the two systems to light of varying wavelengths. The scotopic $V'(\lambda)$ function shows the spectral responsivity of the rods and the photopic $V(\lambda)$ represents the overall sensitivity of the combination of the three types of cones.
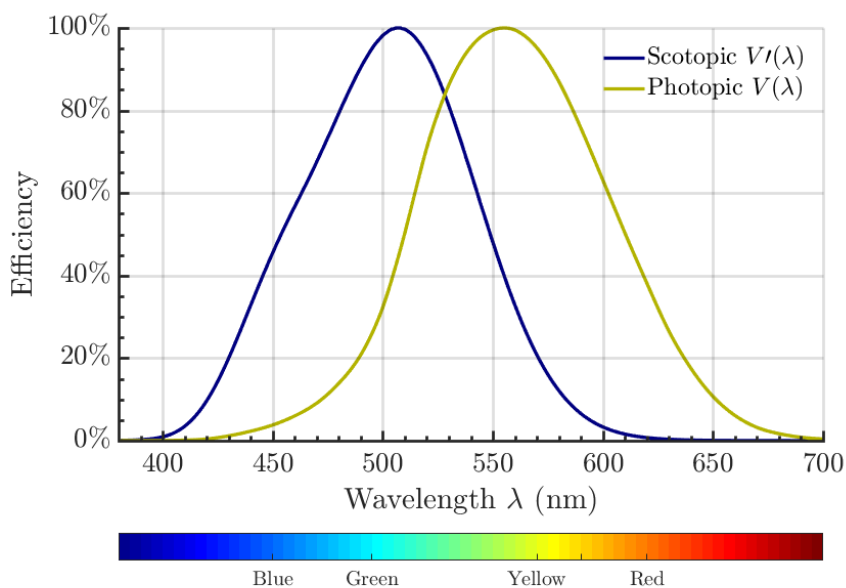
Figure 2.11: The relative luminous efficiency functions, scotopic vision $V'(\lambda)$ (rods vision) and photopic vision $V(\lambda)$ (cones vision). The maximums are at 507 and 555nm, respectively. The photopic function is the basis of photometric measurements of light.

Note that the photopic $V(\lambda)$ is low below about 450nm. Through history $V(\lambda)$ has been lacking of good data for the shortest wavelengths, and it has led to a function that cannot be easily related to a particular physiological mechanism (Valberg, 2007). This problem is due to the considerable differences between the $V(\lambda)$ obtained by different measurement procedures and criterias. An important source of variability is the differing contributions of the L-, M- and S- cones and their retinal pathways to the different types of luminosity tasks. Moreover, there are large differences between the $V(\lambda)$ of individuals with normal vision (Sharpe, Stockman, Jagla, and Jägle, 2005), but the standard $V(\lambda)$ was derived from an average of many individuals and represents no individual observer (Lennie, Pokorny, and Smith, 1993). Moreover, these studies mostly used young male observers. It is important to know that individuals have different relative photometric sensitivities and it might differ for women, children, or older men. For example, even if the spectral sensitivity of the cones may be the same for each individual, the relative number of cones may vary (Atchison and Smith, 2000). Age is also a factor of individual differences. As we age our sensitivity to short wavelengths decreases because of variations in the spectral transmittance of elements in our eye. For example, through age our eye lens absorbs more blue light and the density of the yellow pigment of the macula changes.

Nowadays, the CIE recommends a standard set of the cone fundamentals based on the Stiles & Burch (1959) 10° CMFs (Stockman and Sharpe, 2000) and is not limited to agree with the flawed $V(\lambda)$ (Sharpe et al., 2005). In addition, a more modern version of the $V(\lambda)$ from 1924, is the Judd-modified luminous efficiency curve $V_M(\lambda)$ from 1951. The modern measurements of $V(\lambda)$ suggests that the curve results from the sum of L- and

M- cones sensitivities and S- cones seem to contribute little (Smith and Pokorny, 1975; Lennie et al., 1993). New measurements of $V(\lambda)$ are based solely on the minimum flicker techniques, like heterochromatic flicker photometric (HFP) and minimally distinct border (MDB) which provides reliable and consistent photometric measurements (Sharpe et al., 2005).

As illustrated in Figure 2.12, modern theories of opponent mechanisms can be explained in a simple manner. Opponent color mechanisms are explained with combinations of the L-, M- and S- cones. For example, the L- and M- cones are connected, L- cones with excitatory output, the M- cones with inhibitory output to produce $L - M$ opponent cells or a red-green opposing channel. The S- cones are connected with the L- and M- cells to produce $(L + M) - S$ opponent cells or a yellow-blue opposing channel. The non-color opponent cells $L + M$ output carries luminance information resembling to $V(\lambda)$.
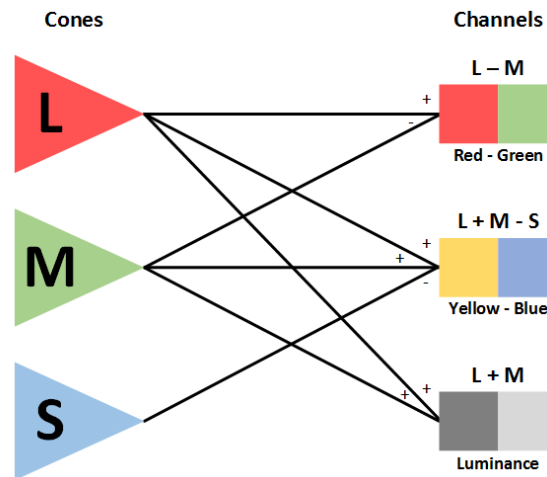
Figure 2.12: Connections of L-, M- and S- cones to produce different opposing channels. The combination $L - M$ opponent cells produce a red-green opposing channel. The combination $(L + M) - S$ opponent cells produce a yellow-blue opposing channel. And $L + M$ produce a channel with just luminance information similar to $V(\lambda)$.

2.3 Color Models

2.3.1 Color Matching Functions

After the luminous efficiency function $V(\lambda)$ was determined, a system was constructed based on the three primaries RGB and the laws of additive color mixture as illustrated in equation 2.2. A matching experiment was done with three monochromatic lights, red (700nm), green (546nm), and blue (435nm) such as the levels of each primary was adjusted to match monochromatic lights of different wavelengths. It is assumed that these primaries are enough to match any test light. This experiment resulted in the color

matching functions (CMFs) $\bar{r}(\lambda)$, $\bar{g}(\lambda)$ and $\bar{b}(\lambda)$. With this system any color stimuli can be converted from their spectral power distribution to the amount of primaries R, G and B needed (tristimulus values RGB). The CIE RGB CMFs are shown in Figure 2.13. The tristimulus values RGB for a stimulus with a spectral power distribution $\phi(\lambda)$ can be calculated with the equations 2.3.

$$R = \int \phi(\lambda)\bar{r}(\lambda)d\lambda \quad G = \int \phi(\lambda)\bar{g}(\lambda)d\lambda \quad B = \int \phi(\lambda)\bar{b}(\lambda)d\lambda \qquad (2.3)$$
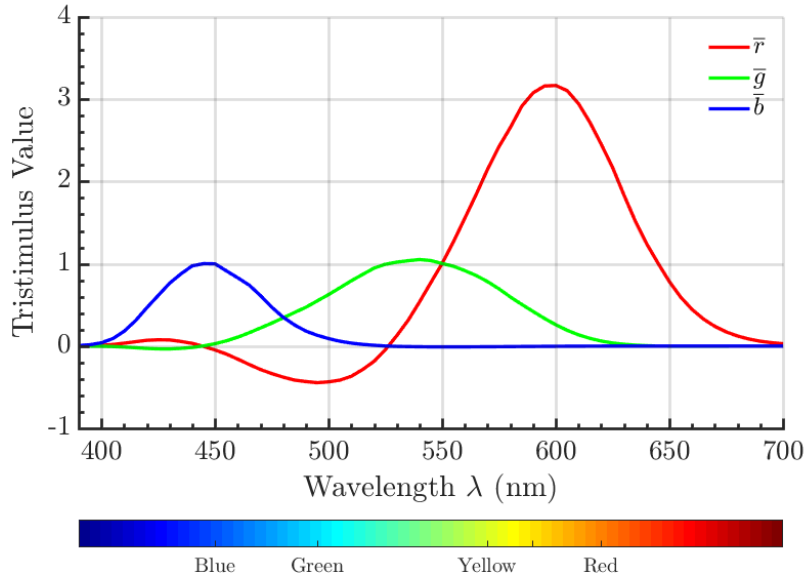
Figure 2.13: Spectral tristimulus values for the CIE RGB CMFs standard with three monochromatic primaries at 435.8, 546.1, and 700.0nm

CIE decided to transform to another set of primaries to eliminate the negative values of this color matching function. In addition, one primary is forced to match the photopic luminous efficiency function $V(\lambda)$. These primaries are known as XYZ and the color matching functions are given by $\bar{x}(\lambda)$, $\bar{y}(\lambda)$ and $\bar{z}(\lambda)$ as shown in Figure 2.14. The three primaries XYZ can be calculated with equations 2.4.

$$X = k \int \phi(\lambda)\bar{x}(\lambda)d\lambda \quad Y = k \int \phi(\lambda)\bar{y}(\lambda)d\lambda \quad Z = k \int \phi(\lambda)\bar{z}(\lambda)d\lambda \qquad (2.4)$$

In these equations k is a normalizing factor. In absolute values it is equal to 683 lumen/W. In relative colorimetry k is calculated with the relative spectral power distribution of the light source $S(\lambda)$ as equation 2.5.

$$k = \frac{100}{\int S(\lambda)\bar{y}(\lambda)d\lambda} \qquad (2.5)$$
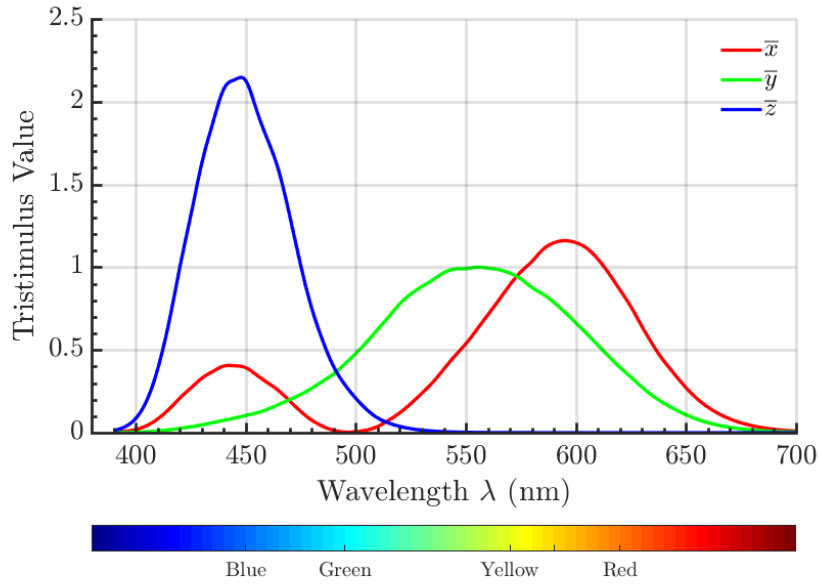
Figure 2.14: Spectral tristimulus values for the CIE XYZ 2006.

2.3.2 Cone Fundamentals

Another set of tristimulus values are known as LMS and they can be derived from the cone fundamentals. These are based on the light absorption and the excitation of the three types of cones, and represented by $\bar{l}(\lambda)$, $\overline{m}(\lambda)$ and $\bar{s}(\lambda)$. Only the relative spectral sensitivity for each one is well known, thus they can be scaled as desired and multiplied by any constant. The human cone spectral sensitivities for a 10° viewing angle derived from the Stiles & Burch 10° color-matching functions were shown in Figure 2.9 (Stockman and Sharpe, 2000). For a given stimulus $\phi(\lambda)$, the tristimulus values LMS are calculated with equations 2.6 and normalized with equations 2.7.

$$L = \int \phi(\lambda)\bar{l}(\lambda)d\lambda \quad M = \int \phi(\lambda)\overline{m}(\lambda)d\lambda \quad S = \int \phi(\lambda)\bar{s}(\lambda)d\lambda \tag{2.6}$$

$$l = \frac{L}{L+M+S} \quad m = \frac{M}{L+M+S} \quad s = \frac{S}{L+M+S} \tag{2.7}$$

2.3.3 Chromaticity Diagrams

Since a color stimulus can be defined by three values in a 3D color space, it is possible to transform these values such that one coordinate represent luminance and two coordinates represent the chromaticity. Therefore, chromaticity can be presented in a two dimensional space, known as a chromaticity diagram. To achieve this the tristimulus values are normalized to remove luminance information. This can be understood as a perspective projection of a three-dimensional space onto a two dimensional plane of the same space. For example, consider the normalization of the tristimulus values XYZ from equations

2.8.

$$x = \frac{X}{X+Y+Z} \quad y = \frac{Y}{X+Y+Z} \quad z = \frac{Z}{X+Y+Z} \tag{2.8}$$

As shown in Figure 2.15, a complete representation of this chromaticity diagram can be obtained with just x and y. It makes sense, since any point in a two dimensional space is represented by two coordinates. In this case, the z value can be calculated as shown in equation 2.9.

$$z = 1 - x - y \tag{2.9}$$
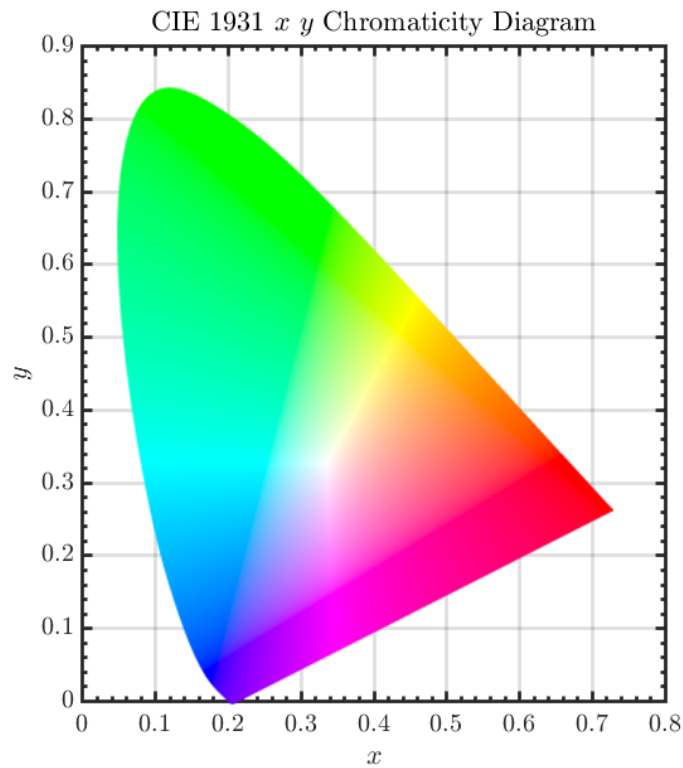
Figure 2.15: The CIE 1931 xy chromaticity diagram.

Given two coordinates x and y, we can transform back to the tristimulus values XYZ with the addition of luminance information represented with the Y tristimulus value. It is also useful to keep the tristimulus values as xyY. The reverse transformation is done as equations 2.10.

$$X = \frac{xY}{y} \quad Y = Y \quad Z = \frac{(1 - x - y)Y}{y} \tag{2.10}$$

A more perceptually uniform chromaticity diagram was proposed by the CIE convention in 1976 as shown in Figure 2.16. It is based on the CIE 1960 that was the result of several studies (MacAdam, 1937, MacAdam, 1971). This is the chromatic diagram that

it is currently recommended by the CIE for general use. it can be obtained from a simple transformation of x and y as shown in equations 2.11 and the reverse transformation in equations 2.12.

$$u\prime = \frac{4X}{X + 15Y + 3Z} = \frac{4x}{-2x + 12y + 3}$$
$$v\prime = \frac{9Y}{X + 15Y + 3Z} = \frac{9y}{-2x + 12y + 3}$$

(2.11)

$$x = \frac{9u\prime}{6u\prime - 16v\prime + 12}$$
$$y = \frac{4v\prime}{6u\prime - 16v\prime + 12}$$

(2.12)
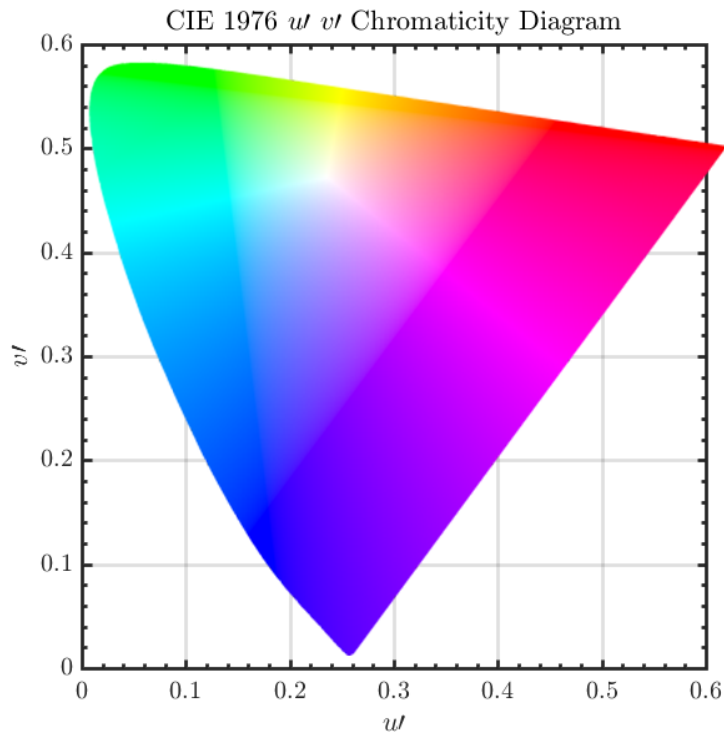
Figure 2.16: The CIE 1976 $u\prime$ $v\prime$ chromaticity diagram.

2.4 Flicker Perception

Flicker is the impression of temporal variation in luminance or color. Light that fluctuates between two luminance levels, produces a sensation of luminance flicker. If the frequency is high enough the flicker fuses, producing the appearance of a static light. This transition of flicker to fusion occurs at the critical fusion frequency (CFF). Measurements of flicker sensitivity for luminance flicker have shown that cones can follow up to $80 - 90$Hz but rods signals cannot be modulated faster than $10 - 15$Hz (Lee, Pokorny, Martin, Valbergt, and Smith, 1990).

The sensitivity to flicker is often described in terms of the temporal contrast sensitivity function (tCSF). De Lange (1952, 1954, 1958) was the first to measure the observer's tCSFs for a 2° sinusoidal stimuli of many temporal frequencies. A tCSF describes the modulation at which a light fluctuation is just visible as a function of temporal frequency. As illustrated in Figure 2.17, the y-axis is the temporal contrast sensitivity and the x-axis the temporal frequency (Hz). The area underneath represents the conditions where flicker is perceived, and the area outside the curve represent the non-perceivable flicker. The CFF is the projection on the frequency axis of the point where the observer do not perceive flicker anymore for higher frequencies.
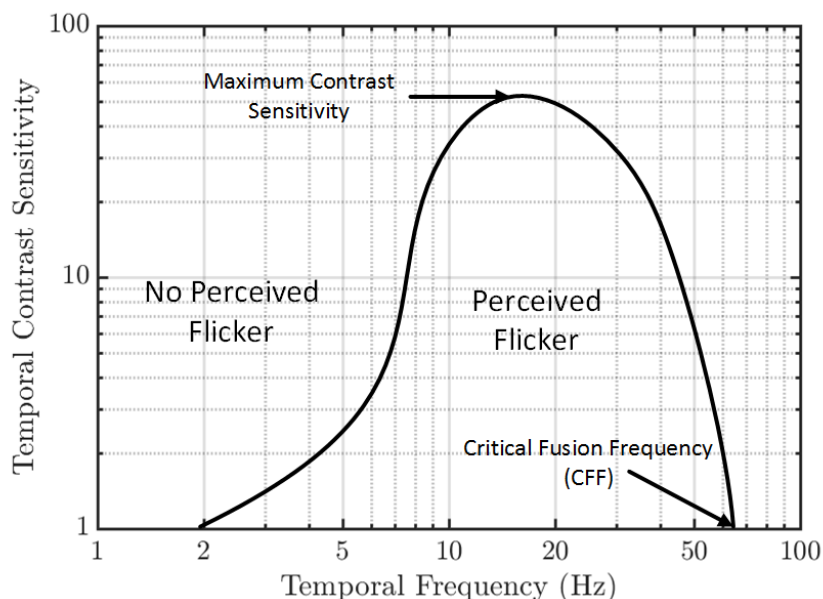
Figure 2.17: Example of a tCSF. The area underneath represents the perceivable flicker, and the area outside the curve represent the non-perceivable flicker. The CFF is the frequency where at higher frequencies the observer do not perceive flicker anymore.

When the two lights are made up of different colors, the fusion frequency occurs at around 25Hz, producing a single perceived color due to the additive mixing of colors (Jiang et al., 2007). If the alternating frequency is lower, the observer perceives what is known as chromatic flicker. Luminance flicker has been well studied by researchers, but limited research has been done to describe chromatic flicker. Among the few studies, most of them only studied red-green chromatic flicker. Some studies found that for luminance and chromatic flicker the human visual system acts like two separate band-pass filters that peak around 8 Hz and 4 Hz, respectively (Shady et al., 2004; Green, 1968). Other studies reported low pass characteristics of the tCSFs for chromatic flicker (Granger and Heurtley, 1973; Van der Horst and Bouman, 1969; Swanson et al., 1987).

In Figure 2.18, we can see that tCSFs for chromatic flicker are distinctly different from tCSFs of luminance flicker (Swanson et al., 1987). For luminance flicker, the band-

pass characteristics and the peak sensitivity increases with the mean luminance. Above 100 troland (31.83 cd/m^2) the bandpass characteristics do not change considerably. For chromatic flicker, the sensitivity depends on mean luminance at all temporal frequencies up to 100 troland (31.83 cd/m^2) and above that value the sensitivity increases only at higher frequencies (Kelly, 1994).
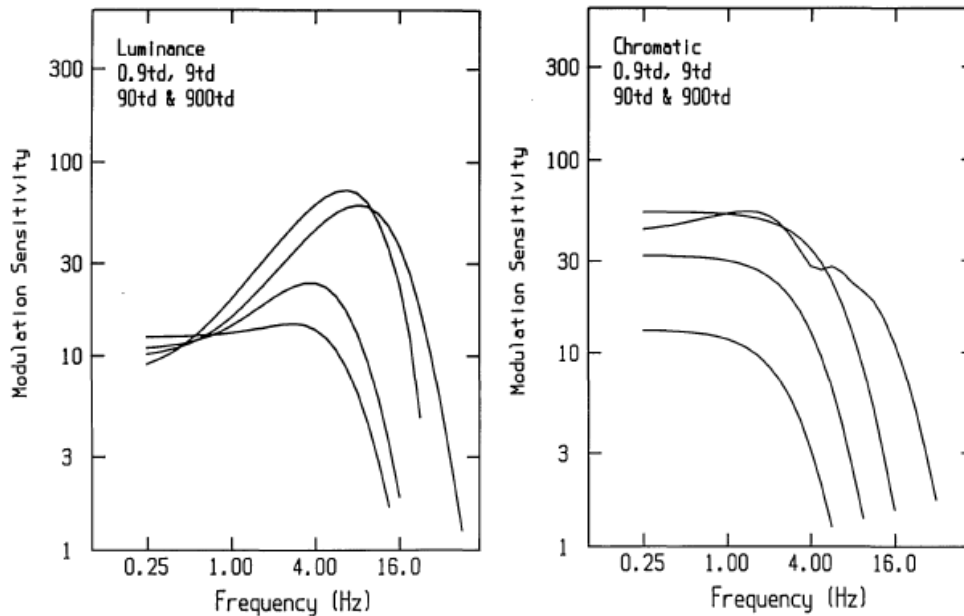
Figure 2.18: Modulation sensitivity as a function of frequency (Hz) for luminance (left) and chromatic (right) flicker. The luminance levels were measured in trolands (td) that corresponds to 0.31 cd/m^2. (Swanson, Ueno, Smith, and Pokorny, 1987)

Different stimulus factors, like the stimulus mean luminance, position and size can influence the CFF for luminance and chromatic flicker (De Valois, 2000; Bodrogi and Khan, 2012; de Lange, 1958). As shown in Figure 2.18 , CFF increases with increasing luminance. For small stimulus sizes, CFF increases with the size of the stimulus field. Furthermore, in the case of luminance flicker for relatively high stimulus luminance levels and a position that stimulates the fovea, the CFF is lower compared to when the fovea and the peripheral area of the eye is stimulated (Bodrogi and Khan, 2012).

Different assumptions have been made in order to measure flicker sensitivity of chromatic and luminance flicker. One important assumption is that the two types of flicker are mediated by separated chromatic and luminance mechanisms, so that it might be possible to isolate one from the other. However, we do not know under which conditions luminance can be considered as constant during chromatic flicker. For example, two lights of equal luminance may not be the same at another luminance. Also, two lights of equal luminance at one frequency may not be equal in luminance at another frequency. Therefore, both chromatic and luminance fluctuations can be visible at the same time. If we change the luminance ratio between the two lights, the impression of flicker will change

and at a certain ratio it will reach a minimum or even disappear. This method is called heterochromatic flicker photometry (HFP) and it is used for determining equal brightness conditions and to minimize the visibility of luminance flicker.

There is evidence that the differences in the shape of the tCSFs might be caused by apparent brightness flicker (Van Der Horst, 1969; De Lange, 1959; Kelly, 1994). In experiments were the luminance of the two chromatic stimuli was corrected to appear equal, the result was a contrast sensitivity function with a low-pass shape (Van der Horst and Bouman, 1969; Kim et al., 2013). In other studies, a contrast sensitivity function of chromatic flicker with a band-pass shape that is more typical of luminance flicker were found (Shady et al., 2004; Green, 1968). Thus, HFP might help to reduce the effect of these residuals of luminance flicker.

2.5   Heterochromatic Flicker Photometry

It is well known that lights of different color and equal in luminance are not always perceived as equally bright (Kaiser and Comerford, 1975). Therefore if two of these lights are temporally alternated, observers might perceive luminance flicker rather than just chromatic flicker. Historically, the method of heterochromatic flicker photometry was based on the assumption that there exist an achromatic mechanism and one or more opponent, chromatic mechanisms of the visual system (B. Lee, Martin, and Valberg, 1989). Consequently, this method can be used to create equal apparent luminance (isoluminant) conditions where only color-sensitive perceptual mechanisms are stimulated and not luminance-sensitive mechanisms. In addition, HFP has been also used to measure the photopic function $V(\lambda)$.

This method enables observers to adjust the luminance ratio of two alternating color lights until the perception of flicker is eliminated or minimized (Bone and Landrum, 2004). One challenge of this method is that researchers have to find the optimal frequency of the modulation to obtain reliable measurements. For example, at low frequencies the sensitivity to chromatic flicker is larger compared to luminance flicker, making it difficult to minimize flicker by changing the luminance ratio. At frequencies above the CFF of chromatic flicker, the two colors are fused, but flicker can be observed as long as the luminance levels of the two colors lights are not matched (Bone and Landrum, 2004). Typically HFP has been used with frequencies around 10 and 20Hz (Lee, Martin, and Valberg, 1988)). This corresponds to the range of frequencies were the sensitivity to luminance flicker is higher.

2.6 Method of Adjustment

In literature, several psychophysical methods have been used to measure visibility thresholds of flicker. Most of these methods can be divided in three categories: method of adjustment, method of limits, and method of constant stimuli. In the method of limits, stimuli are presented in ascending or descending order, and participants must judge whether they can see the stimulus or not. In the method of constant stimuli the threshold is determined by presenting the observer with stimuli of which some are above the threshold and of which some are below. For our study the method of adjustment was chosen to obtain preliminary estimates of the visibility thresholds for chromatic flicker. This can guide the choice of stimulus magnitudes and psychophysical methods for future experiments.

The method of adjustment is a psychophysical procedure introduced by Fechner (1860). It consists of allowing the observer to freely adjust the stimulus to find a threshold. Thus, a direct connection between the input device and the stimulus is made. Experiments generally require observers to repeat this procedure for the same stimulus and the absolute threshold is taken as the average threshold obtained through each repetition. The tasks can be to find the threshold for which participants barely see or not see the stimulus.

One important consideration when using this method is that the order of the starting points has to be randomized to avoid biases like expectation and habituation (Gescheider, 1997). Even if this method is quick and easy to implement, and very simple and straightforward, one big advantage is the amount of active participation an observer has that can help to maintain high performance during the experiments (Fairchild, 2013; Gescheider, 1997). In addition, there is a lot of information that can be stored for every decision made by the observers before settling to a final result (Cunningham and Wallraven, 2011). However, observers may have the tendency of reporting the presence of the stimulus when there is not, so the threshold could be falsely low. They also may have the tendency to be very conservative and report that there is no stimulus when actually there is, so in this case the threshold would be falsely high. This is the main reason why this method is generally considered to be inaccurate for research purposes (Gescheider, 1997).

Chapter III

Methodology

"Always ask oneself: Couldn't this be different? Couldn't this be better? I have found fantasy to be one of the key factors of success in a person's life"

– Anton Philips

This chapter discusses the equipment, and procedures that were used in order to measure and generate chromatic flicker stimuli. First, the equipment is described. Some of them were especially made for this study, but can be easily adapted for future experiments. Second, the general stimuli are introduced. Third, a brief description of the participants is presented. And fourth, the design, procedures and specific details for each experiment is given.

3.1 Equipment

3.1.1 The spectrometer

The spectrometer used to calibrate and measure the spectral properties of the LED system was the Specbos 1201 (see Figure 3.1) developed by JETI Technische Instrumente GmbH. It can be used to measure different quantities, but we were mostly interested in measuring luminance, spectral radiance and xy and $u'v'$ chromatic coordinates. It has a wavelength resolution of 5nm, a total spectral range of 380nm to 780nm and a wavelength accuracy of ± 0.5nm. The luminance range is from 2 cd/m^2 to $7 * 10^4$ cd/m^2 with an accuracy of $\pm 2\%$ and it can measure viewing angles above 1.8°. By default the spectrometer uses $\overline{y}(\lambda)$ of the 2° CIE 1931 color space as $V(\lambda)$ for photometric calculations.
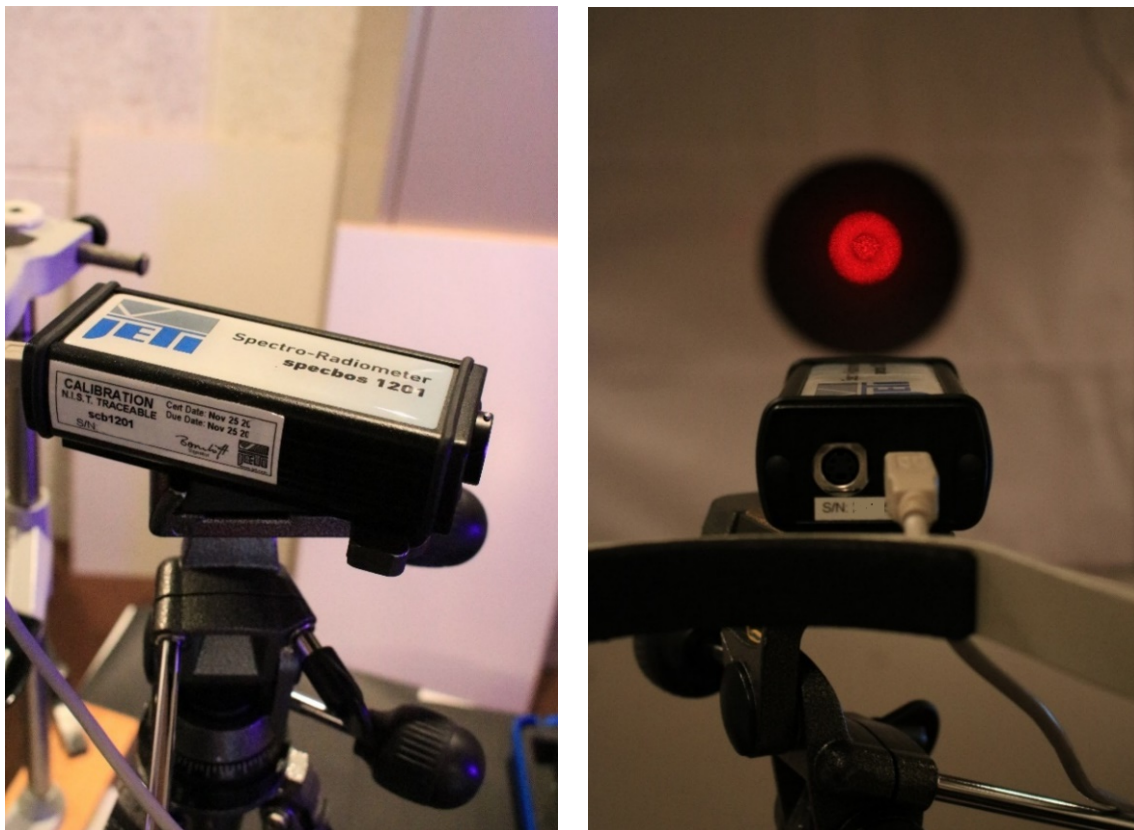
Figure 3.1: Specbos 1201 is a precise and compact VIS spectroradiometer, suitable for the laboratory as well as production environment. Developed by JETI Technische Instrumente GmbH.

3.1.2 LED Flicker System

Stimuli were presented on a LED system specially designed for the purpose of this study. It was designed and developed by Martin Boschman a technical staff from the Human Technology Interaction group of the Eindhoven University of Technology. The system consisted of 36 Cree XP-E LEDs arranged in a squared panel: 12 red, 8 green and 16 royal blue LEDs. The 36 LEDs were divided in 4 banks of 3 Red + 2 Green + 4 Blue LEDs (see Figure 3.2) which were driven by 4 separate addressable drivers as shown in Figure 3.3. A homogenous distribution of light could be achieved by using two banks (1 & 2 or 3 & 4) or all. In our study, just bank 1 and 2 were used.

As specified in the datasheet of the Cree XP-E LEDs, the dominant wavelengths (DWL) of each type of LED could vary between 620 to 630nm for red, 520 to 535nm for green and 450 to 465nm for royal blue. After measuring them with the spectrometer we found that they were within this range with dominant wavelengths of 623nm, 531nm and 453nm, respectively.

(a) Schematic
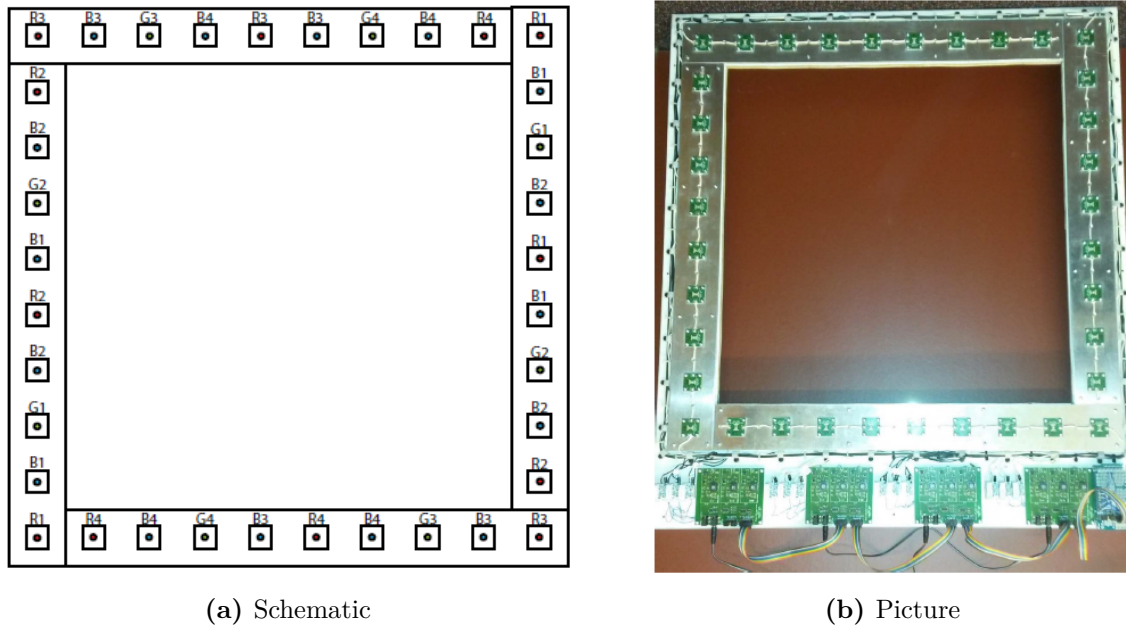
(b) Picture

Figure 3.2: **(a)** Schematic of the placement of 36 LEDs. The numbers next to the RGB letters refer to the banks numbers the LEDs belong to. **(b)** A picture of the squared panel of 36 LEDs, 4 drivers and 1 Arduino Due microcontroller mounted on the bottom-right of the setup.

The panel of LEDs was placed inside a white colored box with smooth and solid walls. The inner walls of the box were painted with white chalk paint by which mat diffuse reflecting surfaces were obtained. Two different configurations of the box are shown in Figure 3.3. The first configuration has a squared shaped window where the light is emitted outside of the box. The second one has a smaller window made by placing a paperboard with a circular hole. In this case, the visible part of the illuminated surface of the back panel acted as a circular stimulus field. For sake of simplicity we call these configurations the big window and small window. The dimensions of the window was 57x57 cm for the big window and 26.5 cm-diameter for the small window.
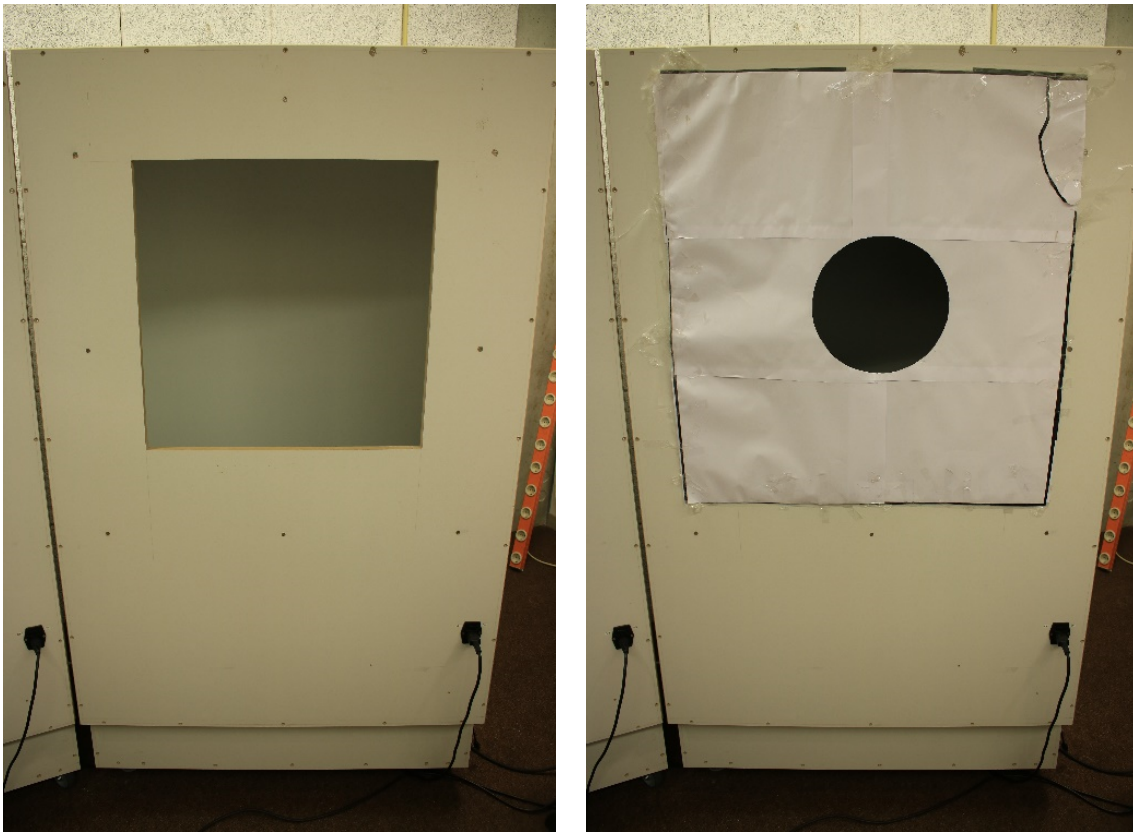
(a) Big window of the box with dimensions 57x57 cm.

(b) Small window made with a paperboard with a 26.5 cm-diameter circular hole.

Figure 3.3: Two different configurations of the LED box.

An 84MHz master clock of an Arduino Due microcontroller board was used to generate high-frequency Pulse Width Modulated (PWM) signals for the LED drivers as shown in Figure 3.4. One period of the PWM was defined as 42000 cycles of the master clock, resulting into a PWM frequency of 2kHz and a period divided in 42000 steps of 11.9ns (i.e. almost a 16-bit resolution). The maximum intensity of the LEDs was achieved when the 42000 steps of the PWM are set to high, as a result the pulse width matches the period and 100% duty cycle is obtained. A duty cycle is defined as $D = (T_H/T) \times 100\%$ where T_H is the pulse width and T the period of the PWM.
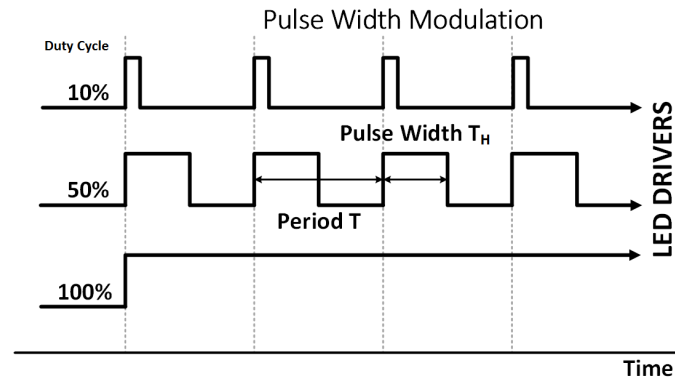
Figure 3.4: Example of different duty cycles of a PWM signal. The system drivers receive these signals to deliver power to the LEDs . The frequency of 2kHz corresponds to a period T of 0.5 ms.

A stable system was of great importance for the experiments presented in this study. The system had to be in constant use for hours, and, since temperature might cause changes in the spectral properties of the LEDs, the color of the light might change over time. As a way to determine these effects the red, green and blue LEDs luminance and spectral power distribution were measured in an hourly basis for 5 hours of continuous warm-up. The spectrometer was set up in front of the small window of the box with the measurement field located at the center of the stimulus field. Warming up the system means that the PWM values for the LEDs were set to the maximum value possible, in this case the duty of the PWM was set to 100% (i.e. full duty cycle). Figure 3.5 shows the temporal variations in the luminance level for each type of LEDs. Stability of luminance can be observed after 1 hour when the luminance drops around 6-8%, 3-5% and 0-1% for the red, green and blue LEDs respectively.
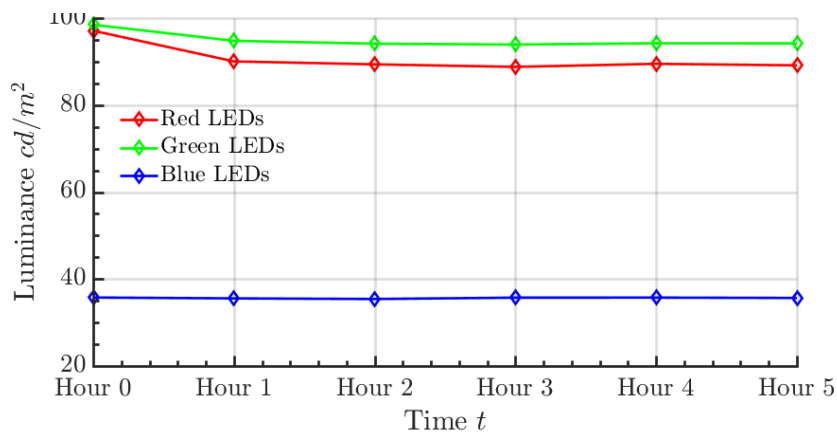
Figure 3.5: Temporal variations in the maximum luminance levels of the red, green and blue LEDs.

The spectral power distribution for each type of LEDs after 1 hour warm-up is shown in Figure 3.6. When the system is stable, the maximum spectral radiance is reduced around

5% relative to the maximum of the initial spectral peak. Temperature also induced a shift of around 1nm for the peak wavelength of the red LEDs.
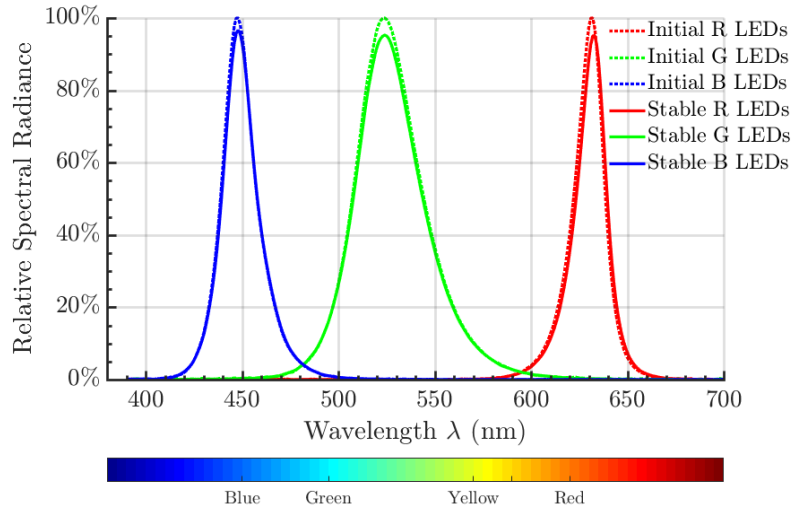
Figure 3.6: The spectral power distribution for the red, green and blue LEDs with maximum PWM values at t = 0 (initial) and after 1 hour (stable).

These shifts caused small variations in the chromatic coordinates $u'v'$ as shown in Figure 3.7. The difference $\Delta u'v'$ between the initial (t = 0) and the last hour (t = 5) for each LED was calculated. The red LEDs had a variation $\Delta u'v'$ of around 0.0031, the green LEDs of 0.0010, and the blue LEDs were very stable from the beginning. The system was left off for a couple of minutes at hour 2 and 3, this might have caused some cool down variations of the chromatic measurements, but afterwards the chromatic point returned to the stable measure.
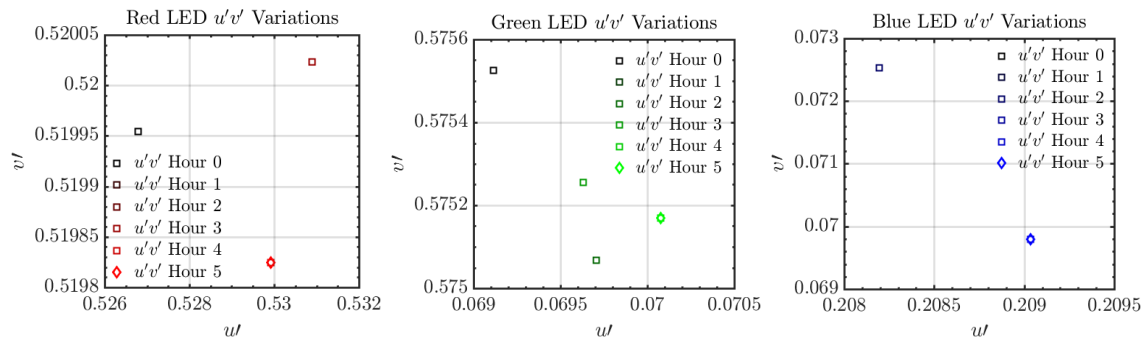
Figure 3.7: Temperature effects on the red, green, blue LEDs chromatic coordinates $u'v'$.

After warming up the LED system the spectral power distribution of red, green and blue LEDs with maximum PWM values were measured. A comparison of the spectrum measured through the big window (BW) and small window (SW) is shown in Figure 3.8. The internal reflections of the box were higher when the paperboard was placed over the big window, therefore a higher percentage of light rays produced were directed out through

the circular hole (small window). In consequence, the spectral radiance for each type of LED was around 15-17% higher than the measure without the paperboard (i.e. through the big window). When the system was stable, there was no big difference between the peak wavelengths of both windows, thus variations in chromatic coordinates $u'v'$ were negligible.
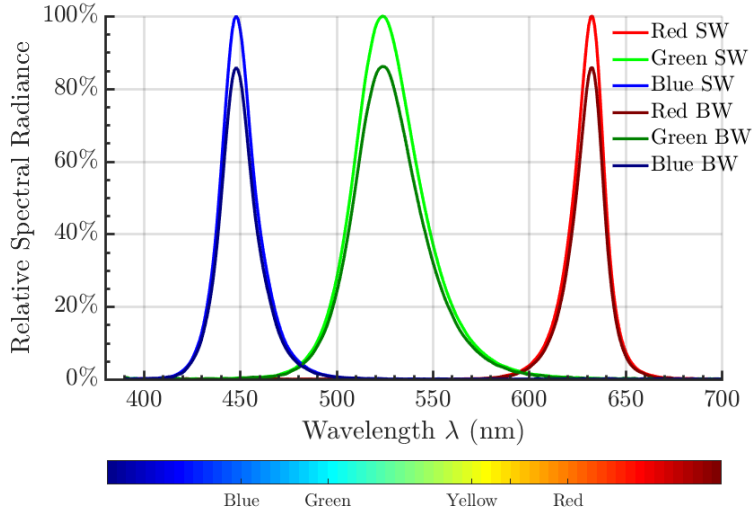
Figure 3.8: Spectral power distribution for the red, green and blue LEDs with maximum PWM values, of both the big window and small window relative to each maximum spectral peak of the big window.

The system had to be calibrated prior to the start of the experiments in order to get accurate $u'v'$ chromatic coordinates. It was important to consider the warm-up time at which the system becomes stable in luminance and chromaticity prior to the calibration procedure. Waiting 1 hour was enough to obtain a calibration file that was well related to the stable spectrum of the system.

The calibration procedure consisted of connecting the LED system and the Specbos 1201 spectrometer to the computer, turning off the lights of the laboratory, directing the measurement field of the spectrometer to the center of the stimulus field, opening a custom software for calibrating the system, selecting the number of PWM values to be measured, and starting the calibration. The software automatically calibrated the system and turned off the computer display. The researcher could leave the lab while the calibration was in process.

After the calibration procedure, we obtained a file specifying 3 chromaticity points in the xy color plane (0.696 , 0.195), (0.303, 0.716) and (0.001, 0.089) and 10 luminance levels for each red, green and blue LEDs measured with 10 PWM from 0 to 42000 in steps of 42000 divided by 10 as shown in Figure 3.9.
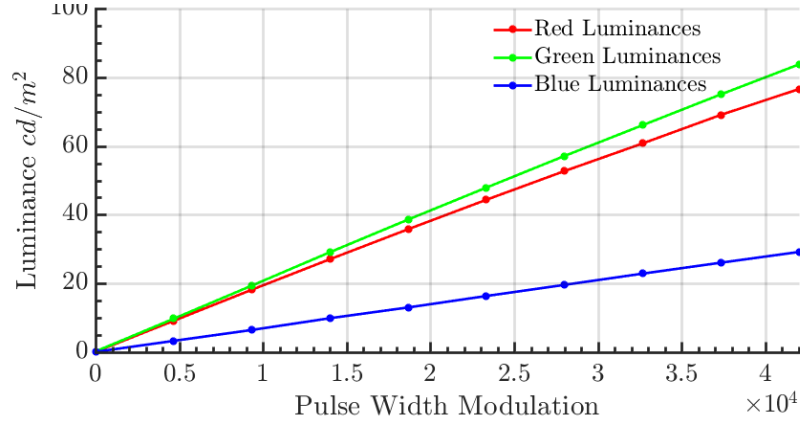
Figure 3.9: Original calibration used for the experiments, 10 luminance levels for each red, green, blue LEDs with varying PWM were measured through the big window. The numeric values are shown in Table A.2 of Appendix A.

The chromaticity points xy helped to define the boundaries of the system's gamut to avoid generating unsupported color points. In addition, the LED system's calibration matrix XYZ_{LED} was obtained from the 3 gamut corners xy_R, xy_G and xy_B to calculate the luminance required for each type of LED (i.e. the R, G and B values) to generate a desired stimuli. First, the 3 gamut corners xy were converted to XYZ_R, XYZ_G and XYZ_B with the set of equations 2.10 shown in chapter 2. The luminance Y was set to 1 and the matrix was calculated as equation 3.1.

$$XYZ_{LED} = \begin{bmatrix} X_R & X_G & X_B \\ 1 & 1 & 1 \\ Z_R & Z_G & Z_B \end{bmatrix} \tag{3.1}$$

Second, in order to know the RGB values for a given $u'v'$ value, first the $u'v'$ coordinates were transformed to xy coordinates with equations 2.12 of chapter 2. Afterwards, these xy coordinates were converted to XYZ (with Y = 1) and it was multiplied by the inverse of the matrix from equation 3.1 to obtain RGB_L, this corresponded to a vector of 3 values, the percentage of luminance for each type of LED.

$$RGB_L = XYZ_{LED}^{-1} \begin{bmatrix} X \\ Y \\ Z \end{bmatrix} \tag{3.2}$$

Because RGB_L do not have luminance information, the wanted overall luminance L was multiplied to obtain the 3 individual luminance levels for each type of LED as equation 3.3.

$$L_{RGB} = RGB_L \times L \tag{3.3}$$

The 10 luminance levels of the calibration were measured to interpolate the desired L_{RGB} luminance levels between 2 measured luminance values and to obtain the PWM values required for each type of LED. In this case, a simple cubic spline interpolation was used. Then, these PWM values were sent to the Arduino to generate the desired stimuli. An additional table with the calibration values is shown in Appendix B.2.

At the beginning, we did not realize that the small and big window would differ in luminance levels. The system was originally calibrated with the measurements through the big window. However, the experiments were carried out with the small window. Therefore, a correction factor had to be calculated to correct for the difference between the big and small window and to know the stimuli that were actually emitted through the small window. As shown in this section, the $u'v'$ chromatic coordinates of the primaries did not considerably vary between the two windows. However, since the calibration used during the experiments was measured a few weeks before the experiments, the correction factors were applied to both chromaticity and luminance levels.

The correction factor was calculated by using a simple relation between two calibration files. One calibration file was the one used during the experiments, it was measured through the big window and the other one was a more recent calibration file measured through the small window. It is important to note that we measured the most recent spectral distribution of the small window, and the used calibration measured through the big window was obtained before the experiments, thus, we expect to see some variations in chromaticity and luminance levels. The correction factors K_{RGB} for the luminance of red, green and blue LEDs was obtained as the average ratio of the luminance between windows as shown in equation 3.4.

$$K_{RGB} = \frac{\sum_{N_{PWM}} L_{RGB}(SW)/L_{RGB}(BW)}{N_{PWM}} \tag{3.4}$$

In this equation, N_{PWM} is the number of measured PWM values. In this case, 10 PWM values were measured, so N_{PWM} equals to 10. The $L_{RGB}(SW)$ are the luminance values measured through the small window and $L_{RGB}(BW)$ are the luminance values measured through the big window. K_{RGB} is a vector of 3 correction factors for the luminance of red, green and blue LEDs. To transform measured luminance levels from the big window to luminance levels of the small window, we simply multiplied these correction factors by the luminance levels of the calibration file used. The correction factors used were approximate to 1.1653, 1.1241 and 1.2144 for the red, green and blue LEDs luminance levels, respectively. This means that both the chromaticity and luminance of the stimuli differed from the intended stimuli. When the correction factors were calculated with a calibration file of the big window that was obtained right after the calibration of the small window, these resulted in 1.1623, 1.1583 and 1.1672 for red, green and blue LEDs. Thus, in this case the stimuli differed mostly in luminance.

Additionally, the ratio of the old calibration of the big window with the recent

calibration was calculated. This resulted in 1.0026 (+ 0.26%), 0.9705 (- ~3%) and 1.0405 (+ ~4%) for red, green and blue spectrum. This means that the spectrum of the system changed through time, thus, we do not know what was the exact spectrum when the experiments were carried.

3.1.3   Software

Figure 3.10: Desktop computer used to communicate with the system. Intel Core i5, 16 GB ram, Windows 7.

A desktop computer (see Figure 3.10) was used to communicate with the Arduino Micro-controller of the LED system through a serial port. In addition, several applications were used, for example, the JETI LiVal software and a custom made software for calibrating the system was used to get measurements from the Specbos 1201 spectrometer. Furthermore, an application was developed to support the different inputs of the experiment tasks, but also as a graphic interface for the experimenter to visualize in real-time the parameters of the experiment (see Figure 3.11). This was extremely helpful while debugging the application and during the pilot experiments, and also to validate that the parameters were set correctly. The data was initially stored in MySQL, then exported to Microsoft Excel and finally analyzed with MATLAB.
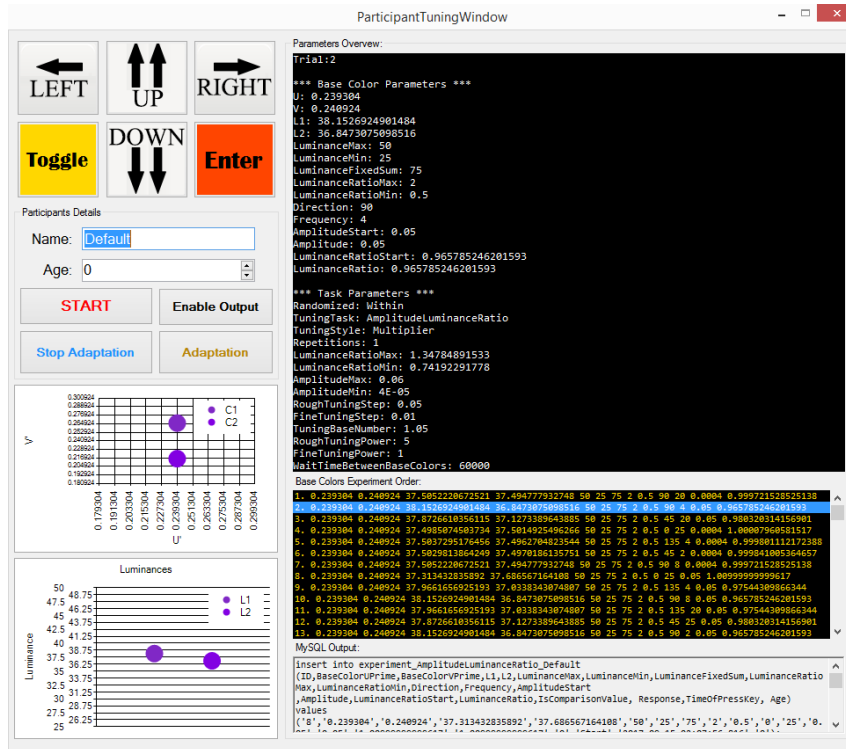
Figure 3.11: Application with a graphic interface used during the experiments. The stimuli was randomly ordered within each base color and shown in form a of a list.

3.2 General Stimuli

In this study, the stimulus was a temporally modulated light field. The chromaticity of the light varied sinusoidally around a base color with a specific amplitude $\Delta u'v'$ in a specific direction θ of the $u'v'$ chromatic diagram and with a specific frequency as shown in Figure 3.12. The two extreme colors (C_1 and C_2) could have a different luminance levels. Therefore, the luminance could also vary over time at the same frequency.
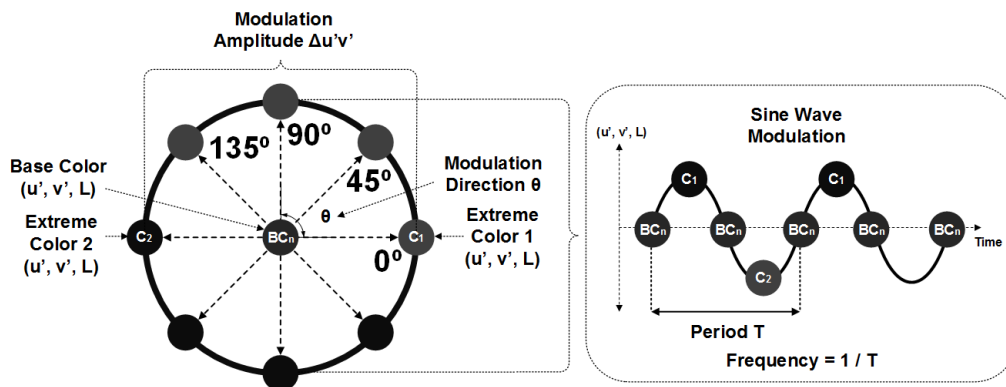
Figure 3.12: Modulation parameters of a flickering stimulus. The two extreme colors of the modulation were defined by the base color, luminance ratio, modulation direction and amplitude.

The modulated luminance level L is given by the ratio R_L of the luminance of the two extreme colors. We defined this relation as equation 3.5, where R_L was constrained by equation 3.6. L_S was defined as the fixed sum of the chosen maximum luminance and the minimum luminance of the system $L_S = L_{max} + L_{min}$.

$$R_L = \frac{L_2}{L_1} \tag{3.5}$$

$$L_2 + L_1 = L_S \tag{3.6}$$

As shown in Figure 3.13, 9 base colors and 4 directions (0°, 45°, 90° and 135°) were selected. Three base color points were placed on the vertices, three others on the middle of each side, one in the center, and two additional on a third of the distance between the vertices and the center. The chromatic coordinates of these base colors depended on limiting factors like the maximum modulation amplitude $\Delta u'v'$ of 0.06 and an offset of 0.01 from the gamut boundaries of the system in order to keep all the colors inside the gamut of the system (see Figure 3.14). An inner gamut triangle was calculated based on these two parameters. This method was just a simple initiative to distribute colors and cover as much as possible the CIE 1976 color space.

id	u'	v'
BC_1	0.127304	0.521309
BC_2	0.225072	0.166347
BC_3	0.450927	0.482579
BC_4	0.289115	0.501944
BC_5	0.176188	0.343828
BC_6	0.337999	0.324463
BC_7	0.267768	0.390078
BC_8	0.239304	0.240924
BC_9	0.389874	0.451745

Table 3.1: Base Colors $u'v'$
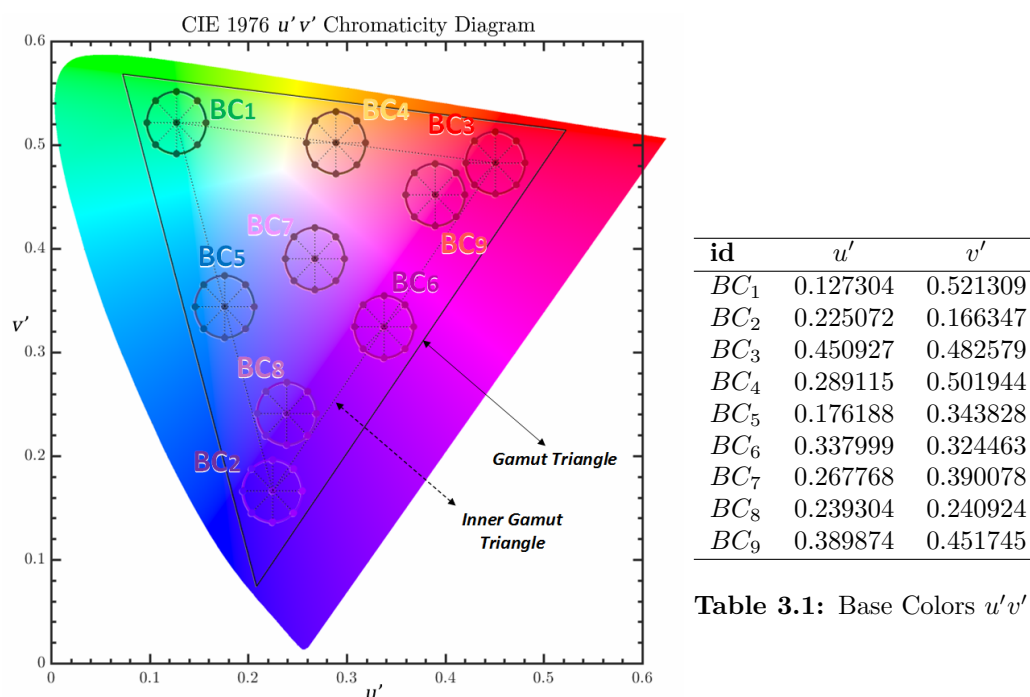
Figure 3.13: 9 base colors specified by their chromatic coordinates $u'v'$ and distributed throughout the CIE 1976 chromatic diagram.
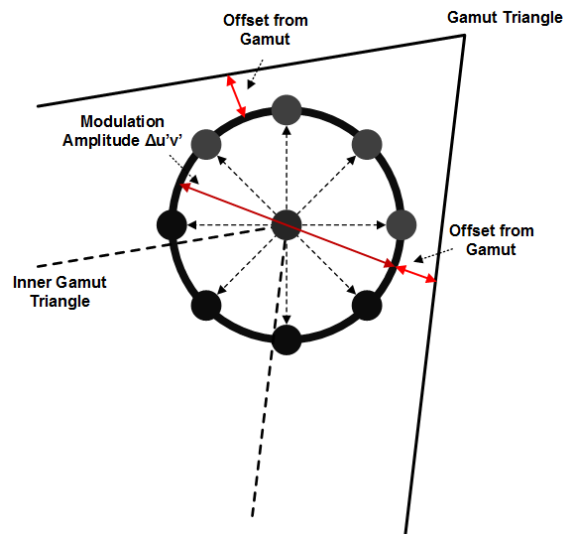
Figure 3.14: Position of base colors relative to the system's gamut triangle.

The luminance range that the system supported for these base colors and extreme colors is shown with yellow lines in Figure 3.15. Based on this, a single range of luminance values was estimated to safely keep every color within their luminance range. The minimum was chosen as 25 cd/m^2 and the maximum as 50 cd/m^2. As explained before, L_S was calculated as $50 + 25 = 75$ cd/m^2 and the mean luminance of the modulation was 37.5 cd/m^2. The extreme colors luminance varied from 37.5 cd/m^2 to 50 cd/m^2 or from 37.5 cd/m^2 to 25 cd/m^2 depending of the given luminance ratio R_L. These luminance values were the ones that we had originally chosen, but after applying the correction factor, the small window luminance values were around 43.5 cd/m^2.
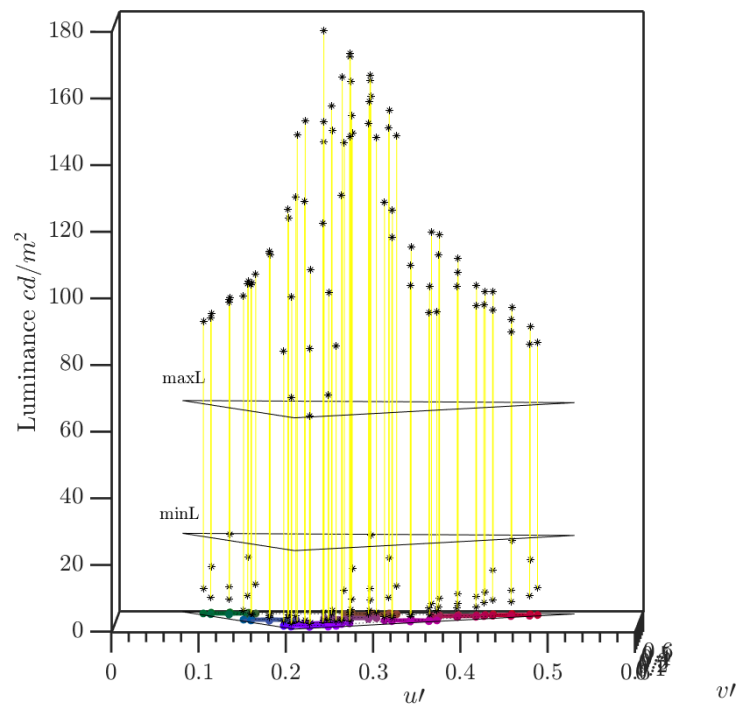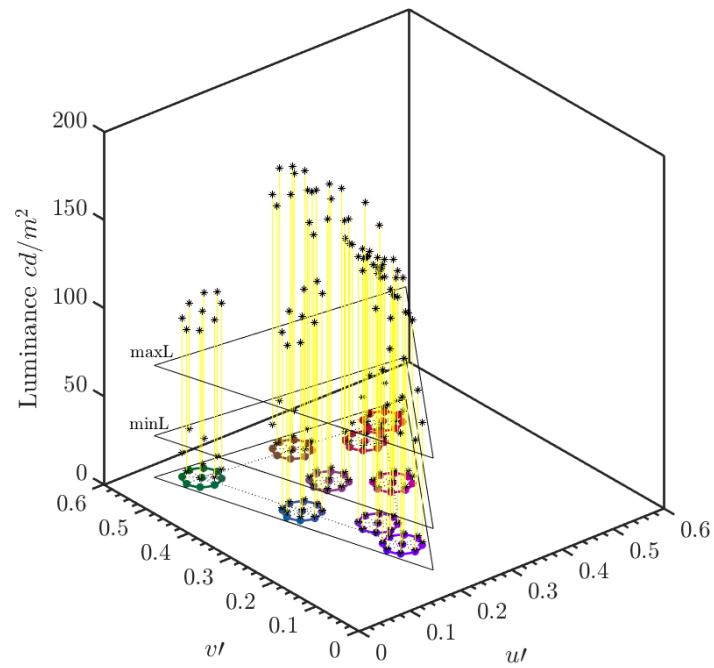
Figure 3.15: Evaluation of the maximum and minimum luminance level for each base colors and extreme colors. The boundaries for the luminance levels that were used during the experiments are shown as two triangles above the $u'v'$ chromatic diagram. The yellow lines are the ranges of luminance levels for individual color points.

3.3 Participants

Three students from the Eindhoven University of Technology, two males and one female in their mid-20s where tested under the same stimuli conditions. Two of the participants were experts on color vision experiments, the author of this thesis and a PhD student working in the lighting domain. For the purpose of the experiments, participants that had experience with the psychophysical method of adjustment were preferred. A naïve participant was trained to perform the experiment tasks, and was included to provide additional data. One participant had corrected vision, the others normal and none of them were susceptible to epileptic attacks. Originally a fourth participant was included in the study, but was excluded due to health problems, he reported feeling ill all day after attending to the laboratory. The experiments were performed in compliance with guidelines approved by the ethical board of the Human-Technology Interaction group and written informed consent was obtained from each participant.

3.4 Laboratory Settings

Participants observed the stimuli from a fixed distance of 150 cm, in a seated position and were kindly asked to use the chin rest, as shown in Figure 3.16. The size of the circular hole (26.5 cm) and the distance in relation to participant's eyes was chosen so as to ensure a 10° field-of-view. As mentioned before, the mayor concentrations of cones exist at the fovea and it corresponds to a 5.2° field-of-view. In addition, most of the existing color models are based on a 10° and 2° field-of-view. During the experiments some reflecting surfaces were covered by a black thick paper, and the computer display was covered as well.

Figure 3.16: The stimuli was observed from a fixed distance of 150 cm, in a seated position and through the chin rest. Some reflective surfaces like the table, were covered with black thick paper.

3.5 Experiment 1 - Luminance Ratio

Several pilot experiments were performed to define the best experimental settings to measure the luminance ratio for which chromatic flicker was least visible. These experiments are presented in the Appendix B. During the pilot experiments, it was discovered that under most conditions the luminance ratio of an isoluminant chromatic stimuli differed from 1 and was different between participants. This means that even if the luminance levels of the two extreme colors of the chromatic flicker stimuli were physically the same, participants perceived luminance flicker. Since every participants has his/her own $V(\lambda)$ function, we had to measure for each participant which luminance ratios had to be used in order to minimize luminance flicker.

3.5.1 Design

For this experiment a within-subject design was employed. With the method of adjustment, participants had to adjust the luminance ratio of the two extreme colors of the chromatic flicker stimulus for all base colors and directions to obtain a percept of minimum flicker. The independent variables were: base color (9 levels), modulation direction (4 levels), starting luminance ratio (2 levels) and repetition (2).

3.5.2 Stimuli

This experiment was performed with 9 base colors and 4 directions that were sinusoidally varying with a fixed frequency of 25 Hz and fixed amplitude $\Delta u'v'$ of 0.05. Two starting luminance ratio were selected, one above 1 (of 1.2201) and one below 1 (of 0.8195). Both luminance ratios corresponded to stimulus where flicker was very noticeable. Each condition was repeated twice. The number of trials generated for this experiment were 144 trials (9 base colors $\times$ 4 directions $\times$ 1 amplitude $\times$ 1 frequency $\times$ 2 starting luminance ratios $\times$ 2 repetitions).

3.5.3 Task

As shown in Figure 3.17, a hypothetical perceptual function was used to explain the task of the participant. Participants were instructed to adjust the luminance ratio between the two extreme colors of the chromatic flicker stimulus. They could use a fine step with a 1.01 multiplier (i.e. 1% change) or a rough step with a 1.01^5 multiplier (i.e. $\sim$5% change) of the luminance ratio. In linear scale, the steps do not have the same intervals, but in logarithmic scale the intervals are the same. The task of the participant was a combination of two smaller strategies.
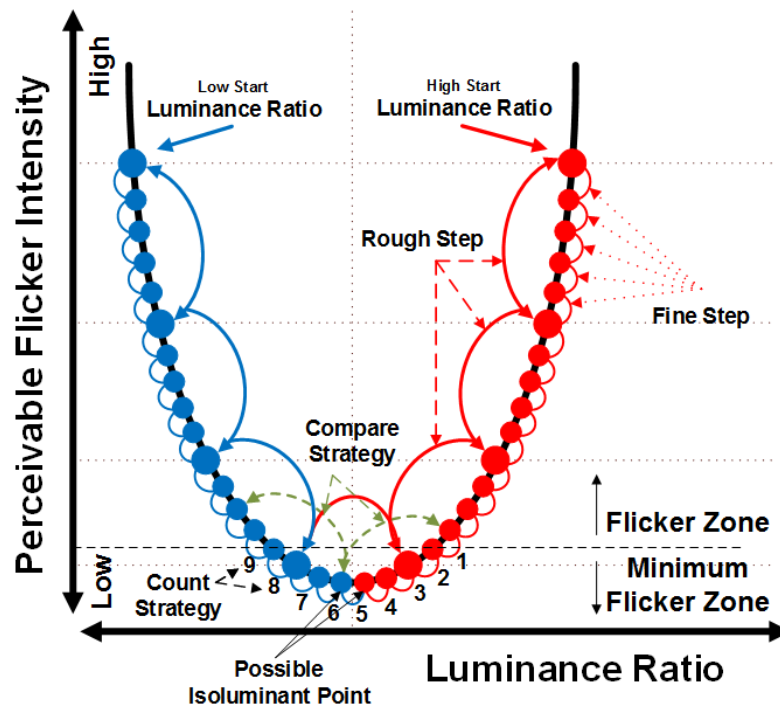
Figure 3.17: Image used to visualize the strategy that participants had to use during this experiment.

Strategy 1 – Count Strategy

1. The participant adjusts the luminance ratio using rough steps and fine steps till he/she perceives less or no flicker.

2. From that point, the participant returns by adjusting the luminance ratio with fine steps till there is an obvious amount of flicker being perceived.

3. The participant has to go back with fine steps while counting the steps till he/she finds the other side with an obvious amount of perceived flicker.

4. The participant has to go back again, but now counting half the steps he/she counted before.

5. Afterwards, the participant uses strategy 2 to make a decision.

Strategy 2 – Compare Strategy

1. From the minimum point found with the first strategy, the participant compares both sides of the flickering stimulus by going 1 rough step up, returning with one rough step down, and then going one rough step down, and returning again with one rough step up.

2. The participant decides if to adjust the luminance ratio with fine steps to balance the amount of flicker of both sides. They can be similar, but not equal.

3. The participant repeats 1 and 2 till he/she makes a decision and continues to the next trial.

4. At this point the participant has to press enter.

3.5.4 Procedure

Participants were introduced to the experiment. A few trials of practice were carried out by the two expert participants, and the naïve participant was instructed with a more extensive training. Before each experiment session it was important to warm up the system for 1 hour prior. Afterwards, the experiment sessions were carried out. The base colors were presented in order from base color 1 to 9, but the order of direction, starting luminance ratio and repetition was randomized. The whole procedure looked like this:

1. A 1-hour training session to get the participant familiar with the method of adjustment, including an explanation of the experimental settings, the stimuli and the strategy. Afterwards, participants were able to do a few practice trials, and the strategy was checked by observing their input during these trials and feedback was given afterwards.

2. A 30-minutes experiment session where the participant had to adjust the luminance ratio of the two extreme colors of the chromatic flicker stimuli towards to a minimum perceivable flicker using HFP. When all the conditions of one base color were measured, the next base color was shown. A 2 mins adaptation time was included for each base color.

3. A 30-minutes rest where participants left the laboratory and moved to an area with natural light.

4. Step 2 and 3 were repeated till the experiment was finished.

5. The data was quickly analyzed to check if there was any inconsistency and the luminance ratio of the measured isoluminant point for each base color and direction was calculated in preparation for experiment 2.

3.5.5 Time estimate

It was estimated that each trial would last around 15 secs to 30 secs. Based on the number of trials of this experiment together with the time estimate for each trial and the 2 mins adaptation time of each base color, it was expected that the experiment would be finished in around $(36 - 72 \text{ mins}) + 2 \text{ mins} \times 9 \text{ base colors} = 54 \sim 90 \text{ mins}$ (see Table A.4

of Appendix A). In addition, the rest time also had to be included in the overall time estimate of the experiment, hence the total time of the experiment was close or above 120 mins (2 hours).

3.6 Experiment 2 – Measuring the Temporal Chromatic Contrast Sensitivity Curve

3.6.1 Design

For this experiment, a within-subject design was used. With the method of adjustment, participants had to adjust the chromatic amplitude $\Delta u'v'$ and find their visibility threshold of chromatic flicker. The independent variables were: base colors (9 levels), frequency (7 levels), modulation direction (4 levels) and starting chromatic amplitude (2 levels).

3.6.2 Stimuli

This experiment was performed with the same 9 base colors and 4 directions but where sinusoidally varying at different frequencies (2, 4, 8, 10, 15, 20 and 25Hz), and the amplitude had to be adjusted by the participants. Two starting amplitudes were selected, one with an obvious amount of flicker ($\Delta u'v'$ of 0.05) and one with non-perceivable flicker ($\Delta u'v'$ of 0.0004). The number of trials generated for this experiment were 504 (9 base colors $\times$ 4 directions $\times$ 7 frequency $\times$ 2 starting amplitude).

We assumed that isoluminant stimuli were achieved by using the luminance ratios measured in the first experiment. During a pilot experiment, it was found that luminance ratio varied as function of the amplitude and the smaller the amplitude is the closer to the luminance ratio to 1. It was also found that a simple function can be used to approximate the luminance ratios as shown in equation 3.7. The luminance ratio $R_{L_{ref}}$ was set to the values found in experiment 1 and amplitude $\Delta u'v'_{ref}$ was 0.05. The variable $\Delta u'v'$ is the current amplitude of the modulation.

$$R_L = R_{L_{ref}}^{\Delta u'v'/\Delta u'v'_{ref}} \tag{3.7}$$

3.6.3 Strategy

Participants were instructed to adjust the modulation amplitude of the chromatic flicker stimulus. They could use a fine step with of 1.05 multiplier (i.e. 5% change) and a rough step of 1.05^5 (i.e. $\sim$25% change) multiplier of the amplitude. Simple and intuitive strategies were used to solve the experiment task.

Strategy 1 − Adjust Strategy

Two starting amplitudes were chosen for this experiment, a small amplitude where flicker would normally be invisible, and a larger amplitude were flicker was very obvious.

1. The participant adjusts using rough step (up or down) till he/she perceives a small amount of chromatic flicker.

2. The participant adjusts with finer steps down till he/she stops perceiving chromatic flicker.

3. Afterwards, the participant uses strategy 2 to make a decision. Sometimes it can get tricky because participants might think there is still flicker when there is not, and they adjust to smaller amplitude values. An additional compare strategy was used to avoid this.

Strategy 2 − Compare Strategy

This strategy was to help participants to make a decision when they were doubting whether or not there was chromatic flicker.

1. The participant do one or two rough step up.

2. The participant has to check if there is an obvious change in the chromatic flicker. In case there is no change, it means that they are far from the threshold point.

3. The participant returns to where he/she perceives flicker, and repeats the adjust strategy with fine steps till a decision is made.

4. At this point the participant has to press enter.

3.6.4   Procedure

After the first experiment, participants left the laboratory and returned another day for the next experiment. They were introduced to the experiment and trained with a different task. Base colors were presented in order from 1 to 9, but the order of modulation direction, frequency and starting amplitude was randomized. The procedure looked like this:

1. A 1-hour training session with an explanation of the experimental settings, the stimuli and the task. Similar to the first experiment, the participant did a few practice trials, and their task was checked by observing her/his input during these trials.

2. A 30-minutes experiment session where the participant had to adjust the amplitude $\Delta u'v'$ till he/she did not perceive chromatic flicker. For reliable results, it was important that the amplitude $\Delta u'v'$ was chosen at the boundary between the perceived

flicker and a non-perceived flicker. A 2 mins adaptation time was included before each base color. If the participant finished a base color within 30 minutes he/she was sent directly to the rest time.

3. A 30-minutes rest where the participant moved to an area with natural light.

4. Step 2 and 3 were repeated till half of the base colors were finished. An additional day was included to finish the rest of the base colors, and point 2 and 3 were repeated again till the experiment was finished.

5. Data was analyzed to check any inconsistency, and the participant was debriefed. The naïve participant received a compensation of 150€ (10€ per hour).

3.6.5   Time estimate

For this experiment, it was estimated that each trial was going to last around 30 secs. The time of each trial together with 2 mins adaptation time for each base color, yielded an experimentation time of around 252 mins + 2 mins × 9 base colors = 270 mins, where the time to finish each base color was estimated to be around 30 mins (see Table A.4 of Appendix A). We included a 30 mins rest after each base color, thus the time to complete the experiment was around 9 hours, split in two experimentation days of 4.5 hours to relief the eye strain that it might be caused by observing flicker for prolonged time. Combining the time of the first experiment and the second experiment, the overall time of the experiments of this study was estimated to be above 11 hours.

3.7   Data Analysis

The data obtained in the second experiment was used to build a model that describes the tCSFs. We were only interested in building a model, the parameters of which might vary from person to person, thus, we did not perform any statistical test, only the goodness of fit of the models and additional explorative analysis was provided. Therefore, we needed a lot of data from a few participants. The whole analysis was done using MATLAB.

For the purpose of this study we considered colors specified in chromatic coordinates $u'v'$ but also their transformation to the LMS color space. First, we had to know the $RGB_\%$ contributions that were sent to the system to generate the stimuli. The PWM values sent to each type of LED to generate a specific stimuli were divided by the maximum PWM value of 42000 to obtain the $RGB_\%$ contributions as shown in equation 3.8.

$$R_\% = \frac{PWM_R}{42000} \quad G_\% = \frac{PWM_G}{42000} \quad B_\% = \frac{PWM_B}{42000} \tag{3.8}$$

The full spectral power distribution of red $P_R(\lambda)$, green $P_G(\lambda)$ and blue $P_B(\lambda)$ LEDs

were measured and multiplied by the R, G and B % contributions to obtain the spectrum of the measured stimuli $SPD(\lambda)$ with MATLAB as equation 3.9.

$$\begin{aligned} SPD(\lambda) &= SPD_R(\lambda) + SPD_G(\lambda) + SPD_B(\lambda) \\ SPD_R(\lambda) &= R_\% \times P_R(\lambda) \\ SPD_G(\lambda) &= G_\% \times P_G(\lambda) \\ SPD_B(\lambda) &= B_\% \times P_B(\lambda) \end{aligned} \tag{3.9}$$

Then, the transformation to LMS was simply done by applying the human cone spectral sensitivities $\bar{l}_{10°}(\lambda)$, $\overline{m}_{10°}(\lambda)$ and $\overline{s}_{10°}(\lambda)$ for a $10°$ viewing angle derived from the Stiles & Burch $10°$ color-matching functions. This was done with the set of equations 2.6 shown in chapter 2. In addition, the normalized values of LMS were considered as equations 2.7.

Before analyzing the data, the MATLAB calculations and corrections of the spectral power distribution of each color stimulus were checked to see if they corresponded to the measured stimuli. Surprisingly, the conversions were very consistent. A comparison with the MATLAB calculations of the 9 base colors measured with the spectrometer through the small window are shown in Figure 3.18.
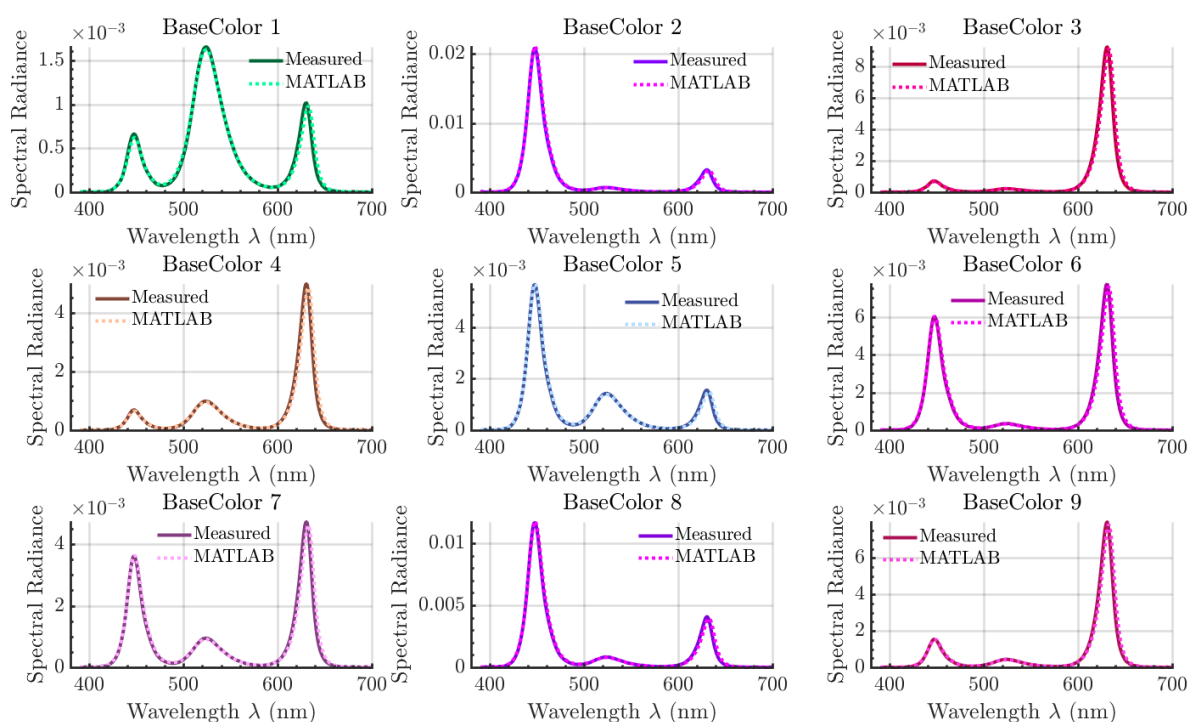
Figure 3.18: Comparison between the measured spectral power distribution and the MATLAB calculation.

The transformation from thresholds $\Delta u'v'$ to ΔLMS was done by first calculating the extreme colors with coordinates $u'_1v'_1$ and $u'_2v'_2$ with the threshold $\Delta u'v'$, base color coordinates $u'v'$, the direction θ as shown in equations 3.10

$$u'_1 = u' + \frac{\Delta u'v'}{2}cos\theta$$

$$v'_1 = v' + \frac{\Delta u'v'}{2}sin\theta$$

$$u'_2 = u' - \frac{\Delta u'v'}{2}cos\theta \qquad (3.10)$$

$$v'_2 = v' - \frac{\Delta u'v'}{2}sin\theta$$

The luminance L_1 and L_2 of the two extreme color points were calculated with a simple substitution of equations 3.5 and 3.6 and the luminance ratio R_L at the threshold.

$$L_1 = \frac{L_S}{1 + R_L}$$

$$L_2 = R_L L_1 \qquad (3.11)$$

Then, the extreme colors were individually converted to LMS and the absolute difference was calculated $\Delta LMS = |LMS_2 - LMS_1|$. In addition, Δlms was calculated by normalizing the individual extreme colors in LMS color space to obtain lms_1 and lms_2.

The modeling of the tCSFs was done by first transforming the thresholds to the inverse of the contrast C to obtain the sensitivity S. Where contrast was defined as the logarithm of the threshold given in $\Delta u'v'$, ΔLMS and Δlms. A model was chosen based on the shape of the tCSFs expressed as the three sensitivities shown in equation 3.12.

$$S_{UV} = \frac{1}{C_{UV}} = \frac{1}{log\Delta u'v'}$$

$$S_{LMS} = \frac{1}{C_{LMS}} = \frac{1}{log\Delta LMS} \qquad (3.12)$$

$$S_{lms} = \frac{1}{C_{lms}} = \frac{1}{log\Delta lms}$$

Chapter IV

Results

"The purest and most thoughtful minds are those which love color the most."

– John Ruskin

4.1   Experiment 1 – Luminance ratio

For this experiment, the method of heterochromatic flicker photometry (HFP) was used to measure for each participant (MIJ, ANN & KON) the luminance ratios that minimize luminance flicker for 9 base colors and 4 directions of the chromatic modulation. The frequency was fixed at 25Hz and the modulation amplitude $\Delta u'v'$ at 0.05. The effort was made to prepare isoluminant stimuli for experiment 2.

The participant responses were thoroughly checked to see if there were inconsistencies. In general, participants were very consistent. For example, the responses of participant ANN for all directions of BC_3 are illustrated in Figure 4.1. The combination of fine steps and rough steps shows clearly that the two strategies explained in chapter 3 were followed carefully until a decision was made. The 4 curves show the responses of 4 trials (2 repetitions $\times$ 2 starting luminance ratio). The red curves are the trials when the starting luminance ratio was high, and the blue curves when it was low. The dotted line is the mean of all the luminance ratios where the participant pressed enter.

In Figure 4.2 are shown the ratios that minimized luminance flicker for each par-
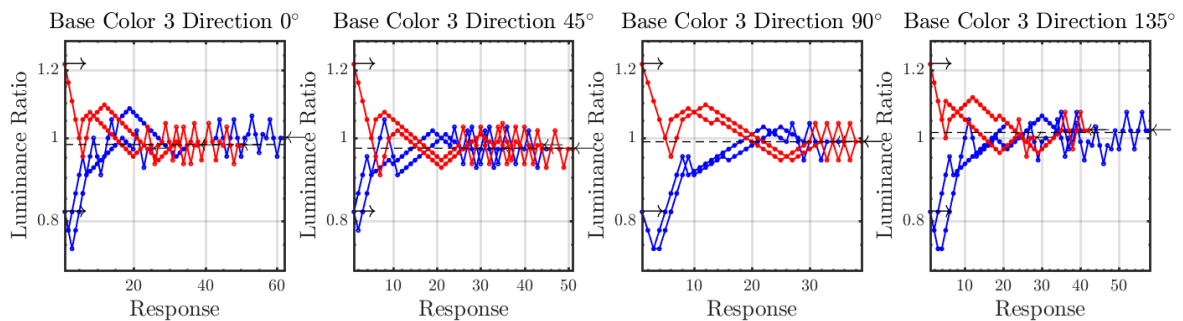
Figure 4.1: The rough steps, fine steps and enter responses for BC_3 trials of participant ANN. The red curves are the trials when the starting luminance ratio was high and the blue curves when it was low.

ticipant, base color and modulation direction. For some directions and base colors the luminance ratio was close to 1 but for others they differed from 1. We assumed that at these luminance ratios the apparent brightness of the two extreme colors were equal.
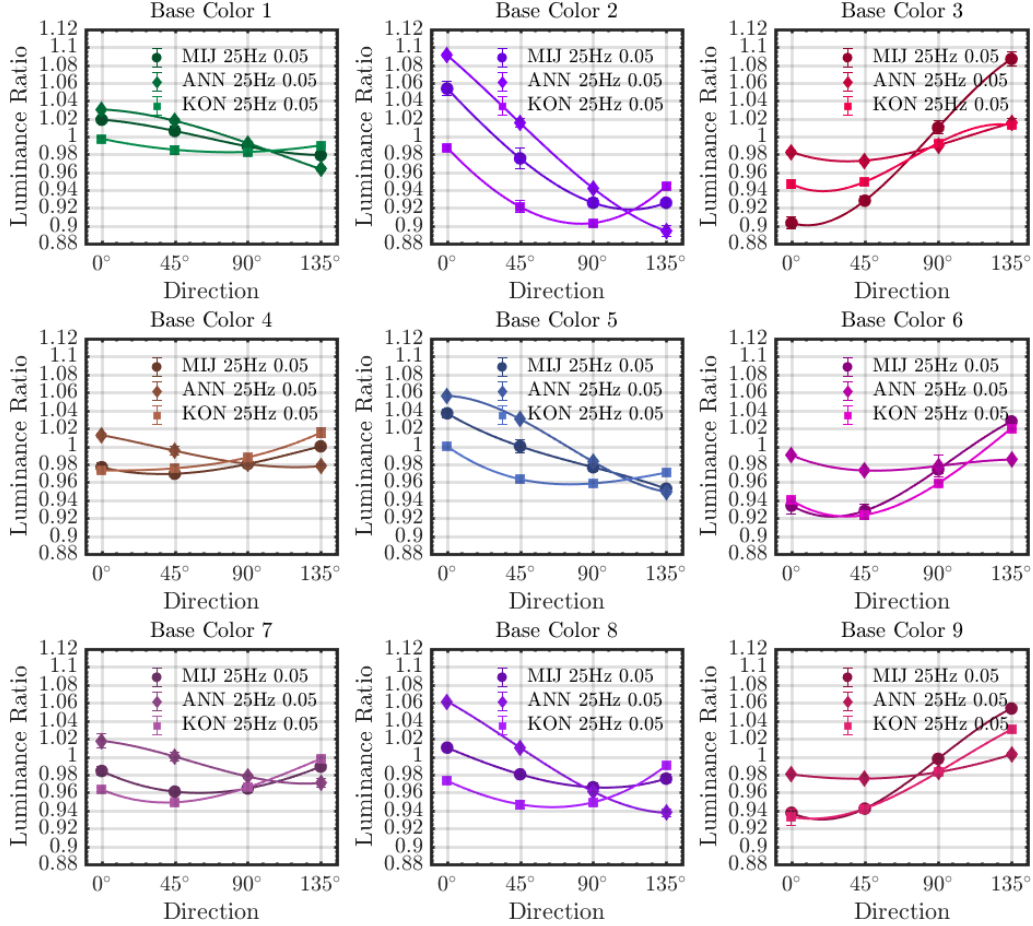
Figure 4.2: Luminance ratio that minimizes luminance flicker for each participant, base color and direction averaged over the two repetitions.

For each base color and direction, the two extreme colors of the chromatic flicker stimulus at the corresponding luminance ratio were converted to LMS color space. Then, the difference of the cones excitation between extreme colors were obtained as ΔL, ΔM and ΔS. And, the normalized cones excitation were calculated as Δl, Δm and Δs. This was done in order to understand better what is happening with the excitation of the L-, M- and S- cones at isoluminance. The participant's luminance ratio together with the absolute ΔL, ΔM and ΔS and the normalized excitation Δl, Δm and Δs as red, green and blue bars are shown in Figure 4.3 , 4.4 and 4.5. In most graphs, we see that the difference in S-cones response between the two colors (ΔS) is larger than for the L- and M-cones. When observing the absolute difference of the excitation of cones, we see that BC_2 and BC_8 present the larger excitations of all base colors, especially for the S-cones (ΔS).
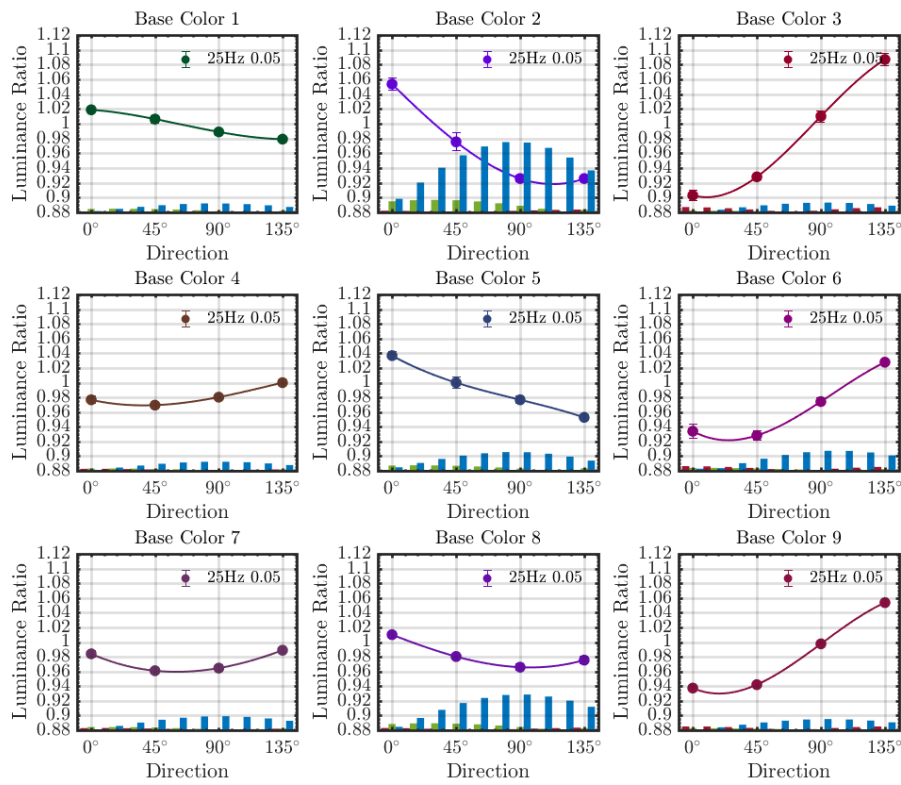
(a) Luminance ratios & the absolute difference of excitation of cones ΔL, ΔM and ΔS.
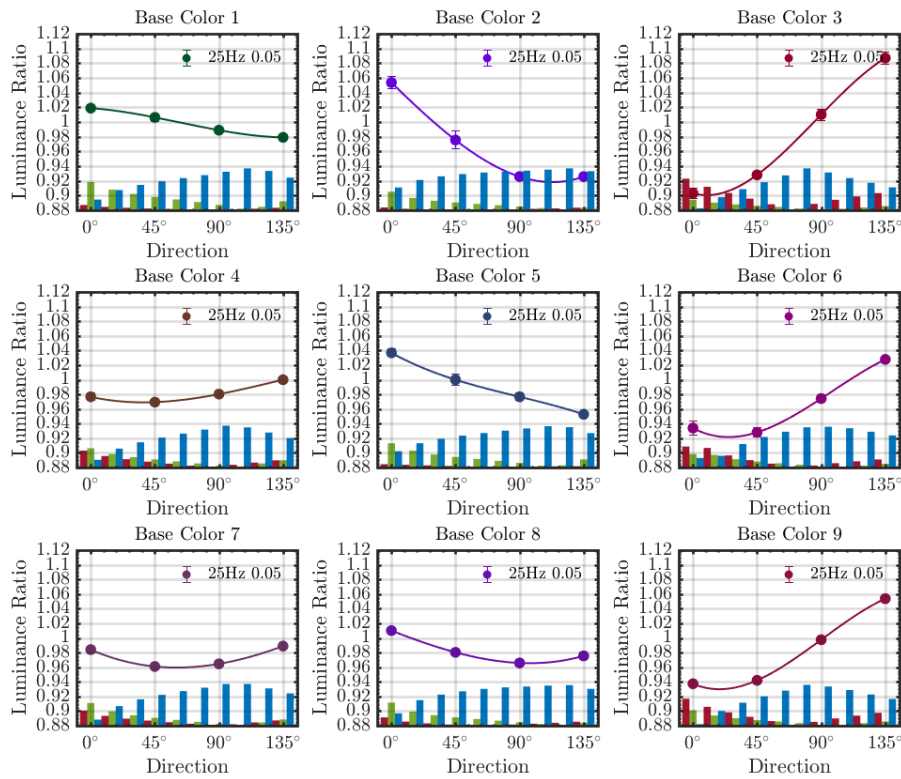
(b) Luminance ratios & normalized difference of excitation of cones Δl, Δm and Δs.

Figure 4.3: Experiment 1 Results - Participant **MIJ**
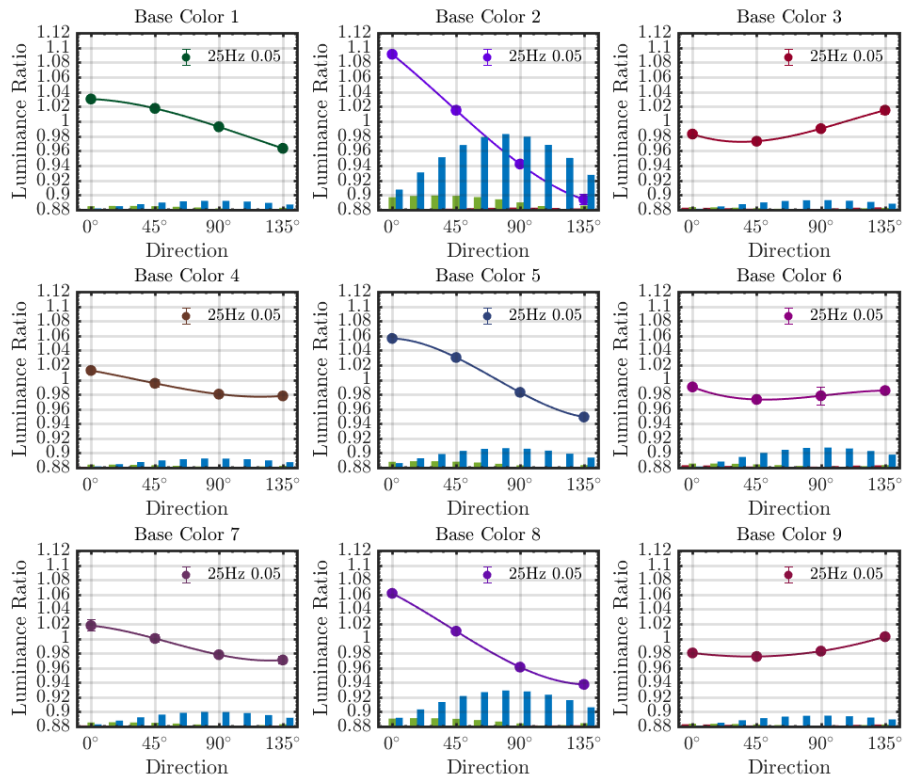
(a) Luminance ratios & the absolute difference of excitation of cones ΔL, ΔM and ΔS.
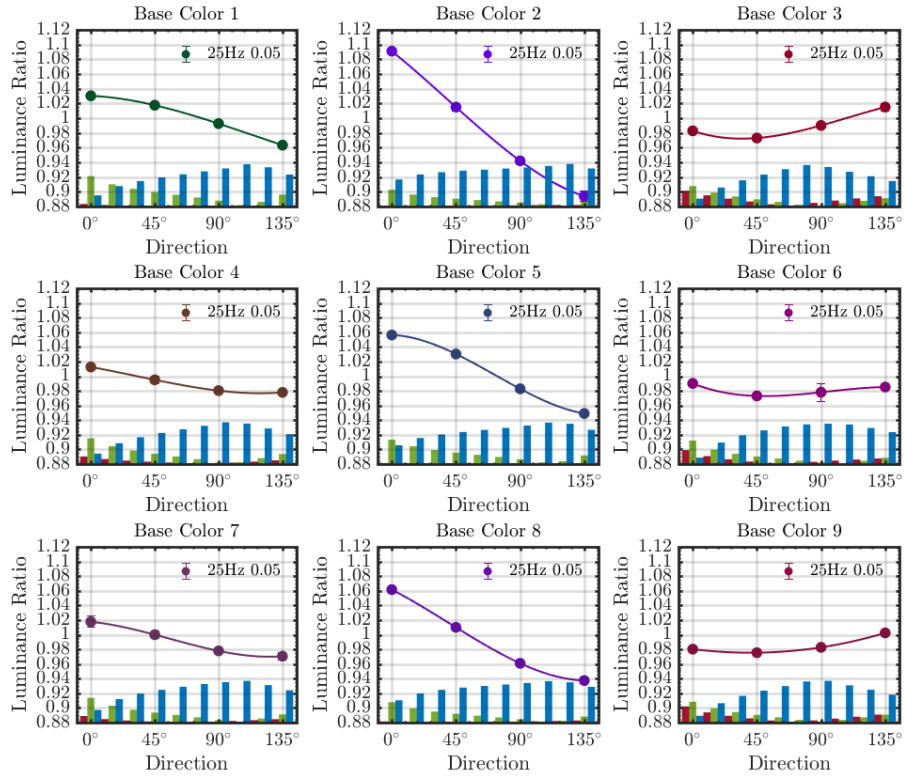
(b) Luminance ratios & normalized difference of excitation of cones Δl, Δm and Δs.

Figure 4.4: Experiment 1 Results - Participant **ANN**
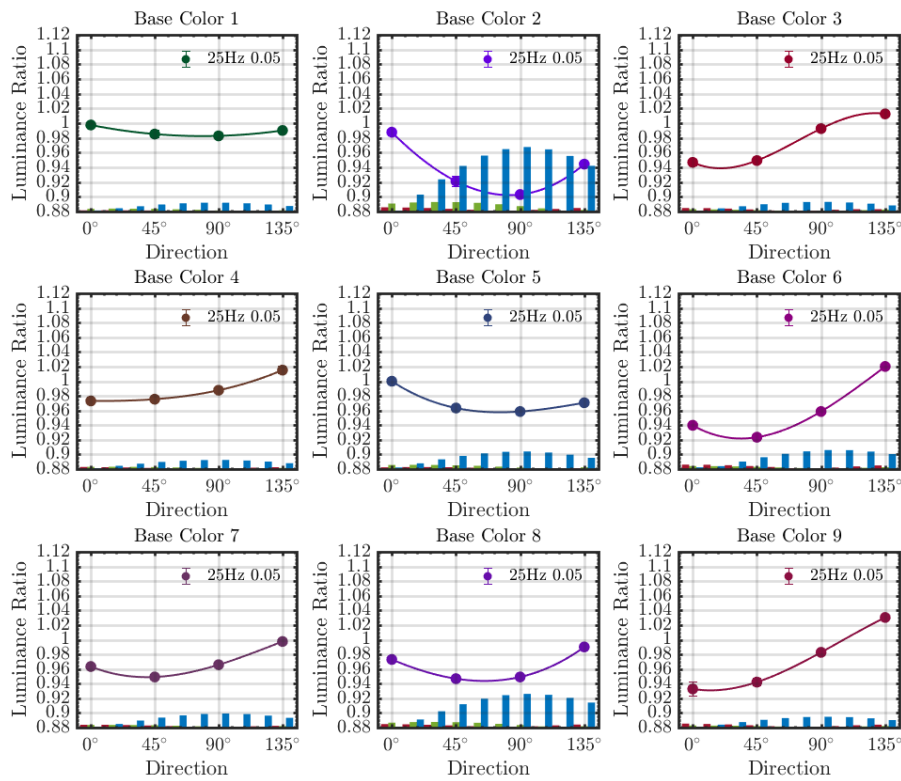
(a) Luminance ratios & the absolute difference of excitation of cones ΔL, ΔM and ΔS.
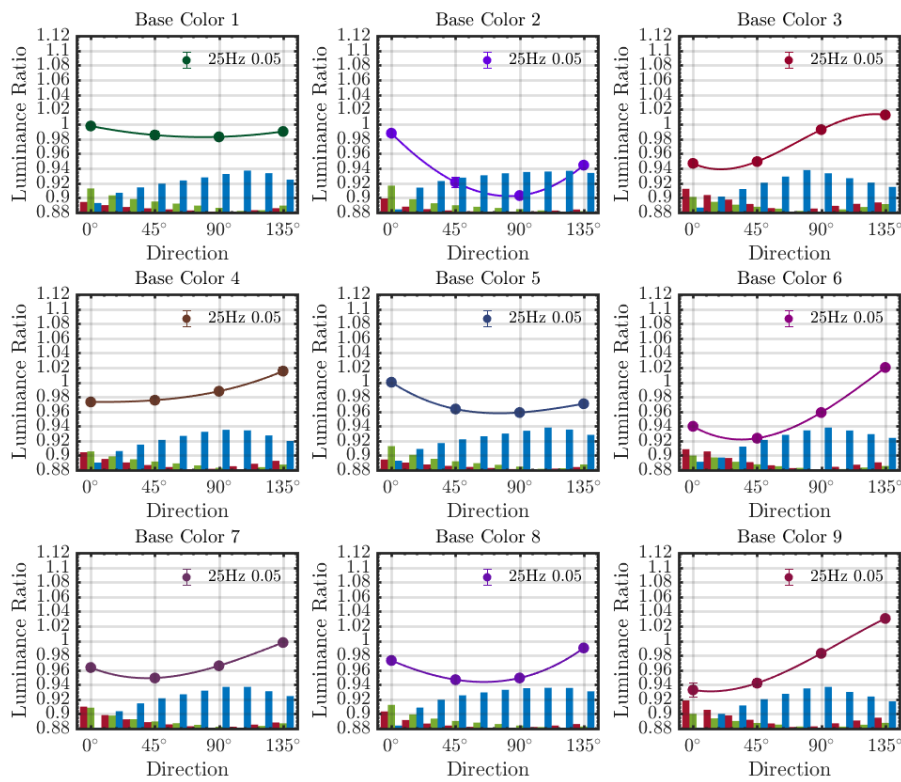
(b) Luminance ratios & normalized difference of excitation of cones Δl, Δm and Δs.

Figure 4.5: Experiment 1 Results - Participant **KON**

Additionally, the difference between ΔL, ΔM and ΔS of the measured luminance ratio and the ΔL_{ref}, ΔM_{ref} and ΔS_{ref} of the reference luminance ratio of 1 is shown in Figures 4.6, 4.7 and 4.8. From these graphs, we can observe that the luminance ratios are mostly adjusting the S-cones responses (ΔL) especially for the blue base colors.
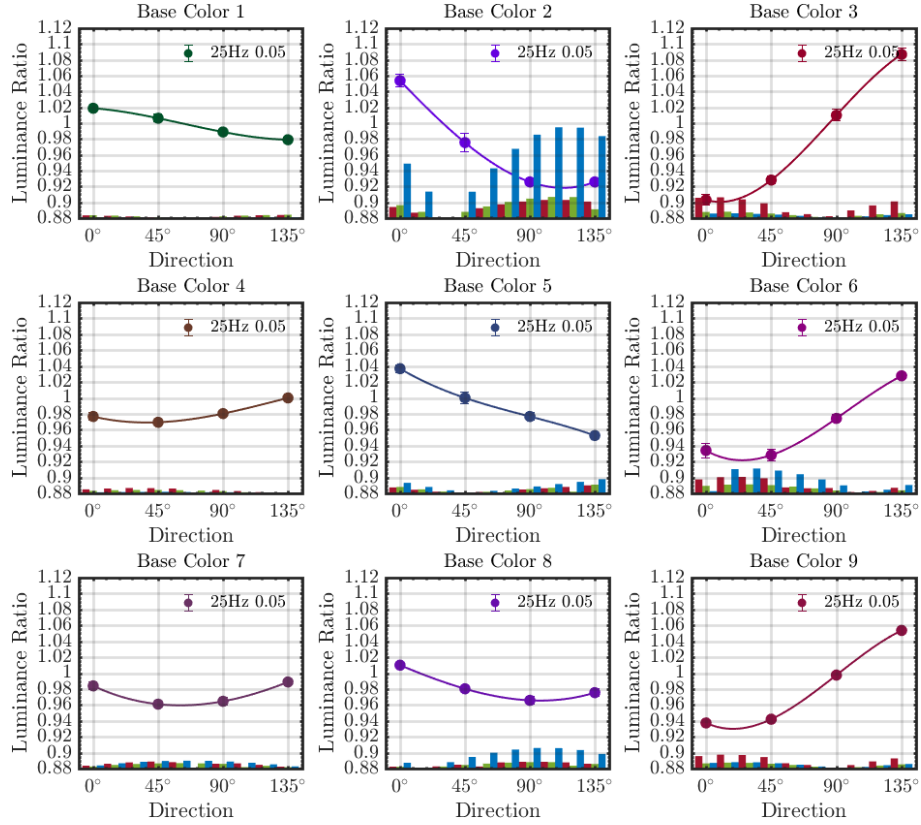
Figure 4.6: Luminance ratios & the difference between ΔL, ΔM and ΔS of the measured luminance ratio and the ΔL_{ref}, ΔM_{ref} and ΔS_{ref} of the luminance ratio reference of 1 of **MIJ**
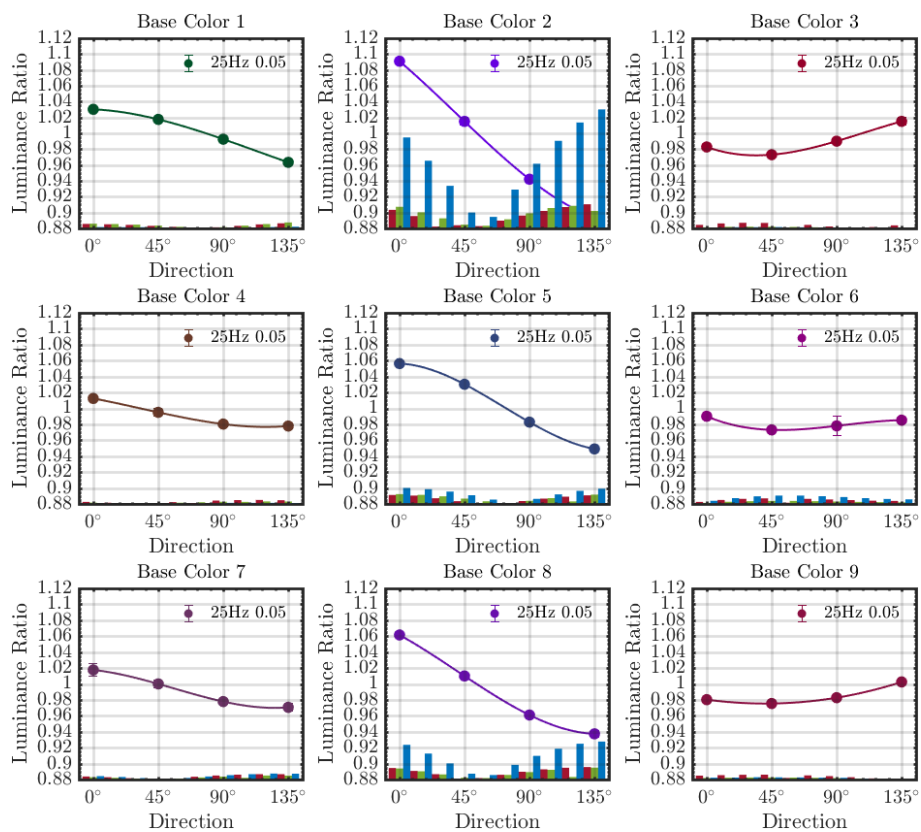
Figure 4.7: Luminance ratios & the difference between ΔL, ΔM and ΔS of the measured luminance ratio and the ΔL_{ref}, ΔM_{ref} and ΔS_{ref} of the luminance ratio reference of 1 of **ANN**
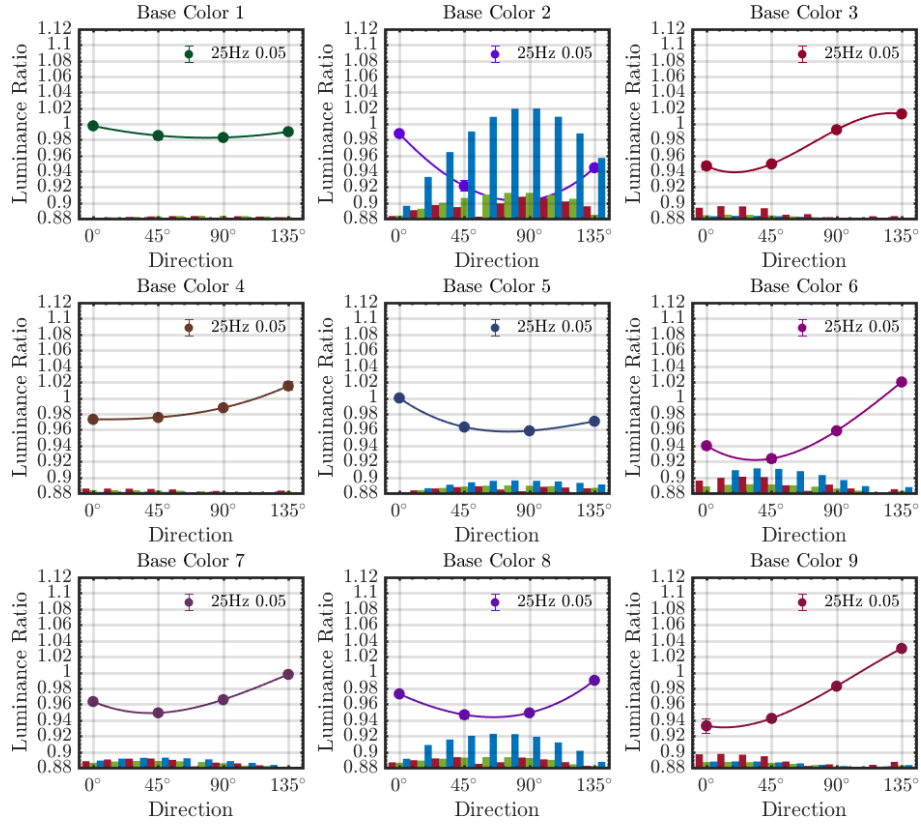
Figure 4.8: Luminance ratios & the difference between ΔL, ΔM and ΔS of the measured luminance ratio and the ΔL_{ref}, ΔM_{ref} and ΔS_{ref} of the luminance ratio reference of 1 of **KON**

A function $D(\lambda)$ was created as equation 4.1 to express the difference in spectra of all two extreme colors of the modulation. This function was defined as the weighted sum of the difference of spectral power distribution $\Delta SPD = |SPD_2 - SPD_1|$ for each base color and modulation direction θ, where SPD_1 and SPD_2 correspond to the spectral power distribution of the two extreme colors of the modulation. The $SPD(\lambda)$ of each color was calculated with equation 3.8 of chapter 3.

$$D(\lambda) = \sum_{BC_n,\theta} |\log(R_L)| \times \Delta SPD_{BC_n,\theta} \tag{4.1}$$

The function $D(\lambda)$ for each participant is shown in Figures 4.9. If $V(\lambda)$ was correct, equal apparent brightness would be achieved with a luminance ratio R_L of 1, this would result in an empty function $D(\lambda)$, since all contributions are eliminated ($|\log(R_L)| = 0$). However, this was not the case for our experiments, we found that there are major contributions at short wavelengths of the difference spectrum, but also at long wavelengths when luminance ratio is different than 1. In addition, there are some individual differences between participants that the standard $V(\lambda)$ do not consider.

(a) Function $D(\lambda)$ of participant **MIJ**.

(b) Function $D(\lambda)$ of participant **ANN**.

(c) Function $D(\lambda)$ of participant **KON**.
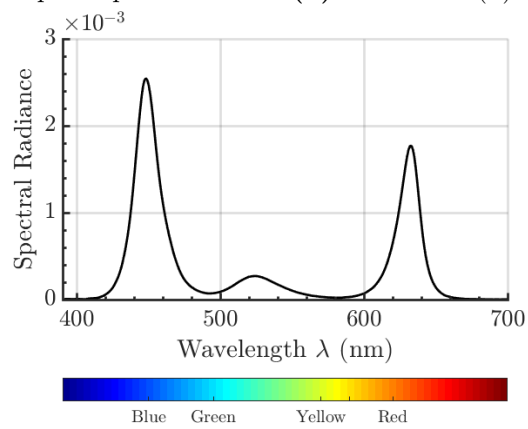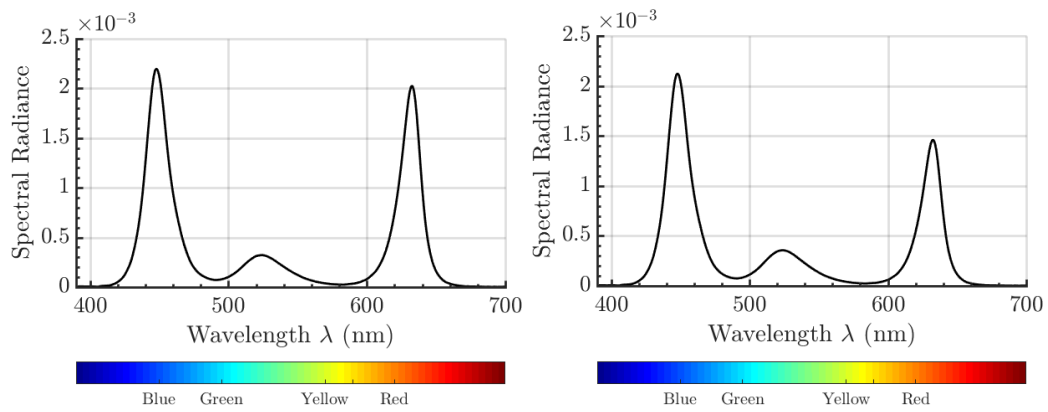
Figure 4.9: Function $D(\lambda)$

4.2 Experiment 2 – Modeling of the Temporal Contrast Sensitivity Function

In this experiment, participants had to adjust the chromatic amplitude $\Delta u'v'$ to find their visibility threshold of chromatic flicker. As explained before, 9 base colors and 4 modulation directions at 7 different frequencies were used. In total, 504 trials were carried out by the participants, and 36 tCSFs were obtained (9 base colors $\times$ 4 directions).

The results were regularly checked by observing the responses of the participants during the experiment. In Figure 4.10, we can see an example of the rough steps, fine steps and enter responses for each trial of participant ANN.
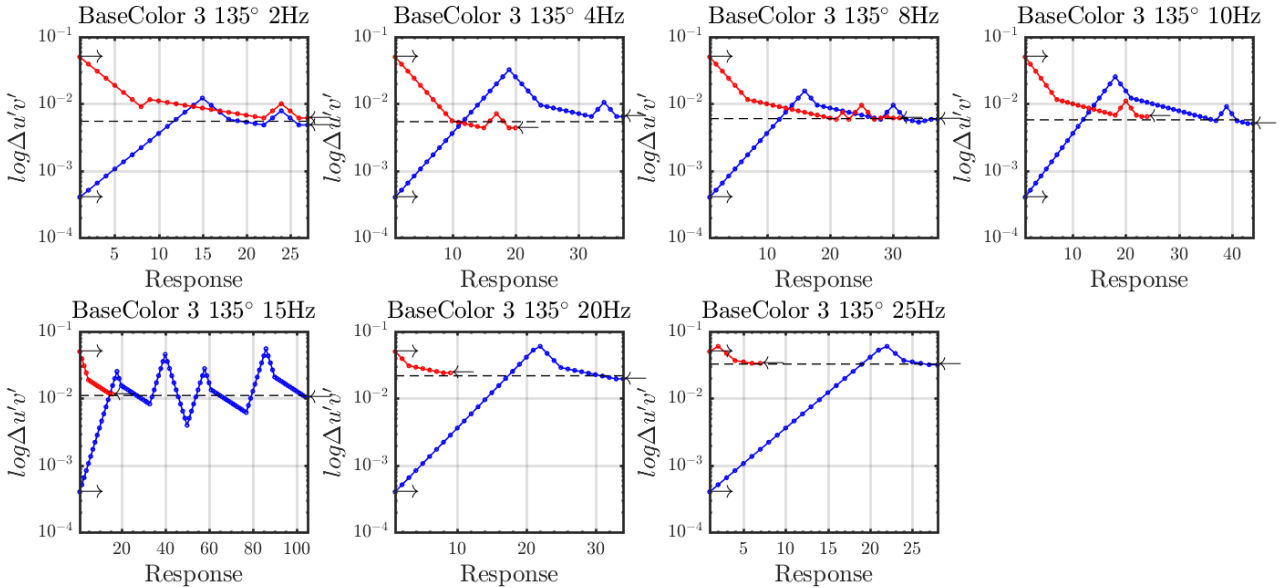
Figure 4.10: The rough steps, fine steps and enter responses for BC_3 trials of participant **ANN** of the second experiment. The red curves are the trials when the starting amplitude was high and the blue curves when it was low. The dotted line is the average threshold.

The red curve is the trial when the starting amplitude $\Delta u'v'$ was high, and the blue curve when it was low. The results are consistent when both trials fall close to the horizontal line at the moment of pressing enter. Afterwards, both enter responses are averaged to obtain the visibility threshold $\Delta u'v'$ (dotted line) for the corresponding modulation frequency, base color and direction. As we can see in the example, participant ANN was very consistent for these stimuli. During the task, these plots were constantly checked to give feedback to the participants and to improve the results for next sessions. In general, participants followed the task very carefully, so they were very consistent with their thresholds.

First, the measured threshold data was plotted to hypothesize the model to fit. An

example, of the raw data is shown in Figure 4.11 for participant MIJ. The x-axis corresponds to the frequencies of the modulation and the y-axis corresponds to the visibility thresholds measured as $\Delta u'v'$. For this example, the average thresholds are shown as a green curve. The shape of the curves gives a hint of a possible exponential model to be used as the model. The rest of the raw thresholds for all base colors and participants are shown in Appendix C.
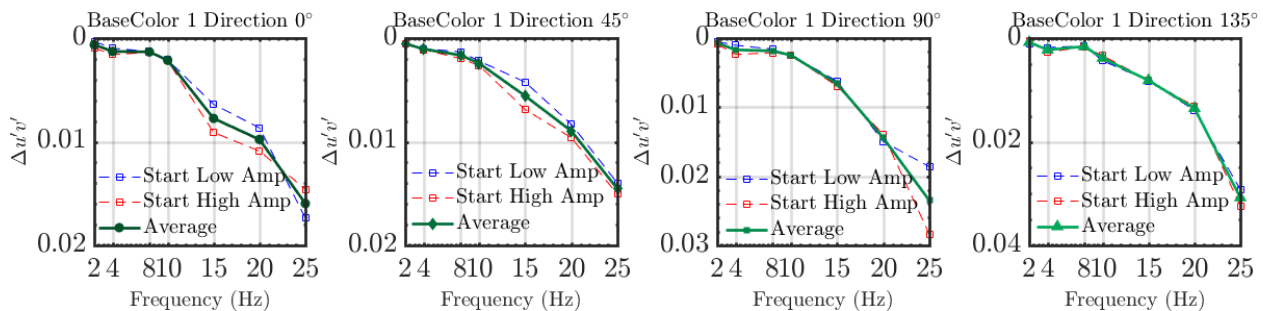
Figure 4.11: The raw thresholds $\Delta u'v'$ of BC_1 for each direction of participant **MIJ**. The red curves are the thresholds when the starting amplitude was high and the blue thresholds when it was low. The average thresholds $\Delta u'v'$ are shown as a colored line.

The modeling part was done in three color spaces: the $u'v'$ color space, the LMS cone space and the normalized lms cone space. The respective transformations were shown in chapter 2. To obtain the tCSFs, the thresholds were transformed to a logarithmic scale, and then the inverse was obtained to get the sensitivities as shown in equations 4.2 of chapter 3. Following the example above, the thresholds of BC_1 expressed as tCSFs in three different color spaces are shown in Figures 4.12. The tCSFs were plotted for every participant, base color and modulation direction and it was hypothesized that an exponential model (a linear fit on log scale) may describe the results rather well. The model used is shown in equation 4.2. S is the fitted sensitivity, the coefficient β_1 is the slope of the fit, f is the frequency and β_0 is the intercept.

$$S = \beta_1 f + \beta_0 \tag{4.2}$$

(a) tCSFs $1/log\Delta u'v'$

(b) tCSFs $1/log\Delta LMS$

(c) tCSFs $1/log\Delta lms$
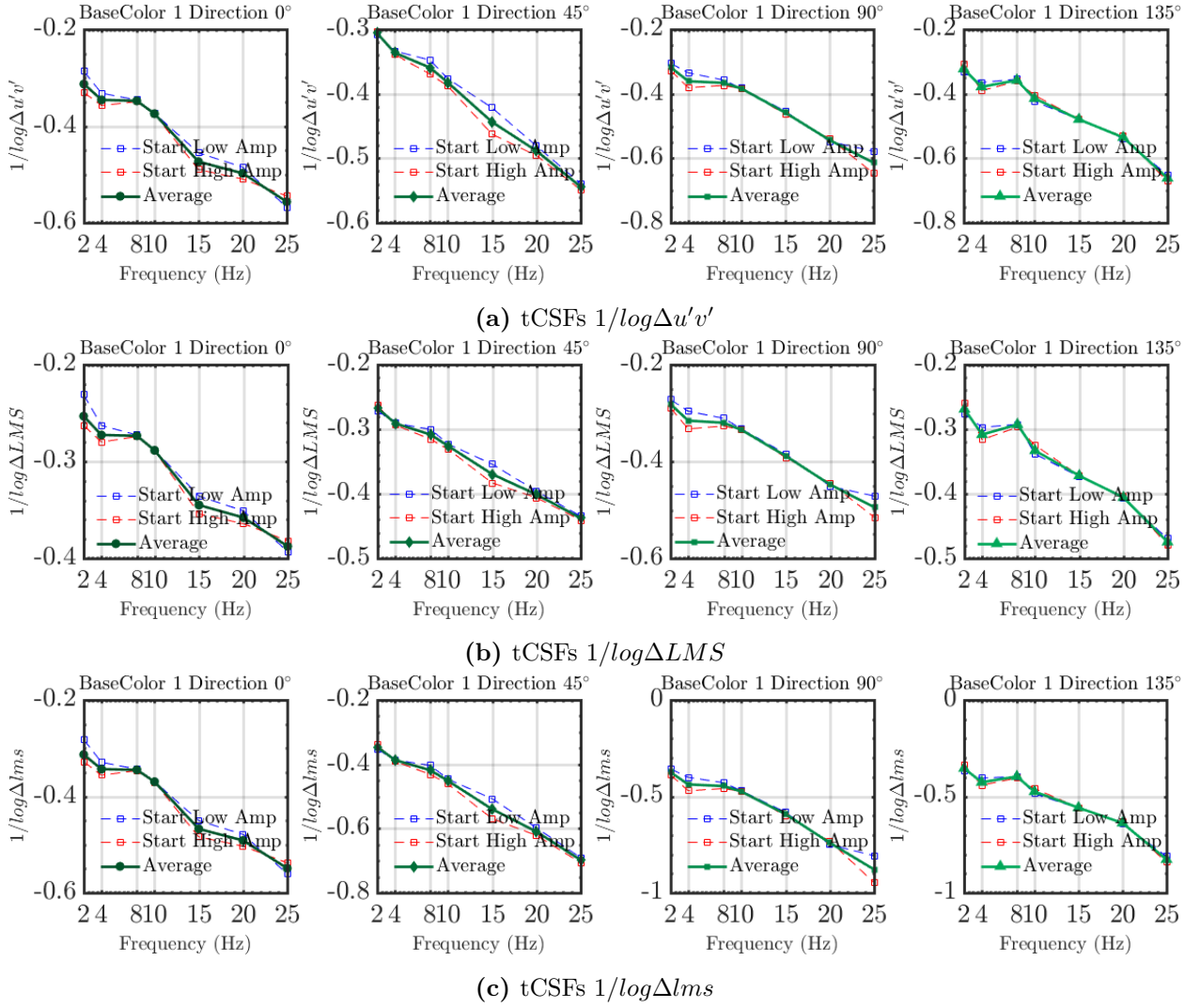
Figure 4.12: The tCSFs of BC_1 for participant **MIJ**

As an example, the fits for all the tCSFs in cone space LMS of participant MIJ are shown in Figure 4.13. The goodness of fit R^2 was obtained for each participant, base color and modulation direction. Then, the average R^2 for each base color and the overall average R^2 for all base colors was calculated as shown in Table 4.1. We obtained an average goodness of fit R^2 close to 96%, 87% and 94% for participant MIJ, ANN and KON, respectively. Also, there was not a large difference between the R^2 of the tCSFs in the three color spaces $\Delta u'v'$, ΔLMS and Δlms. All the graphs of the fits for each participant, base color, direction and color space are shown in Appendix D.
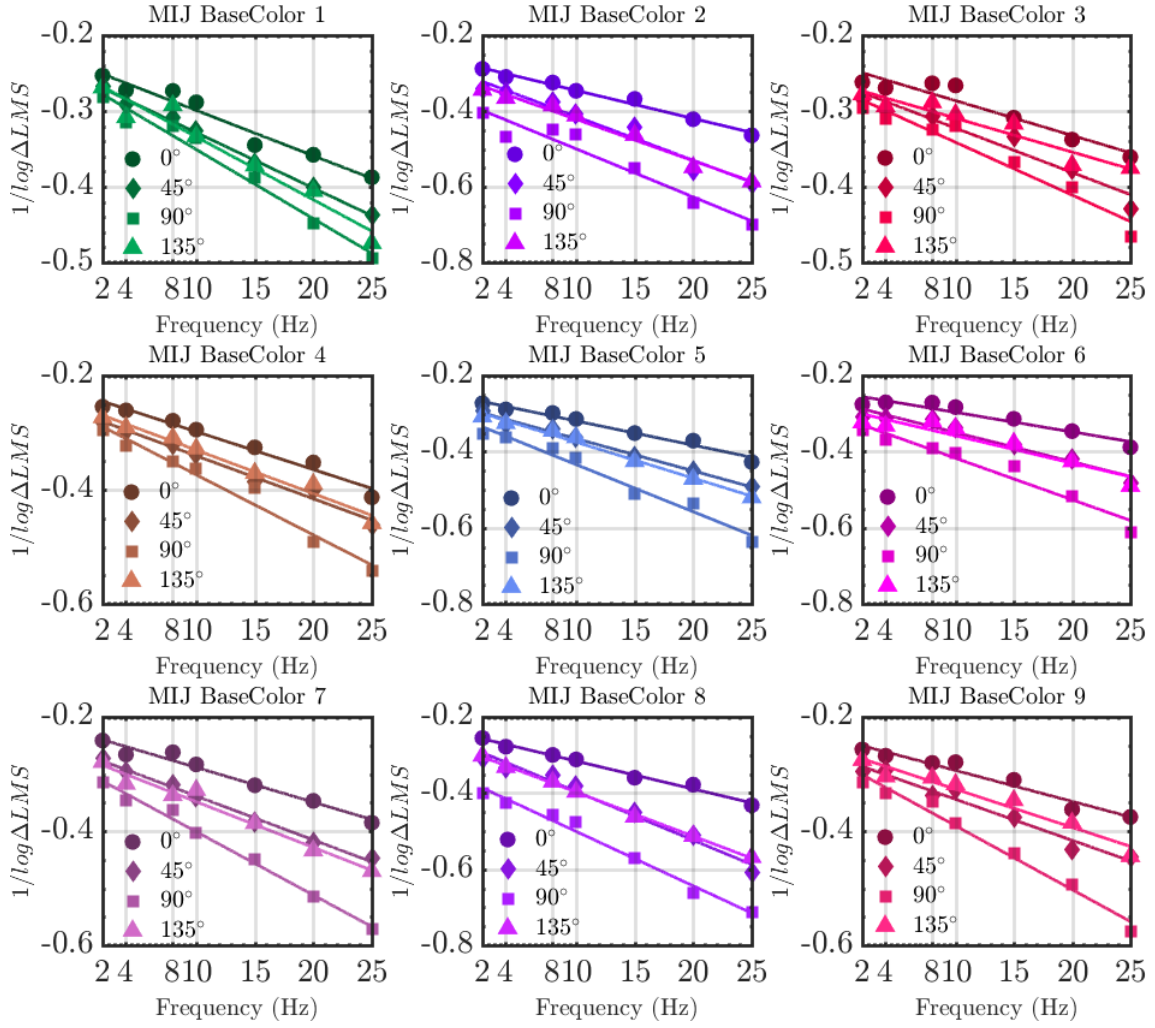
Figure 4.13: tCSFs ($1/\log \Delta LMS$) & linear fits on a logarithmic scale for participant **MIJ.**

ID	tCSFs	BC_1 R^2	BC_2 R^2	BC_3 R^2	BC_4 R^2	BC_5 R^2	BC_6 R^2	BC_7 R^2	BC_8 R^2	BC_9 R^2	**Avg** R^2
MIJ	$1/\log \Delta u'v'$	0.96658	0.96826	0.92132	0.96351	0.97811	0.92054	0.98095	0.98616	0.95471	0.96001
	$1/\log \Delta LMS$	0.96926	0.96656	0.92313	0.97542	0.98098	0.92390	0.98181	0.98633	0.96162	0.96322
	$1/\log \Delta lms$	0.96091	0.96849	0.90588	0.95240	0.97679	0.91576	0.97938	0.98603	0.94705	0.95474
ANN	$1/\log \Delta u'v'$	0.91754	0.88473	0.84246	0.86039	0.95942	0.79873	0.89272	0.89514	0.79537	0.87183
	$1/\log \Delta LMS$	0.91977	0.88191	0.84265	0.85259	0.95923	0.79723	0.88671	0.89674	0.79718	0.87044
	$1/\log \Delta lms$	0.91460	0.88524	0.83554	0.86577	0.96024	0.80040	0.89253	0.89558	0.78733	0.87080
KON	$1/\log \Delta u'v'$	0.96590	0.93642	0.88967	0.95855	0.96120	0.95797	0.95984	0.92764	0.91554	0.94142
	$1/\log \Delta LMS$	0.97060	0.92345	0.89727	0.96812	0.96518	0.95988	0.96562	0.92745	0.92288	0.94449
	$1/\log \Delta lms$	0.95909	0.93482	0.87279	0.94160	0.95860	0.95493	0.95541	0.92583	0.90116	0.93380

Table 4.1: The average goodness of fit R^2 of a exponential model (linear fit on log scale) for each participants, base color and tCSFs transformed to different color spaces.

4.2.1 Additional Analysis

The tCSFs in LMS color space were chosen for further analysis. Plots with the 95% confidence interval of the slopes β_1 and intercepts β_0 of each fit in function of base color and direction are shown per participant in Figure 4.14 and 4.15.
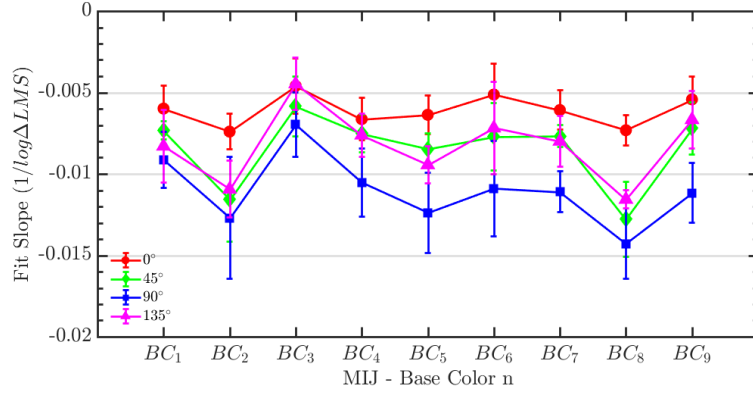
(a) Slopes (β_1) of the fits ($1/\log \Delta LMS$) of participant **MIJ**.
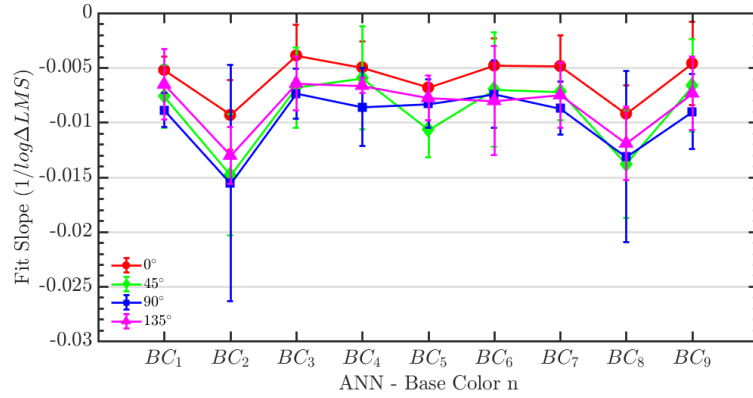
(b) Slopes (β_1) of the fits ($1/\log \Delta LMS$) of participant **ANN**.
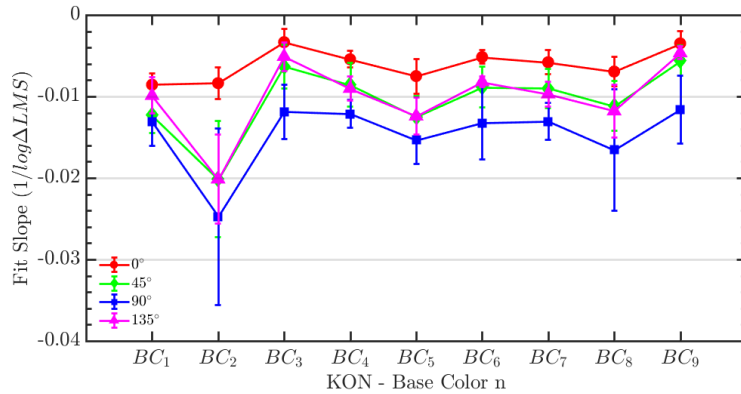
(c) Slopes (β_1) of the fits ($1/\log \Delta LMS$) of participant **KON**.

Figure 4.14: Slopes (β_1) of the fits ($1/\log \Delta LMS$) with the 95% confidence interval in function of base color BC_n and direction.
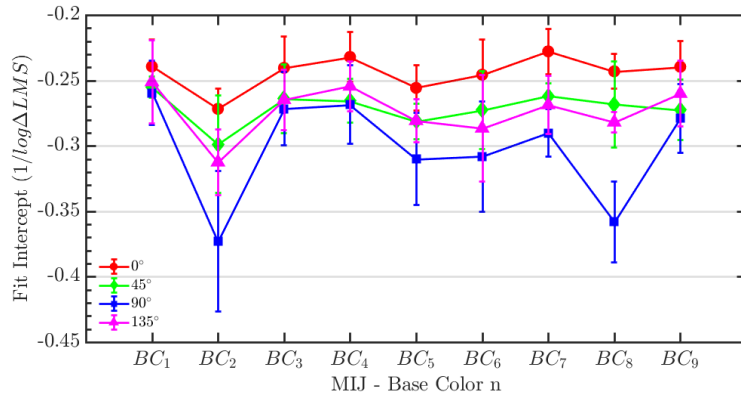
(a) Intercepts of the fits $(1/\log \Delta LMS)$ of participant **MIJ**.
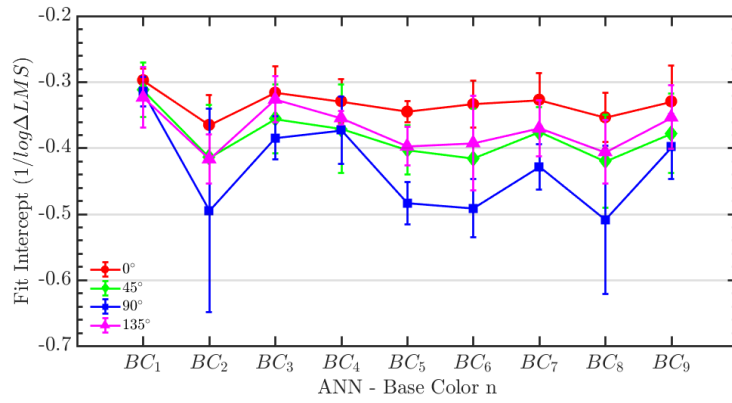
(b) Intercepts (β_0) of the fits $(1/\log \Delta LMS)$ of participant **ANN**.
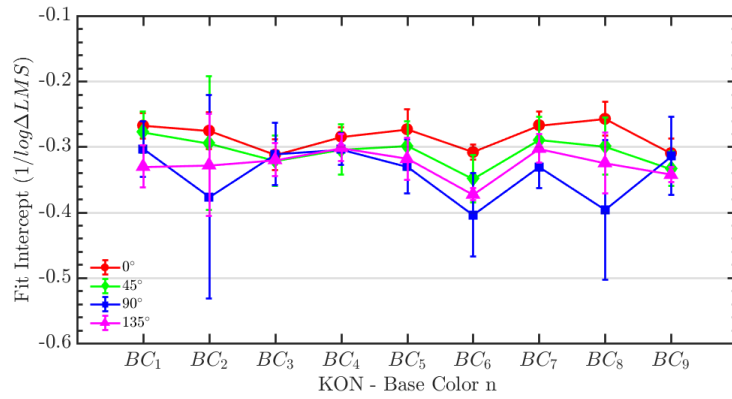
(c) Intercepts (β_0) of the fits $(1/\log \Delta LMS)$ of participant **KON**.

Figure 4.15: Intercepts (β_0) of the fits $(1/\log \Delta LMS)$ with the 95% confidence interval in function of base color and direction.

For most of the base colors the slopes and intercepts at direction $0°$ are above the other curves, at direction $90°$ below and at $45°$ and $135°$ the curves are approximate. However, when direction is $90°$, we can see a large confidence interval at BC_2 and BC_8. It was also expected but interesting to notice that similar colors like BC_2 and BC_8 or BC_3, BC_6 and BC_9 have slopes and intercepts that fall close to the same line. It was reported that

participants had trouble to do the experiments when stimuli was BC_2. In consequence, a similar but less saturated color BC_8 was included. Also, BC_9 was proposed as a less saturated version of BC_3. Even if these colors were separated in $u'v'$ coordinates, the graphs show approximate slopes and intercepts. In addition, some participants mentioned that BC_2 was brighter than the others. We know that this base color have higher components at short wavelengths and that the spectrometer by default measures photometric information with a $V(\lambda)$ that might not represent well short wavelengths. Thus, it might be that the luminance levels of this base color were higher than the ones measured with the device.

To further understand the slopes and intercepts of the fits, we performed an additional analysis. In our study, we had 3 participants, each with 36 slopes and intercepts of the tCSFs fits (thresholds expressed as ΔLMS) obtained from 9 levels (base color) $\times$ 4 levels (modulation direction) of measurements. Thus, a two-way ANOVA with two repeated measures was performed. Across participants, we found for the slopes that the main effects of base color ($F(8,48) = 9.38$, $p < 0.001$) and modulation direction ($F(3,48) = 14.08$, $p = 0.004$) were statistically significant. It was also found that the interaction effects of base color and direction were significant ($F(24,48) = 2.17$, $p = 0.01$). In addition, the same was found for the intercepts, the effect of base color ($F(8,48) = 4.28$, $p = 0.006$), direction ($F(3,48) = 18.34$, $p = 0.002$) and the interaction effects were significant ($F(24,48) = 9.84$, $p < 0.0001$). Participant KON obtained the lowest mean values of slopes, followed by MIJ and ANN with the highest mean values. For the intercepts, MIJ obtained the highest mean values, followed by KON and ANN with the lowest mean values. Moreover, a Tukey HSD pairwise comparison was done to compare base colors and directions. It was found that the slopes and intercepts for direction $45°$ and $135°$ were not significantly different ($p > 0.05$), and that direction $0°$ and $90°$ have the larger mean differences ($p < 0.05$). It was also obtained that BC_2 and BC_8 have the lowest values of slopes, and BC_3 and BC_9 the highest. The lowest intercepts were obtained for BC_2, BC_6 and BC_8 and the highest was BC_1. Furthermore, we decided to repeat the analysis without BC_2, BC_3 and BC_8. In this case, for the slopes there was a statistically significant effect of direction ($F(3, 71) = 17.31$, $p < 0.001$), and the base color and interaction effect were not significant ($p > 0.05$). However, the effects for the intercepts were still significant for base color ($F(5, 71) = 4.44$, $p = 0.02$), direction ($F(3, 71) = 4.79$, $p < 0.001$) and interaction effects ($F(15, 71) = 4.79$, $p < 0.001$). In all the analysis, the effect of participant was statistically significant ($p < 0.05$).

To illustrate better the effects of base color, direction and frequency, the color points of their respective thresholds were plotted in the $u'v'$ color space and the data was connected with dotted lines for each direction of corresponding frequency. The data was fitted by using the conic representation of an ellipse as shown in equation 4.3 and the least squares method. For more information of the MATLAB function used see Appendix E.

$$Ellipse = ax^2 + bxy + cy^2 + dx + ey + f = 0 \tag{4.3}$$

The ellipse fits of participant KON are shown in Figure 4.16 for high frequencies and Figure 4.17 for low frequencies. Surprisingly, the shape of the ellipses seem to be constant for most of the frequencies within each base colors, except at lower frequencies in some cases. The bigger ellipse is the average of all ellipses and it illustrates their overall shape and orientation. The ellipses correspond to the frequencies of the chromatic modulation from 25Hz(lighter color) to 2Hz(darker color). We can observe that the size of the ellipse is dependant of the frequency, this means that the visibility thresholds become smaller for decreasing frequency, but in some cases at lower frequencies the shapes seem to be different. In addition, participant MIJ obtained the smallest ellipses of all participants. This might be due to subjective bias or because his sensitivity to color changes is greater than the other participants.

In Figure 4.18, the ellipse fits for all base colors of participant KON are plotted to illustrate their overall shape and orientation within the $u'v'$ color space. The ellipses seem to have a smaller radius in their x-axis and a larger radius in their y-axis, thus, they are close to have a vertical orientation. In other words, the y-axis of the ellipses represents lower sensitivities and corresponds to larger thresholds $\Delta u'v'$, and the x-axis represents higher sensitivities and corresponds to lower thresholds. If we compare these results with the graphs of slopes and intercepts of Figures 4.14 and 4.15, at a direction of $0°$ the curve is above the other curves, in consequence, the sensitivities are higher and the thresholds are lower (remember inverse relationship $S = 1/\log \Delta u'v'$). Then, we have the direction of $45°$ and $135°$, their curves are almost identical, but the sensitivities are lower than at $0°$. At a direction of $90°$ we found the lowest sensitivities, except for ANN that she has slopes very close to $45°$ and $135°$. The ellipses for all participants are shown in Appendix E.

Figure 4.16: The ellipse fits (Zoomed out to high frequencies) of participant **KON** from 25Hz(lighter color) to 2Hz(darker color). The bigger ellipse is the average shape and orientation of all ellipses.
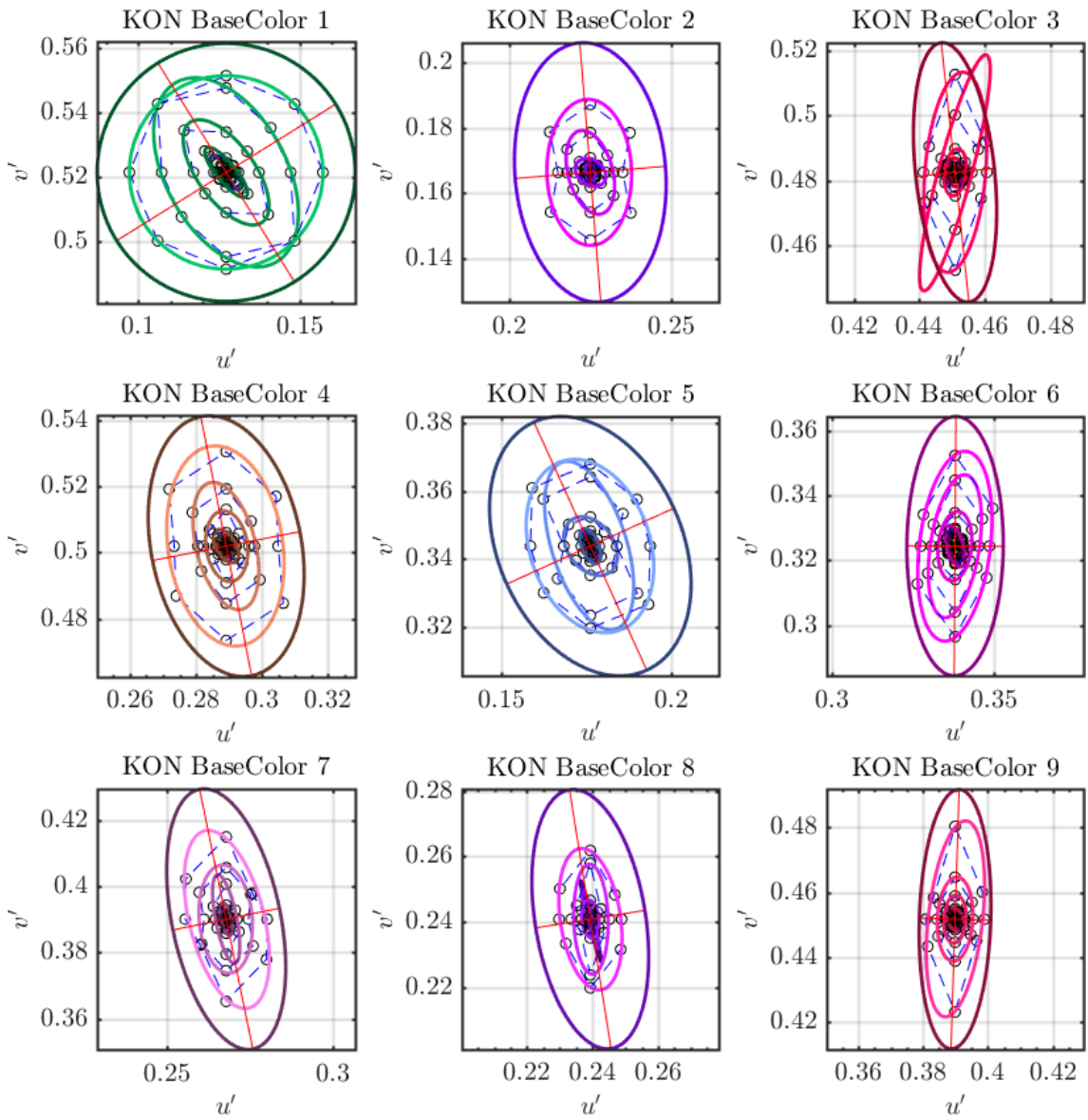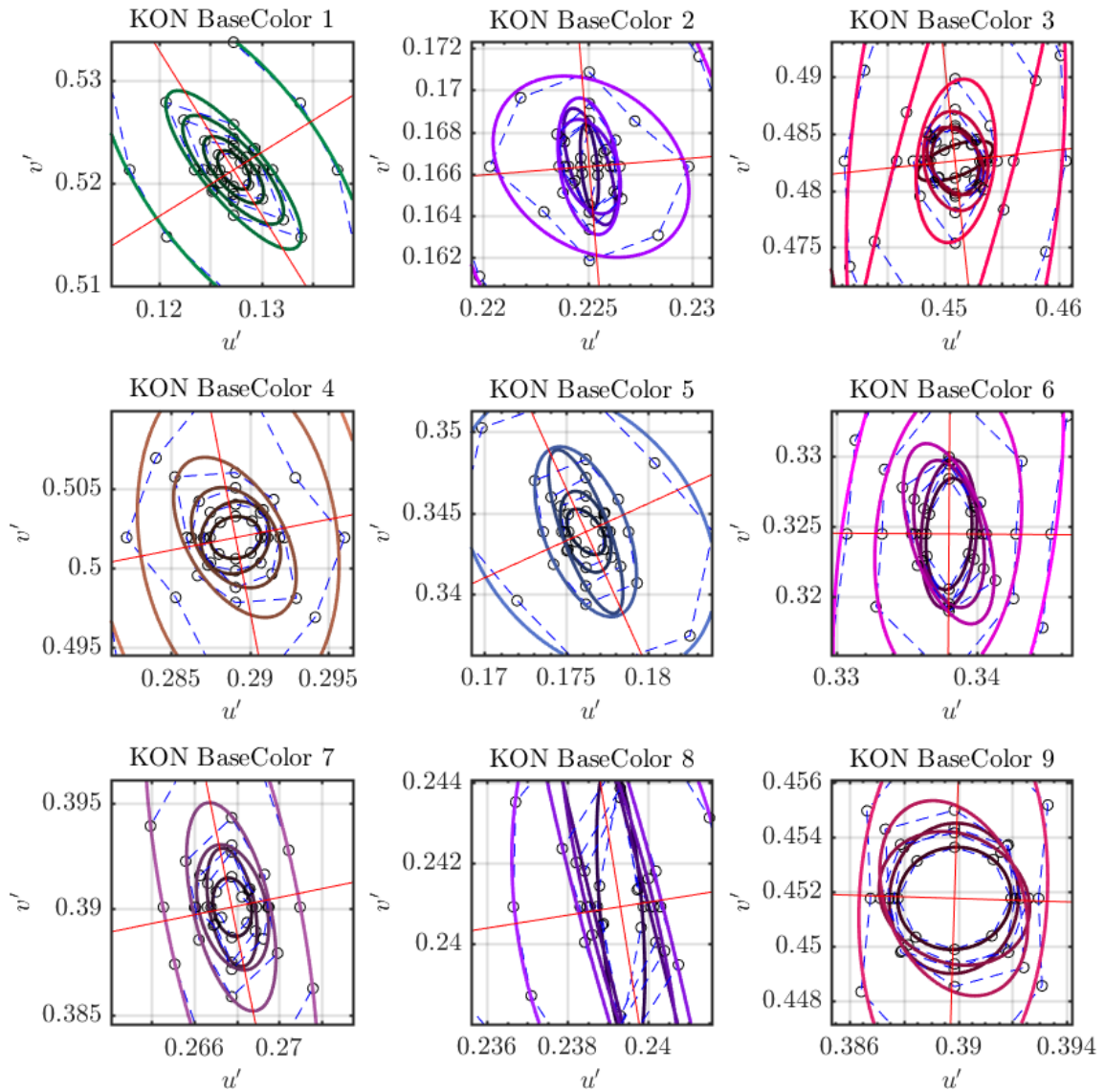
Figure 4.17: The ellipse fits (Zoomed in to low frequencies) of participant **KON** from 25Hz(lighter color) to 2Hz(darker color). The bigger ellipse is the average shape and orientation of all ellipses.
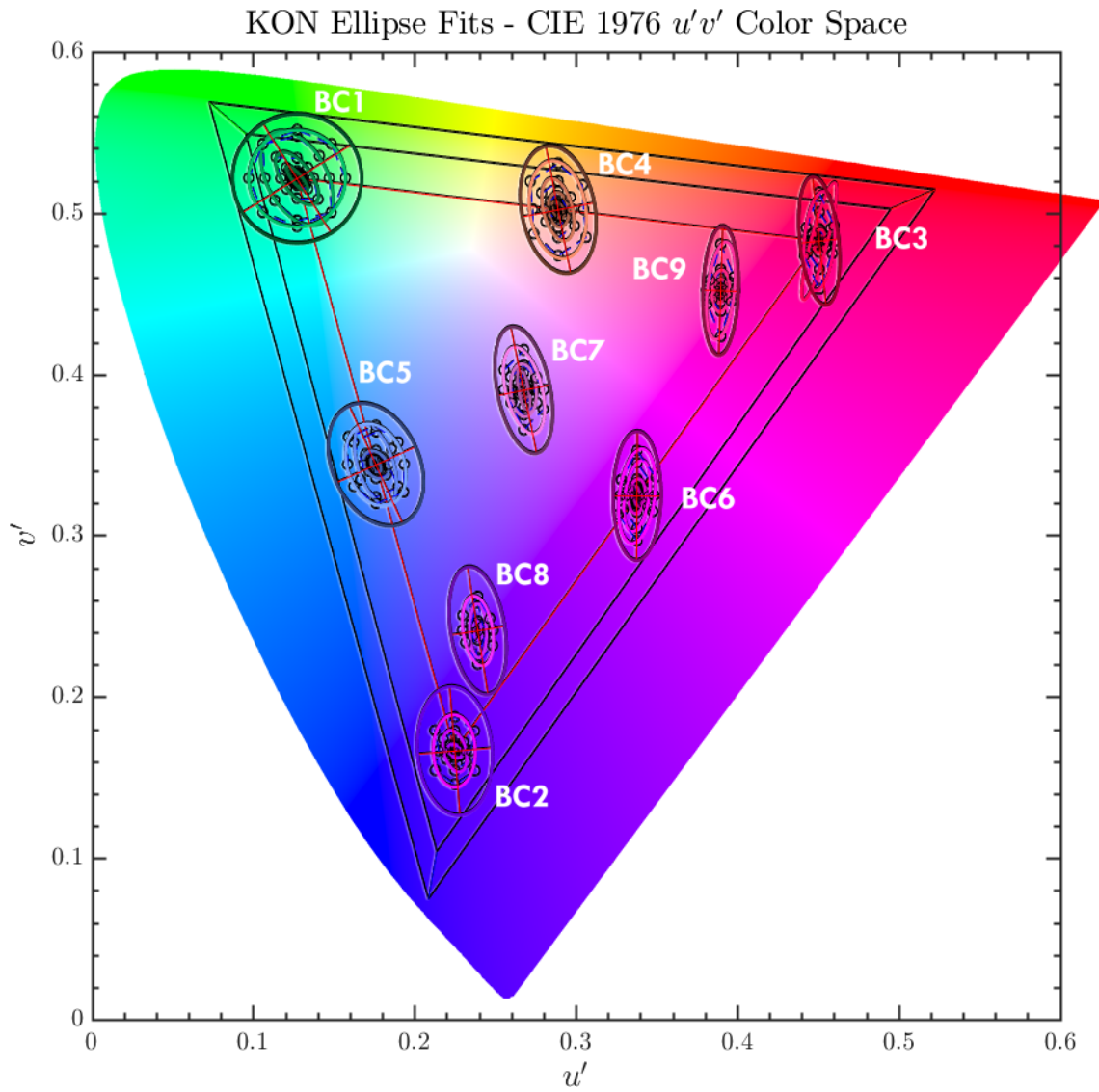
Figure 4.18: The ellipse fits plotted on the $u'v'$ color space to illustrate the overall shapes and orientation of the ellipses of participant **KON**.

Chapter V

Discussion

In this study, two experiments were carried out. First, the isoluminant point for 9 base colors and 4 directions was measured with the method of heterochromatic flicker photometry (HFP) at a frequency of 25Hz and an modulation amplitude $\Delta u'v'$ of 0.05. Second, the temporal contrast sensitivity functions (tCSFs) for chromatic flicker of 9 base colors, 4 directions and 7 frequencies was obtained.

In the first experiment the importance of finding the isoluminant point was highlighted. It was confirmed that there were conditions with luminance ratios different than 1. In addition, the function $D(\lambda)$ expressed the extend at which the luminance ratios were different from 1 and at which wavelengths the difference spectrum was mostly adjusted by these luminance ratios. This function was calculated with the sum of the difference between the two extreme colors spectral radiance weighted by the logarithm of the luminance ratio at isoluminance. We found that major compensations were at short wavelengths and long wavelengths. In addition, the luminance ratios different than 1 were mostly adjusting the S-cones responses between the two extreme colors (ΔS), more than for the L- and M-cones responses and especially for base colors with components at short wavelengths. According to literature, the photopic function $V\lambda$ used to do photometric measurements (i.e. to measure luminance) wrongly represents the individual observer, and underestimates short wavelengths (Valberg, 2007). This means that the $V(\lambda)$ used to create colors at equal luminance is not perfect, and should be corrected. By default the spectrometer (specbos 1201) uses $\overline{y}(\lambda)$ of the 2° CIE 1931 color space as $V(\lambda)$ for photometric calculations. If this is the case, a flawed $V(\lambda)$ should not be used to calibrate the LED system. As a suggestion, we could first consider the most recommended $V(\lambda)$ to measure individual differences with HFP and correct this $V(\lambda)$. Then, in preparation for the second experiment the system can be calibrated with the corrected $V(\lambda)$ for each participant. If it is possible to achieve isoluminance with this $V(\lambda)$, then, we could replace the first experiment by an experiment to obtain individual $V(\lambda)$ that might be less time consuming.

In the second experiment, an exponential model (a linear fit on log scale) of the tCSFs chromatic flicker resulted in a high goodness of fit. The parameters of the tCSFs depended on participant, base color and direction, thus, generalizations of the temporal chromatic mechanisms cannot be done with only red-green flicker as measured in literature. In addition, there was not a large difference between the goodness of fit of the tCSFs with

thresholds expressed as $\Delta u'v'$, ΔLMS and Δlms. Furthermore, the curves of the slopes and intercepts of the fits in function of base color and direction were plotted. For most of the base colors at direction 0° the curves were above the other directions, at direction 90° below, and at direction 45° and 135° the curves were very similiar. The slopes and intercepts across participants were analyzed with a two-way ANOVA of two repeated measures (base colors and directions). It was found that the effects of base color, direction and their interaction were statistically significant. But, when BC_2, BC_3 and BC_9 were removed from the analysis, it was shown that effects on the slope was only significant for direction, but not significant for base color and their interaction. However, all the effects were still significant for the intercepts. Also, the effect of participants was found significant through all the analysis. The effect of base color, direction and frequency was illustrated with the thresholds plotted in the $u'v'$ color space and fitted with ellipses. The size of ellipses seems to be dependent of the frequency of the modulation, but in some cases at low frequencies the ellipses have different shapes. Also, the ellipses are close to have a vertical orientation, meaning that the sensitivities are higher in the x-axis (shorter thresholds) and lower in the y-axis (larger thresholds). This can also be infered from the graphs of slopes and intercepts. These findings have shown that the sensitivity of the human visual system to chromatic flicker cannot be described by a simple function but is a complex function of the chromaticity, modulation direction and frequency.

In some cases, for the tCSFs of the naïve participant a peak appeared at lower frequencies, indicating either a band pass characteristic of the tCSFs or that the participant was still perceiving brightness flicker. In literature, it was found that this characteristic was typical of experiments were luminance flicker was not minimized (Shady et al., 2004; Green, 1968). On the other hand, a low pass characteristic of the tCSFs and a higher goodness of fit than the naïve participant was found for the expert participants. Similiary, a low pass characteristic of the tCSFs was found for studies were luminance flicker was minimized (Van Der Horst, 1969; Kim et al., 2013). However, we cannot conclude if this is related to the experience with the tasks or to individual visual differences. Furthermore, the difficulty of the task of this experiment depended on the frequency, especially at low frequencies it became more difficult.

It is interesting to note that the difficulty of the task of the first experiment depended on the base color and direction. For some base colors, participants had trouble to find the point of minimal flicker because they were always perceiving some amount of flicker. For example, some participants mentioned that the most difficult base colors were BC_2 (a saturated blueish-purple color) and BC_3 (a saturated red color). The luminance ratios of these two base colors were mostly farther from 1. Interestingly, the trends of luminance ratios are similar for colors that are close to this two colors, for example, the BC_2 base color is similar to the BC_8 and the BC_3 was similar to the BC_6 and BC_9. Some participants mentioned that BC_2 appeared brighter than the other colors. In case the system was

calibrated with the $V(\lambda)$ that is wrong at short wavelengths, then it might be that the luminance levels for BC_2 and BC_8 were much higher than the desired ones.

The LED system was calibrated weeks before the experiments. As a consequence, after finishing the experiments it was found that the spectrum of each red, green and blue LEDs changed around 0.26%, 3% and 4%, respectively. We do not know how the spectrum changed through time, thus, we assume that the measured colors are approximate but different to the desired colors. For future experiments, it is important to consider calibrating the system before each experiment session to ensure accurate measurements, or to consider improving the system's stability. In addition, just the warm up effects of the system were studied with maximum PWM values, but the cool down effects were ignored. Base colors did not use the full power of the LEDs during the experiments, and this might have caused shifts of the chromatic points.

In relation to health issues, every participant reported feeling eye strain. One participant mentioned that the luminance level was too high. Other participant had a strong headache after the first experiment. It was also reported that after all the experiments, a participant could perceive flicker in almost any light and that it was hard to read from a screen. One participant drop out from the experiment because of health issues. He suggested that there could be a problem with the ventilation of the laboratory. In literature, the health effects of flicker can be divided into those that are immediate like epileptic seizures, and those who result of long-term exposure, like malaise, headaches and impaired visual performance. Additionally, suggestions of the design of flickering LED systems can be found in the same literature (Wilkins, Veitch, and Lehman, 2010).

Before a general temporal model can be developed, the study has to be expanded for more participants and a wider range of base colors and directions. However, the biggest problem is the amount of time participants have to spend for the experiments. For this study, it was required more than 11 hours, so increasing the number of stimuli will just considerably increase the time. One of the main findings of this study can yield a solution to this problem. We found that an exponential model (linear fit on log scale) resulted in a high goodness of fit. For that reason, we might be able to measure fewer frequencies (i.e. 3 frequencies) and then fit a line (on log scale) to approximate the tCSFs. This could considerably reduce the number of trials for the second experiment, i.e., 216 trials and the time would be reduced from 9 hours to $\sim$6.6 hours (216×0.5mins $+2 \times 9 = 396$mins).

Additionally, a new design has to be considered to reduce the time without compromising accuracy. For example, the method of adjustment might have contributed to make the task hard and time consuming. Participants mentioned that they had to think for long time before deciding a threshold. Some felt that they were not able to understand if they were perceiving flicker or not. This problem was mentioned before in the book of Geischeider (1997) and can result in thresholds away from the real ones (falsely low or falsely high). It might be of great importance to reconsider the methodology to

eliminate participant's subjective criteria and response bias. For example, a prior study by Veelenturf (2016), it was found that the yes/no staircase method was accurate and the quickest compared to a 2AFC staircase method and a 2AFC constant stimuli method. So, it might be good idea to compare this method with the method of adjustment. During the experiments, the observed responses of the participants for each the adjustment tasks looked similar to the responses generated by a staircase method.

As an additional recommendation, we do not know if we can generalize an exponential model when measuring the tCSFs with different parameters of mean luminance levels and stimulus sizes. In literature, it was mentioned that the CFF depended of this parameters (Bodrogi and Khan, 2012). Also, the shape of the tCSFs and the isoluminance point might differ for different mean luminance levels and stimulus sizes. In the study by Swanson et al. (1987) a mean luminance below of 31.83 cd/m^2 (100 trolands) resulted in a tCSFs for chromatic flicker with a low pass characteristic, but at higher mean luminance the shape had a distorted appearance. It might be useful, to study further these parameters for future experiments.

5.1 Conclusion

Results from the present study indicate that the standard $V(\lambda)$ substantially underestimates the spectral characteristics of individual observers, especially at short wavelengths. Thus, to account for the individual differences, isoluminant conditions of chromatic flicker had to be measured with the method of HFP for each participant. The effort was made to be able to measure the temporal chromatic characteristics for only color-sensitive perceptual mechanisms and not luminance-sensitive mechanism. As a consequence, the thresholds plotted as a function of the frequency showed an exponential relationship. Furthermore, the tCSFs were obtained as the inverse of the logarithm of the thresholds expressed in three color spaces as $\Delta u'v'$, ΔLMS and Δlms. An exponential model (linear fit of tCSFs on log scale) resulted in a high goodness of fit R^2 for all participants and base colors. In addition, there was not a large difference between the goodness of fit of the tCSFs represented in different color spaces. These results opens up the possibility of reducing the amount of frequencies to measure the tCSFs. As a consequence, the time of the experiments can be reduced, so that the range of base colors and directions can be expanded for further study.

During the study, our gratitude is due to the interest of few participants and their consistent responses, and the welcomed support and feedback from the supervisors. This contributed to the cleanness of the findings reported in this study, but, most important, to the present purpose of understanding the temporal characteristics of color perception.

Bibliography

1. Atchison, D. & Smith, G. (2000). *Optics of the human eye.* Butterworth-Heinemann.

2. Bodrogi, P. & Khan, T. (2012). *Illumination, color and imaging: Evaluation and optimization of visual displays.* John Wiley & Sons.

3. Bone, R. & Landrum, J. (2004). Heterochromatic flicker photometry. *Archives of biochemistry and biophysics, 430*(2), 137–142.

4. Conway, B. (2002). *Neural mechanisms of color vision: Double-opponent cells in the visual cortex.* Springer Science & Business Media.

5. Cunningham, D. W. & Wallraven, C. (2011). *Experimental design: From user studies to psychophysics.* CRC Press.

6. De Valois, K. K. (2000). *Seeing.* Academic Press.

7. de Lange, H. (1958). Research into the dynamic nature of the human fovea→cortex systems with intermittent and modulated light. ii. phase shift in brightness and delay in color perception. *JOSA, 48*(11), 784–789.

8. Fairchild, M. (2013). *Color appearance models.* John Wiley & Sons.

9. Fechner, G. (1860). Elements of psychophysics. translation, h. *Adler. Brietkoph & Härtel, 1.*

10. Gescheider, G. (1997). Chapter 3. the classical psychophysical methods. *Psychophysics: the fundamentals. 3rd ed. Mahwah: Lawrence Erlbaum Associates.*

11. Granger, E. & Heurtley, J. (1973). Visual chromaticity-modulation transfer function. *JOSA, 63*(9), 1173–1174.

12. Green, D. (1968). The contrast sensitivity of the colour mechanisms of the human eye. *The Journal of physiology, 196*(2), 415–429.

13. Jiang, Y., Zhou, K., & He, S. (2007). Human visual cortex responds to invisible chromatic flicker. *Nature neuroscience, 10*(5), 657–662.

14. Kaiser, P. & Comerford, J. (1975). Flicker photometry of equally bright lights. *Vision research, 15*(12), 1399–1402.

15. Kelly, D. (1994). *Visual science and engineering: Models and applications.* Marcel Dekker, Inc.

16. Kim, K., Mantiuk, R., & Lee, K. (2013). Measurements of achromatic and chromatic contrast sensitivity functions for an extended range of adaptation luminance. In *Human vision and electronic imaging* (86511A).

17. Kuehni, R. (2003). *Color space and its divisions: Color order from antiquity to the present.* John Wiley & Sons.

18. Lee, B., Martin, P., & Valberg, A. (1989). Sensitivity of macaque retinal ganglion cells to chromatic and luminance flicker. *The Journal of physiology*, *414*(1), 223–243.

19. Lee, Martin, P., & Valberg, A. (1988). The physiological basis of heterochromatic flicker photometry demonstrated in the ganglion cells of the macaque retina. *The Journal of physiology*, *404*(1), 323–347.

20. Lee, Pokorny, J., Martin, P., Valbergt, A., & Smith, V. (1990). Luminance and chromatic modulation sensitivity of macaque ganglion cells and human observers. *JOSA A*, *7*(12), 2223–2236.

21. Lennie, P., Pokorny, J., & Smith, V. C. (1993). Luminance. *JOSA A*, *10*(6), 1283–1293.

22. MacAdam, D. L. (1937). Projective transformations of ici color specifications. *JOSA*, *27*(8), 294–299.

23. MacAdam, D. L. (1971). Geodesic chromaticity diagram based on variances of color matching by 14 normal observers. *Applied optics*, *10*(1), 1–7.

24. Malacara, D. (2011). Color vision and colorimetry: Theory and applications. SPIE Washington.

25. Murdoch, M., Sekulovski, D., & Seuntiëns, P. (2011). The influence of speed and amplitude on visibility and perceived subtlety of dynamic light. In *Color and imaging conference* (Vol. 2011, *1*, pp. 265–269). Society for Imaging Science and Technology.

26. Raghavachary, S., Pharr, M., Luebke, D., & Strothotte, T. (2008). *Rendering ebook collection: Ultimate cd.* Elsevier.

27. Shady, S., MacLeod, D., & Fisher, H. (2004). Adaptation from invisible flicker. *Proceedings of the National Academy of Sciences of the United States of America*, *101*(14), 5170–5173.

28. Sharpe, L. T., Stockman, A., Jagla, W., & Jägle, H. (2005). A luminous efficiency function, v*(lambda), for daylight adaptation. *Journal of Vision*, *5*(11), 3–3.

29. Smith, V. & Pokorny, J. (1975). Spectral sensitivity of the foveal cone photopigments between 400 and 500 nm. *Vision research*, *15*(2), 161–171.

30. Stockman, A. & Sharpe, L. (2000). The spectral sensitivities of the middle- and long-wavelength-sensitive cones derived from measurements in observers of known genotype. *Vision research*, *40*(13), 1711–1737.

31. Swanson, W., Ueno, T., Smith, V., & Pokorny, J. (1987). Temporal modulation sensitivity and pulse-detection thresholds for chromatic and luminance perturbations. *JOSA A*, *4*(10), 1992–2005.

32. Valberg, A. (2007). *Light vision color*. John Wiley & Sons.

33. Van Der Horst, G. J. (1969). Chromatic flicker. *JOSA*, *59*(9), 1213–1217.

34. Van der Horst, G. & Bouman, M. (1969). Spatiotemporal chromaticity discrimination. *JOSA*, *59*(11), 1482–1488.

35. Veelenturf, J. (2016). *Comparison of methodologies for measuring chromatic flicker perception* (Master's thesis, Eindhoven University of Technology).

36. Vogels, I., Sekulovski, D., & Rijs, B. (2007). Discrimination and preference of temporal color transitions. In *Color and imaging conference* (Vol. 2007, *1*, pp. 118–121). Society for Imaging Science and Technology.

37. Wilkins, A., Veitch, J., & Lehman, B. (2010). Led lighting flicker and potential health concerns: Ieee standard par1789 update. In *Energy conversion congress and exposition (ecce), 2010 ieee* (pp. 171–178). IEEE.

Appendix A.

Chapter III Additional Tables

LED	Min DWL (nm)	Max DWL (nm)	Approx DWL (nm)	L BW(cd/m^2)	L SW(cd/m^2)
Red	620	630	623	76.56	90
Green	520	535	531	83.74	94.4
Royal Blue	450	465	453	29.18	35.8

Table A.1: Minimum and maximum dominant wavelength (DWL) specified in the Cree XP-E datasheet, the measured dominant wavelength, the luminance of the big window, and luminance of the small window for each type of LED with maximum duty cycle values.

PWM	L Red cd/m^2	L Green cd/m^2	L Blue cd/m^2
0	0.118	0.231	0.108
4666	9.141	9.754	3.308
9333	18.190	19.390	6.475
14000	27.070	29.110	9.902
18666	35.790	38.600	13.030
23333	44.350	47.890	16.360
28000	52.710	57.100	19.600
32666	60.750	66.060	22.870
37333	69.050	75.010	26.050
42000	76.560	83.740	29.180

Table A.2: The calibration values measured through the big window and used during the experiments of this study. The gamut's chromaticity points in the xy color plane were (0.696 , 0.195), (0.303, 0.716) and (0.001, 0.089).

Parameter	Value
Maximum Amplitude ($\Delta u'v'$)	0.06
Minimum Amplitude ($\Delta u'v'$)	0.0004
Offset from Gamut ($\Delta u'v'$)	0.01
Maximum Luminance (cd/m^2)	50
Minimum Luminance (cd/m^2)	25
Fixed Sum of Luminance (cd/m^2)	75
Directions	0, 45, 90, 135

Table A.3: Parameters for the definition of the base colors and extreme colors.

Experiment	Number of Trials	Session	Time/trial	Time Estimation
Exp 1 R_L	$9BC \times 4D \times 1A \times$ $1F \times 2SR \times 2Re = 144$	1	15s – 30s	(36 − 72 mins) +2 mins $\times 9BC$ = 54 ∼ 90 mins
Exp 2 $tCSFs$	$9BC \times 4D \times 7F \times 2SA = 504$	2 (BC_1)	30s	$28 + 2 = 30$ mins
		3 (BC_2)	30s	$28 + 2 = 30$ mins
		4 (BC_3)	30s	$28 + 2 = 30$ mins
		5 (BC_4)	30s	$28 + 2 = 30$ mins
		6 (BC_5)	30s	$28 + 2 = 30$ mins
		7 (BC_6)	30s	$28 + 2 = 30$ mins
		8 (BC_7)	30s	$28 + 2 = 30$ mins
		9 (BC_8)	30s	$28 + 2 = 30$ mins
		10 (BC_9)	30s	$28 + 2 = 30$ mins
		All		252 mins + 2 mins $\times 9BC$ = 270 mins
	Experiments Total Time estimate			324 ∼ 360 mins

Table A.4: Time estimates for each experiment, session and trial.

Appendix B.

Pilot Experiments

These pilot experiments were performed to define strategies assumed to give reliable luminance ratios and visual thresholds, but also to highlight the importance of measuring the luminance ratio before proceeding to measure the temporal chromatic contrast sensitivity curve. Pilots were also done, to define parameters like the number of frequencies and how to approximate the luminance ratio as function of the amplitude. These preliminary studies are presented and briefly explained in this appendix.

B.1 Pilot 1 - Luminance Ratio

This pilot experiment was performed to know if the luminance ratio of an isoluminant chromatic flicker differs from 1. The two expert participants performed the experiment with 7 base colors, 4 directions, a frequency of 15Hz and an amplitude $\Delta u'v'$ of 0.01. The task was as the same as experiment 1.

We found that some luminance ratios did not considerably differ from 1 but others differed by as much as 3%. Later, the pilot was repeated but with a frequency of 25Hz and an amplitude $\Delta u'v'$ of 0.05 and we found that the ratios were considerably different from 1 and they differed as much as 10%. However, a question arised whether such difference of luminance ratio really represented a minimized luminance flicker.

B.2 Pilot 2 - Luminance Comparison

A second pilot experiment was carried out to answer the question if these luminance ratios represented a minimized luminance flicker. Stimuli with the reference luminance ratio of 1 were compared to the stimuli with the luminance ratio measured in pilot experiment 1. In this experiment, 7 base colors, 4 directions and a frequency of 15Hz and an amplitude $\Delta u'v'$ of 0.01 were used. Ttwo participants had to choose which of the two stimuli had the smallest amount of perceivable flicker. The stimuli were presented 10 times in random order. If certain stimulus was chosen above or equal to 80% of the time it was very likely ($p < 0.05$) that it represented a stimuli with less or none perceivable flicker. We found that the stimuli with the measured luminance ratio was chosen for 64% of the all the base colors

and directions presented, which was significantly different from chance (p < 0.05). This pilot showed the importance of measuring the luminance ratio were participants perceive none or less luminance flicker.

B.3 Pilot 3 - Luminance Ratio as function of Modulation Amplitude

For the second experiment, it was important to note that when varying the modulation amplitude $\Delta u'v'$ of the chromatic flicker stimulus, the luminance ratio should not be fixed. When the extreme colors are getting closer and closer, the colors should also approximate in luminance levels. When the amplitude $\Delta u'v'$ is 0, then both extreme colors are the same and also their luminance levels, so a luminance ratio of 1 is expected. The problem here was to find what was the best way to approximate the luminance ratio without introducing luminance flicker.

In this pilot experiment, the luminance ratio was measured for stimuli of 25Hz and amplitudes $\Delta u'v'$ of 0.05, 0.03 and 0.01. Two expert participants completed the pilot. At the end, a simple relation was used to the approximate this luminance ratios:

$$R_L = R_{L_{ref}}^{\Delta u'v'/\Delta u'v'_{ref}} \tag{B.1}$$

We plotted and computed the mean squared error to find which reference values, the luminance ratio $R_{L_{ref}}$ and amplitude $\Delta u'v'_{ref}$ approximated better the luminance ratios. The average mean squared error was 1.7536×10^{-5}. The values measured from 25Hz and an amplitude $\Delta u'v'$ of 0.05 were found to give the best interpolation of luminance ratios as shown in Figure B.1 for 6 base colors.

B.4 Pilot 4 - Frequencies

The number of frequencies used for the second experiment is what made the experiment time consuming. As a way to reduce the time of the experiment, a pilot was done to know which frequencies do not convey interesting information for the purpose of this study. For this pilot experiment, 9 frequencies were measured; 1, 2, 4, 8, 10, 15, 20, 25, 30 Hz. After this pilot, we decided to remove 1Hz and 30Hz and just 7 frequencies were measured in the study. The frequency of 1Hz appeared to be very difficult and the participant spent considerable amount of time trying to find the visibility threshold at that frequency. Furthermore, the chromatic flicker was hardly visible at 30Hz, and it might be that the fusion frequency is below this frequency.
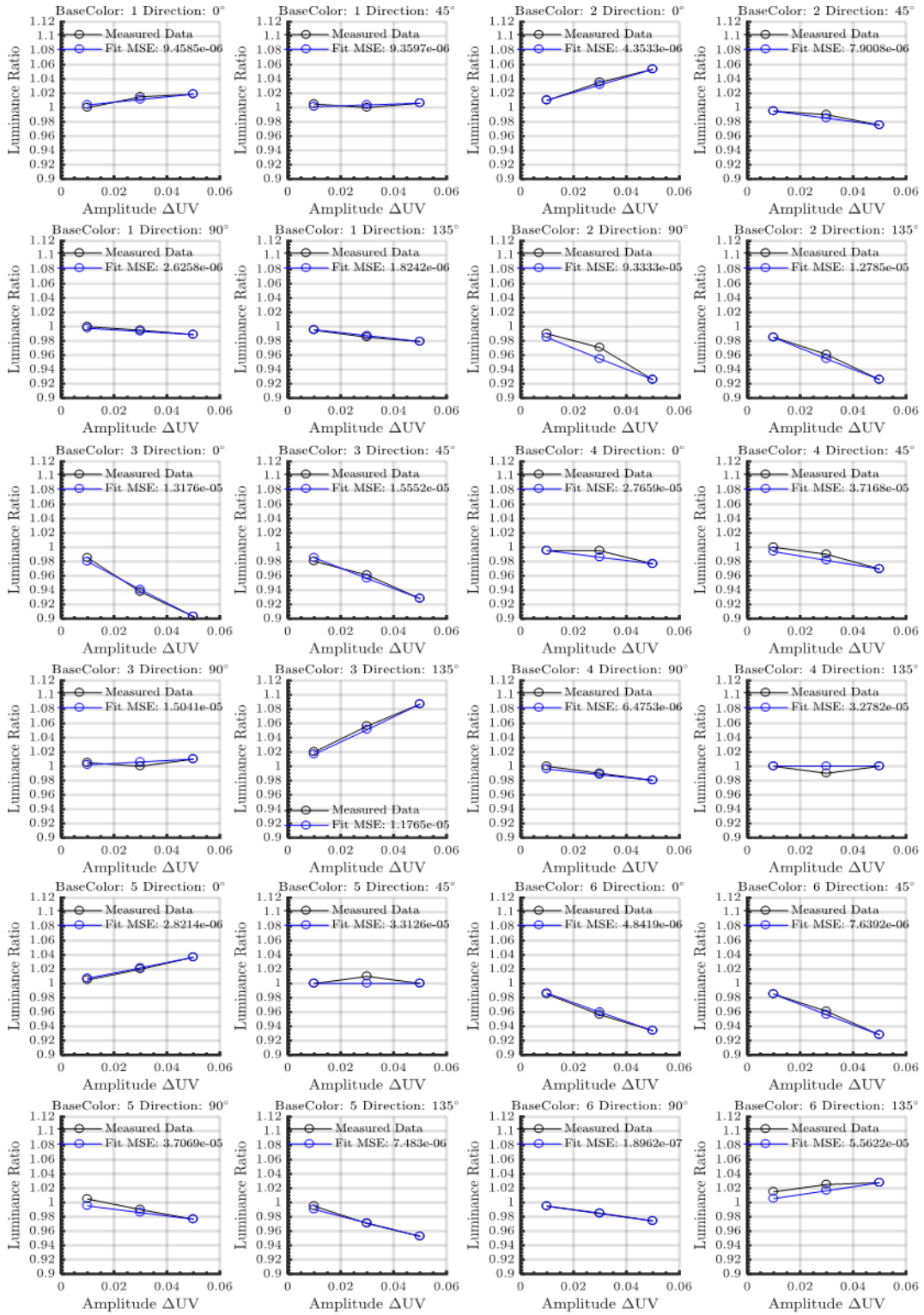
Figure B.1: Interpolation of the luminance ratios of 6 base colors versus amplitude using the luminance ratio of the amplitude 0.05 as the reference.

Appendix C.
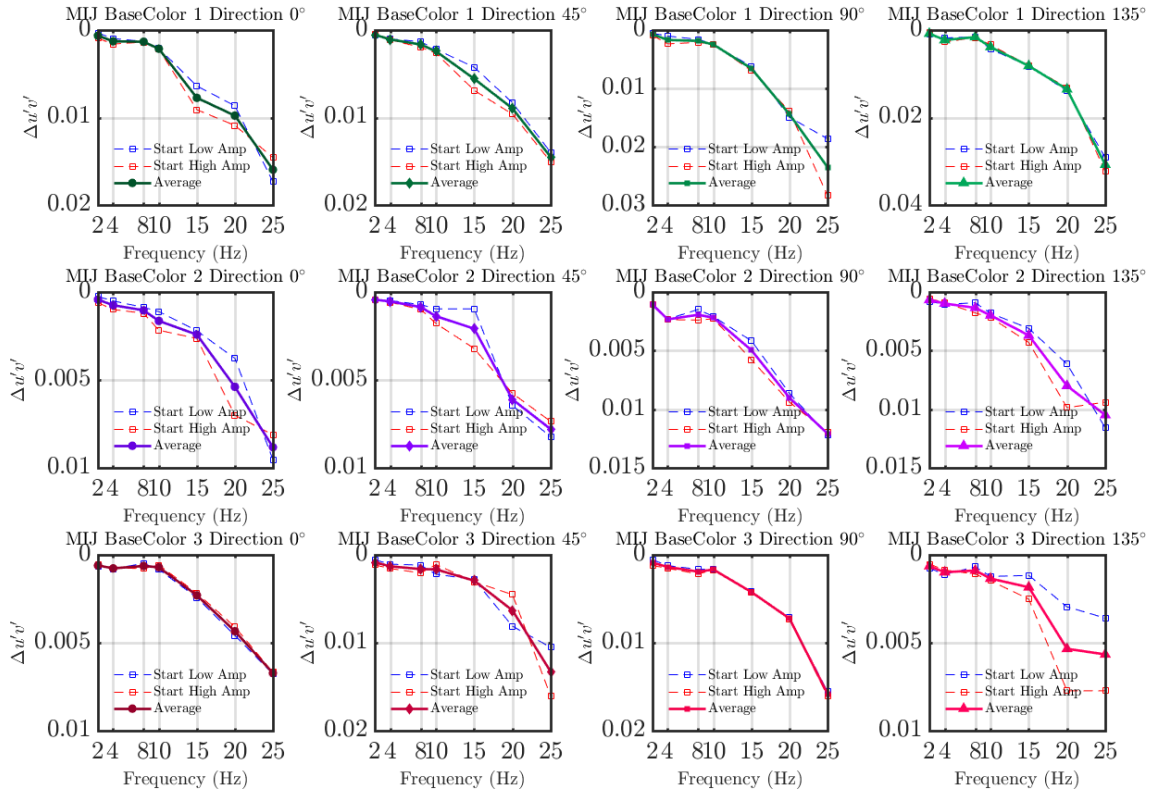
Raw thresholds $\Delta u'v'$

Figure C.1: The raw thresholds $\Delta u'v'$ of $BC_1 - BC_3$ of participant **MIJ**.
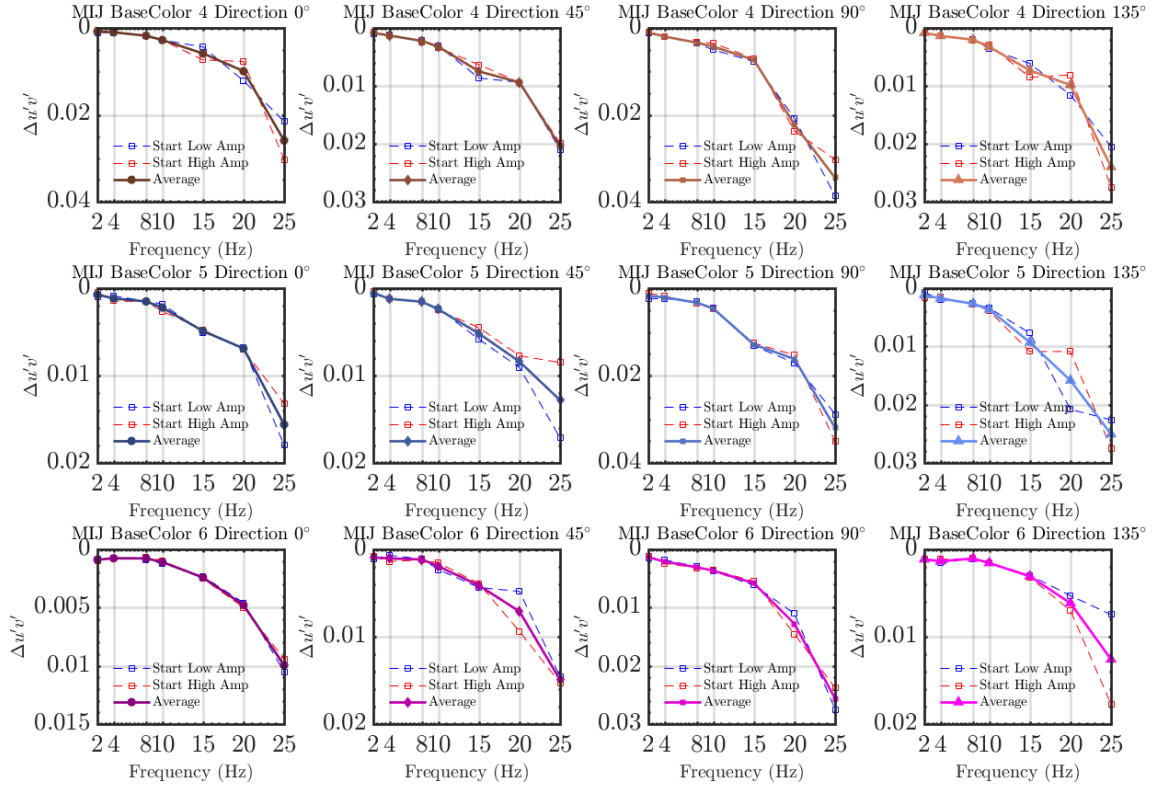
C. Raw thresholds $\Delta u'v'$

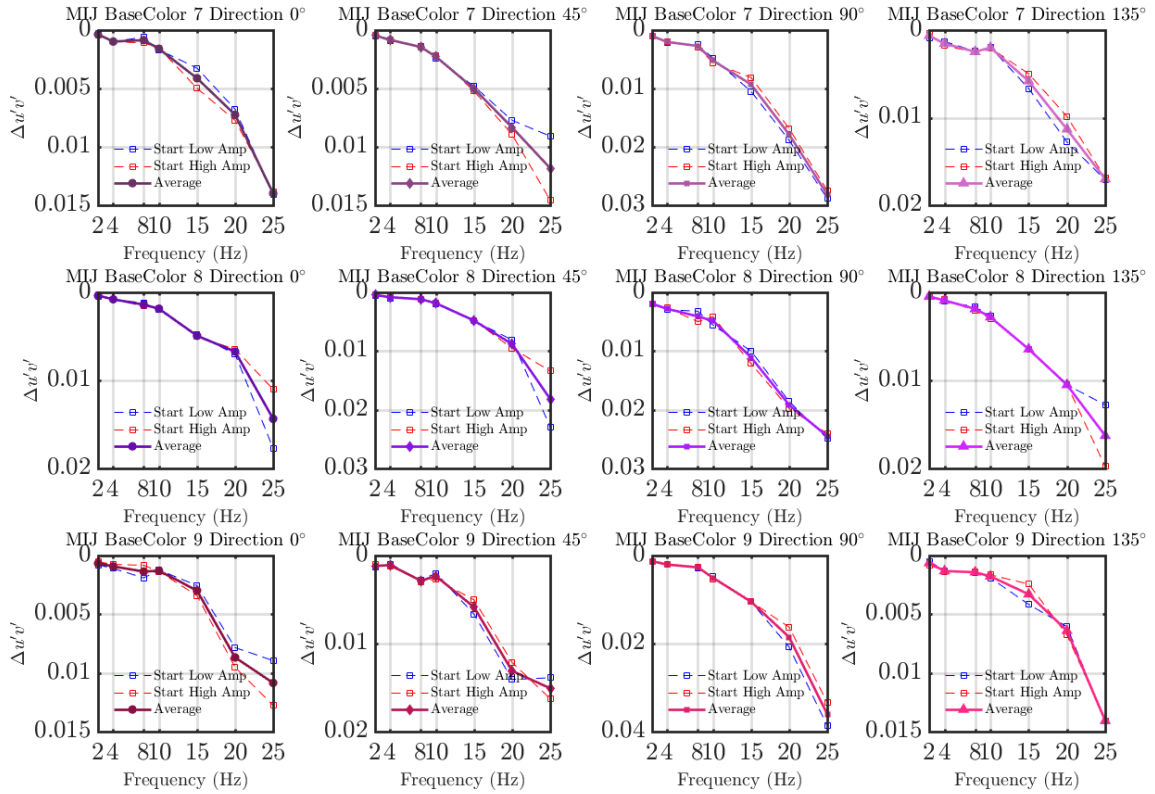**Figure C.2:** The raw thresholds $\Delta u'v'$ of $BC_4 - BC_6$ of participant **MIJ**.

Figure C.3: The raw thresholds $\Delta u'v'$ of $BC_7 - BC_9$ of participant **MIJ**.
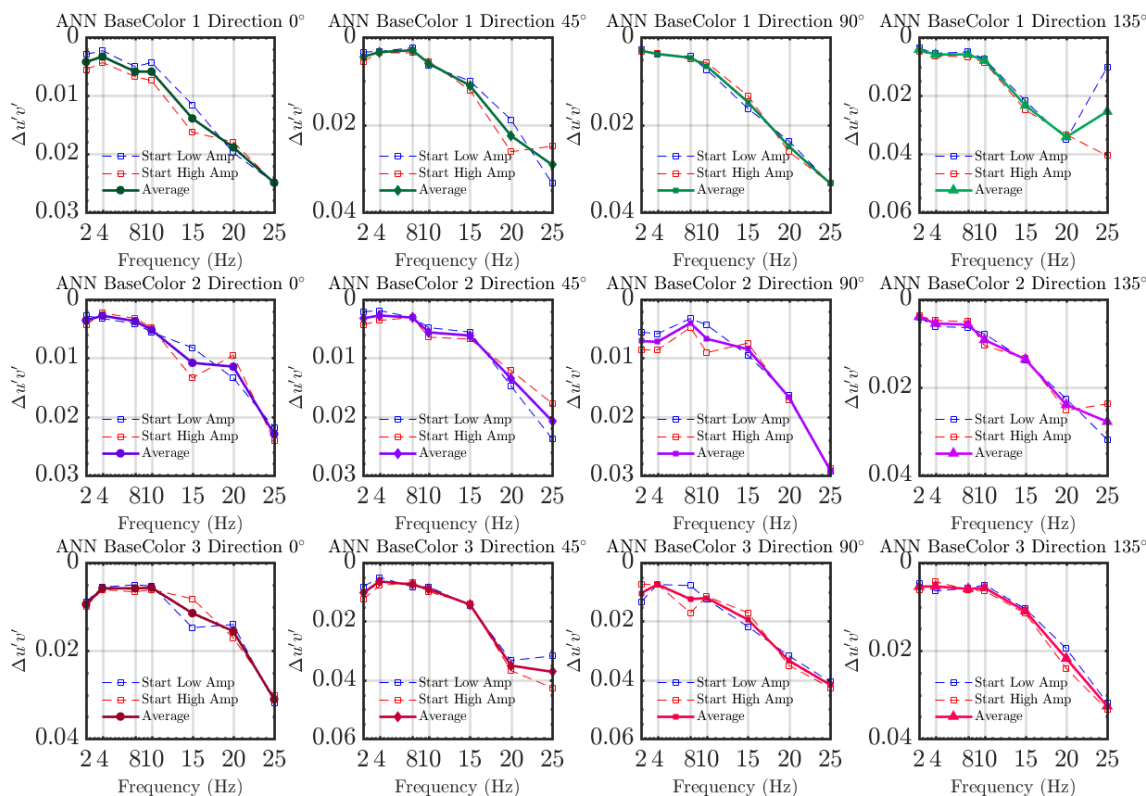
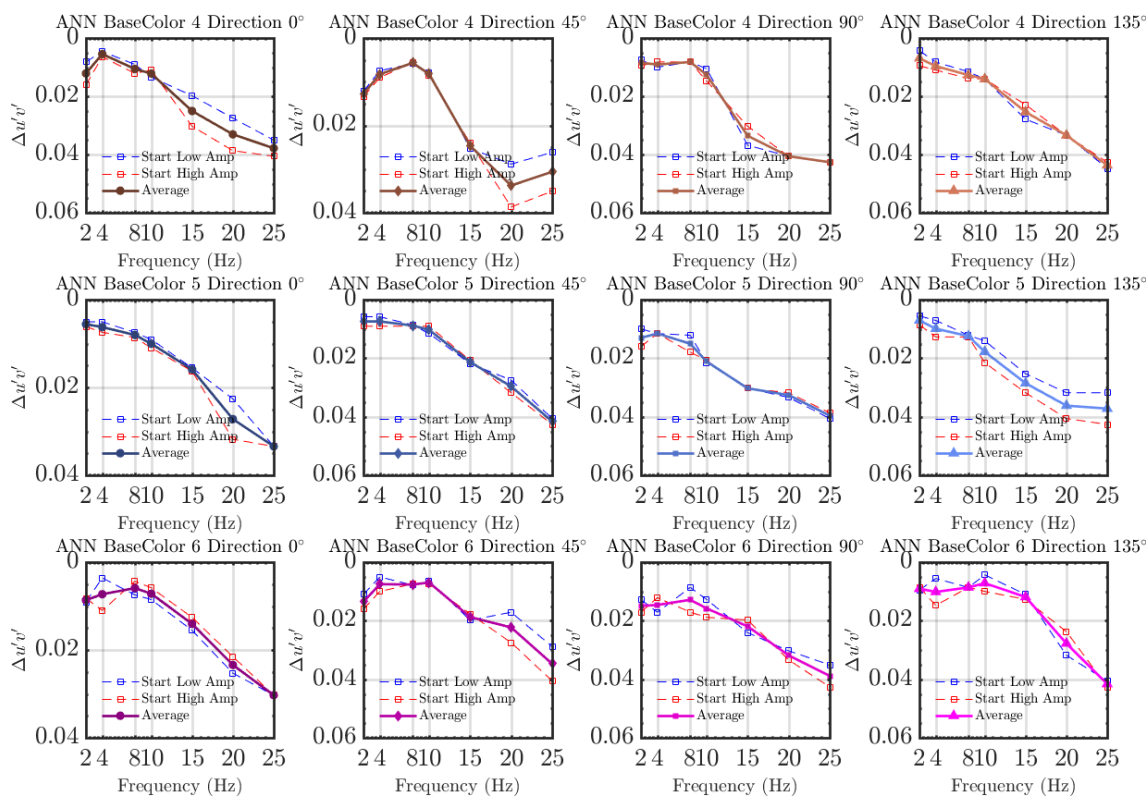**Figure C.4:** The raw thresholds $\Delta u'v'$ of $BC_1 - BC_3$ of participant **ANN**.

Figure C.5: The raw thresholds $\Delta u'v'$ of $BC_4 - BC_6$ of participant **ANN**.
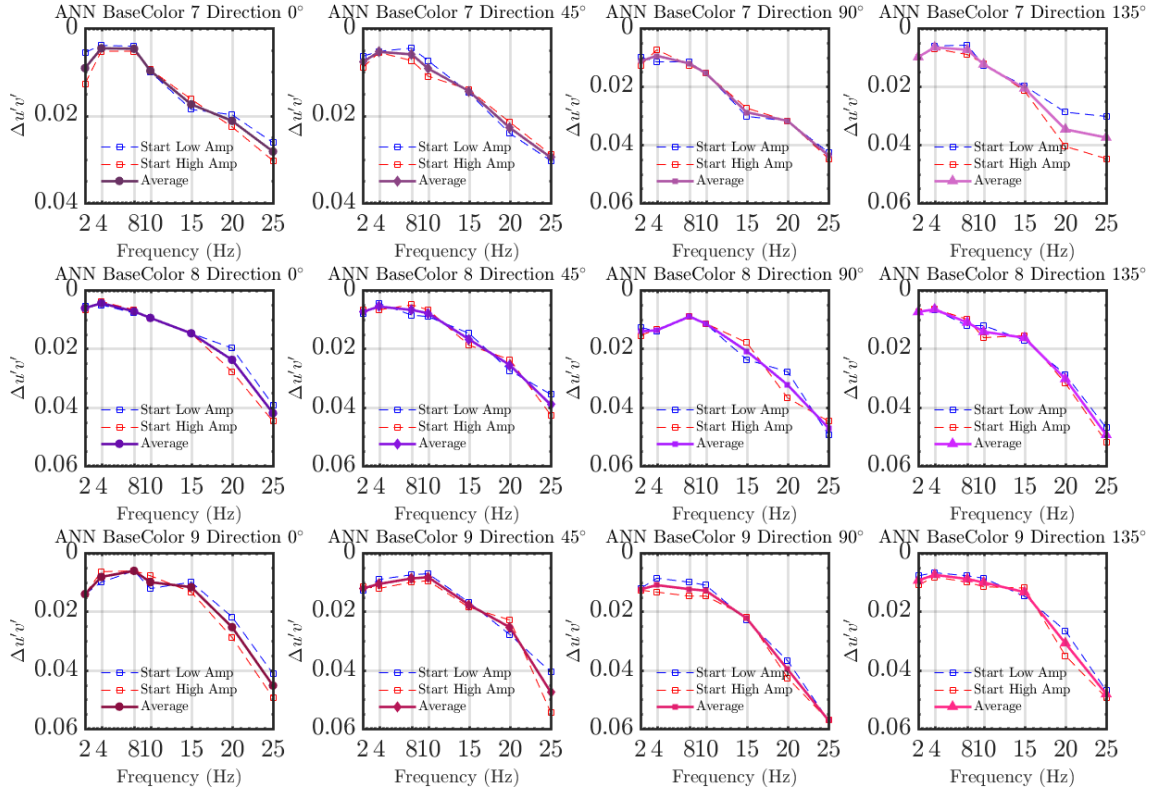
Figure C.6: The raw thresholds $\Delta u'v'$ of $BC_7 - BC_9$ of participant **ANN**.
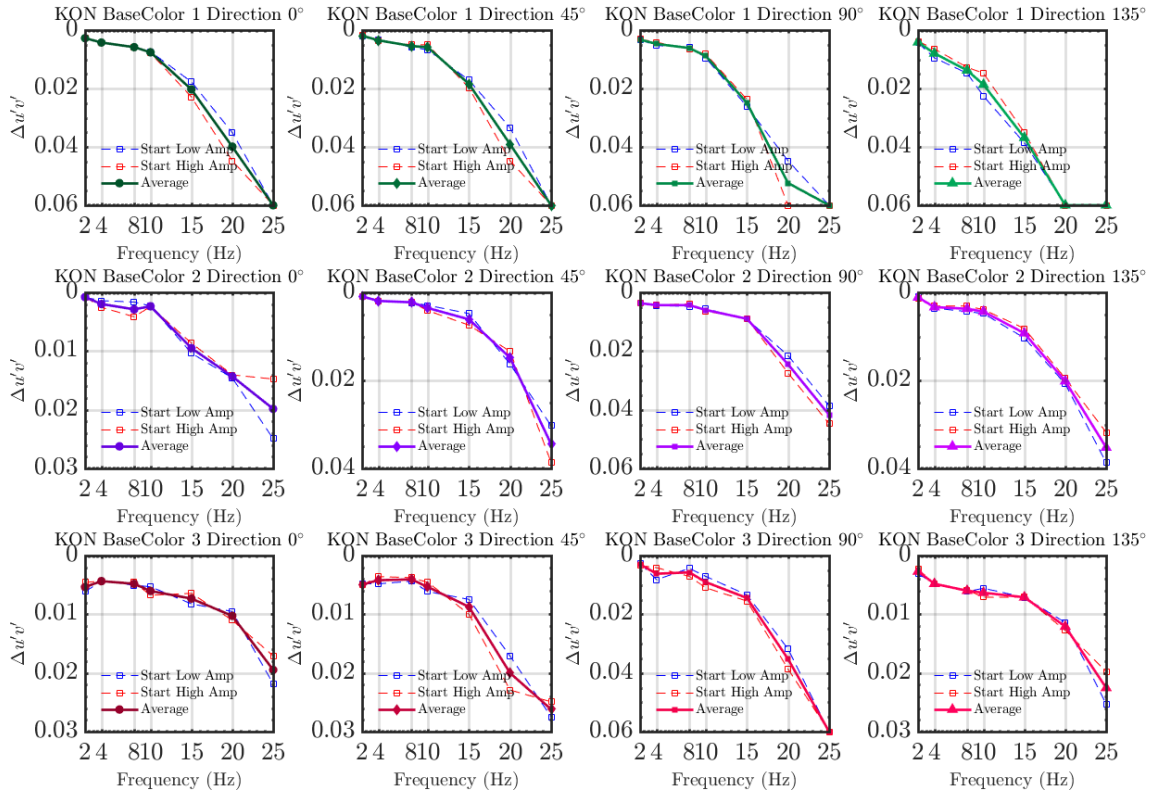

Figure C.7: The raw thresholds $\Delta u'v'$ of $BC_1 - BC_3$ of participant **KON**.
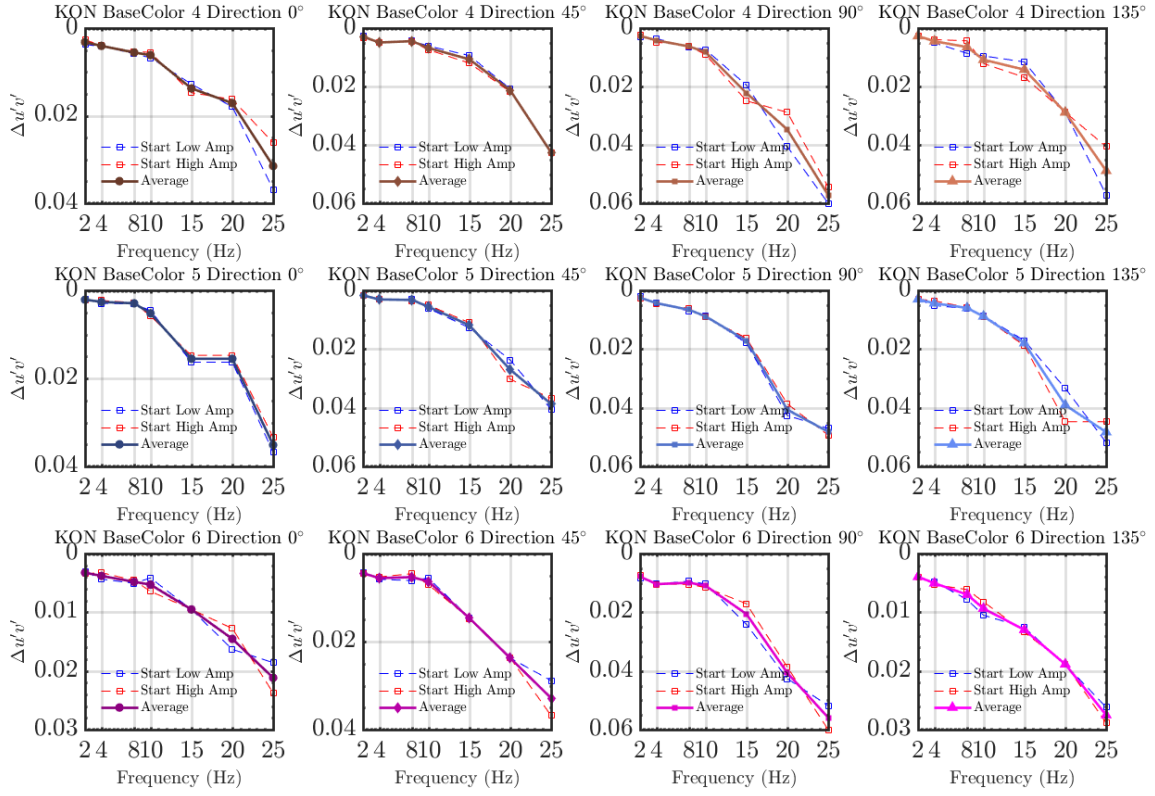
Figure C.8: The raw thresholds $\Delta u'v'$ of $BC_4 - BC_6$ of participant **KON**.
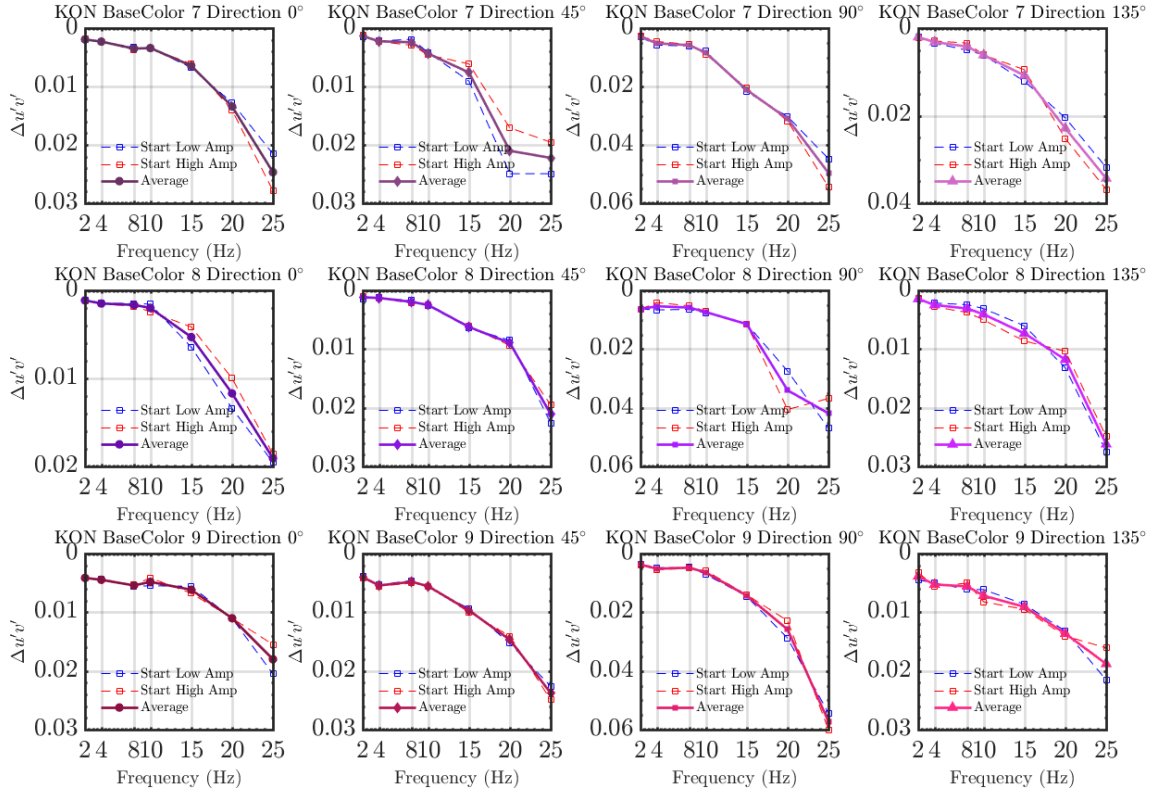

Figure C.9: The raw thresholds $\Delta u'v'$ of $BC_7 - BC_9$ of participant **KON**.

83

Appendix D.

TCSFs Fits

Figure D.1: tCSFs $(1/\log \Delta u'v')$ & linear fits on a logarithmic scale for participant **MIJ**.

Figure D.2: tCSFs $(1/\log \Delta LMS)$ & linear fits on a logarithmic scale for participant **MIJ**.

Figure D.3: tCSFs $(1/\log \Delta lms)$ & linear fits on a logarithmic scale for participant **MIJ**.
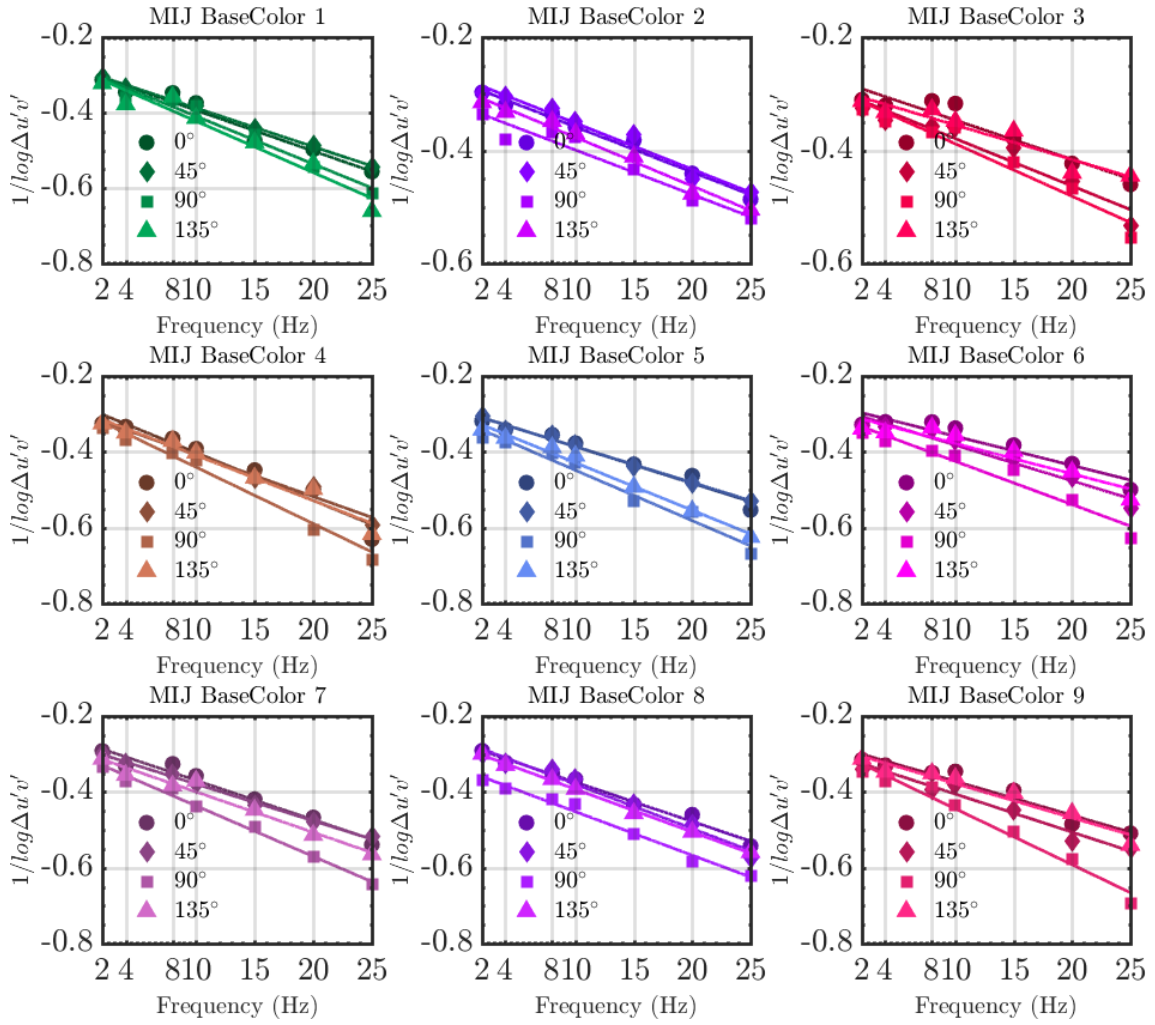
Figure D.4: tCSFs $(1/\log \Delta u'v')$ & linear fits on a logarithmic scale for participant **ANN**.

Figure D.5: tCSFs $(1/\log \Delta LMS)$ & linear fits on a logarithmic scale for participant **ANN**.

Figure D.6: tCSFs $(1/\log \Delta lms)$ & linear fits on a logarithmic scale for participant **ANN**.

Figure D.7: tCSFs $(1/\log \Delta u'v')$ & linear fits on a logarithmic scale for participant **KON**.
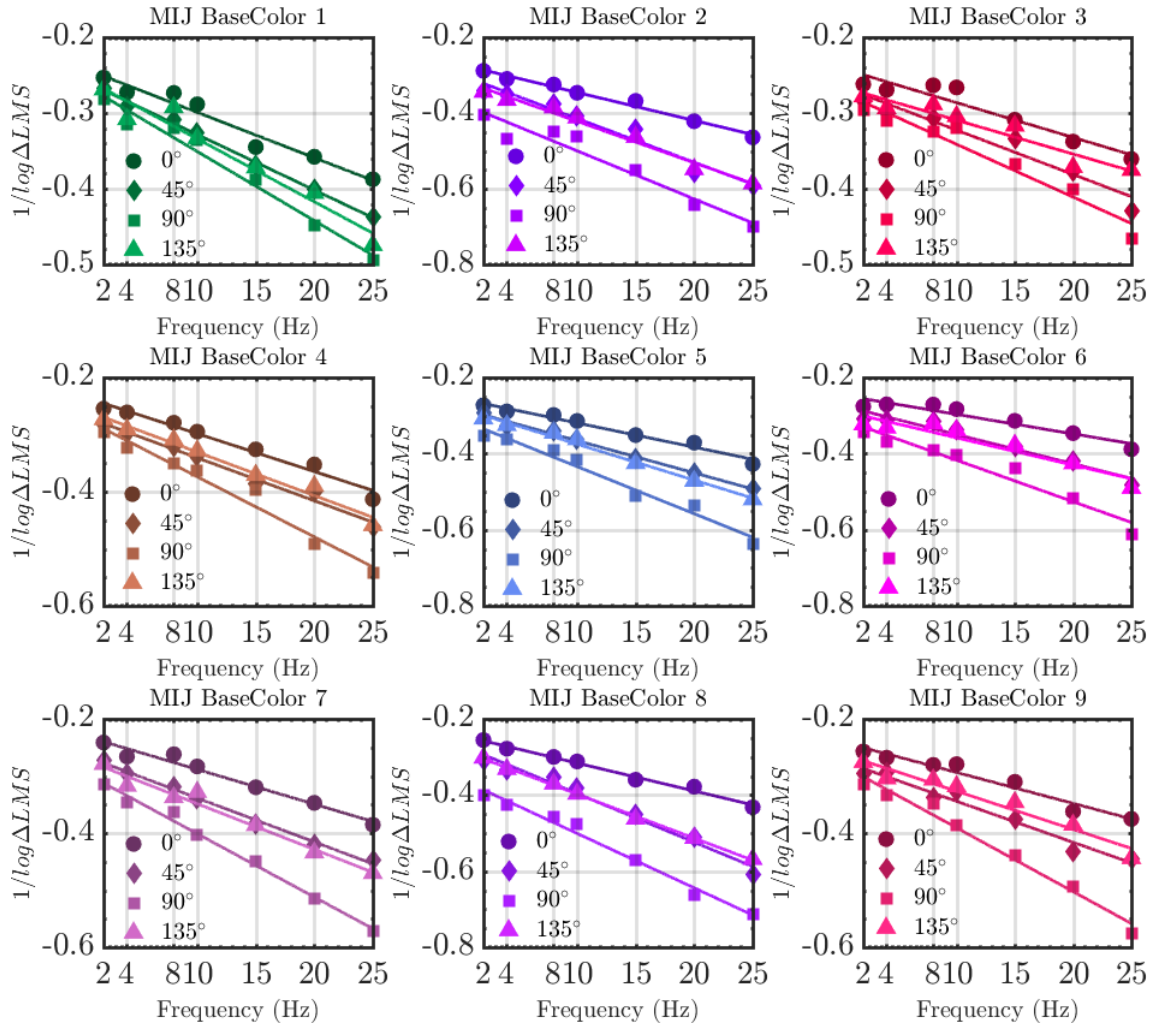
Figure D.8: tCSFs $(1/\log \Delta LMS)$ & linear fits on a logarithmic scale for participant **KON**.
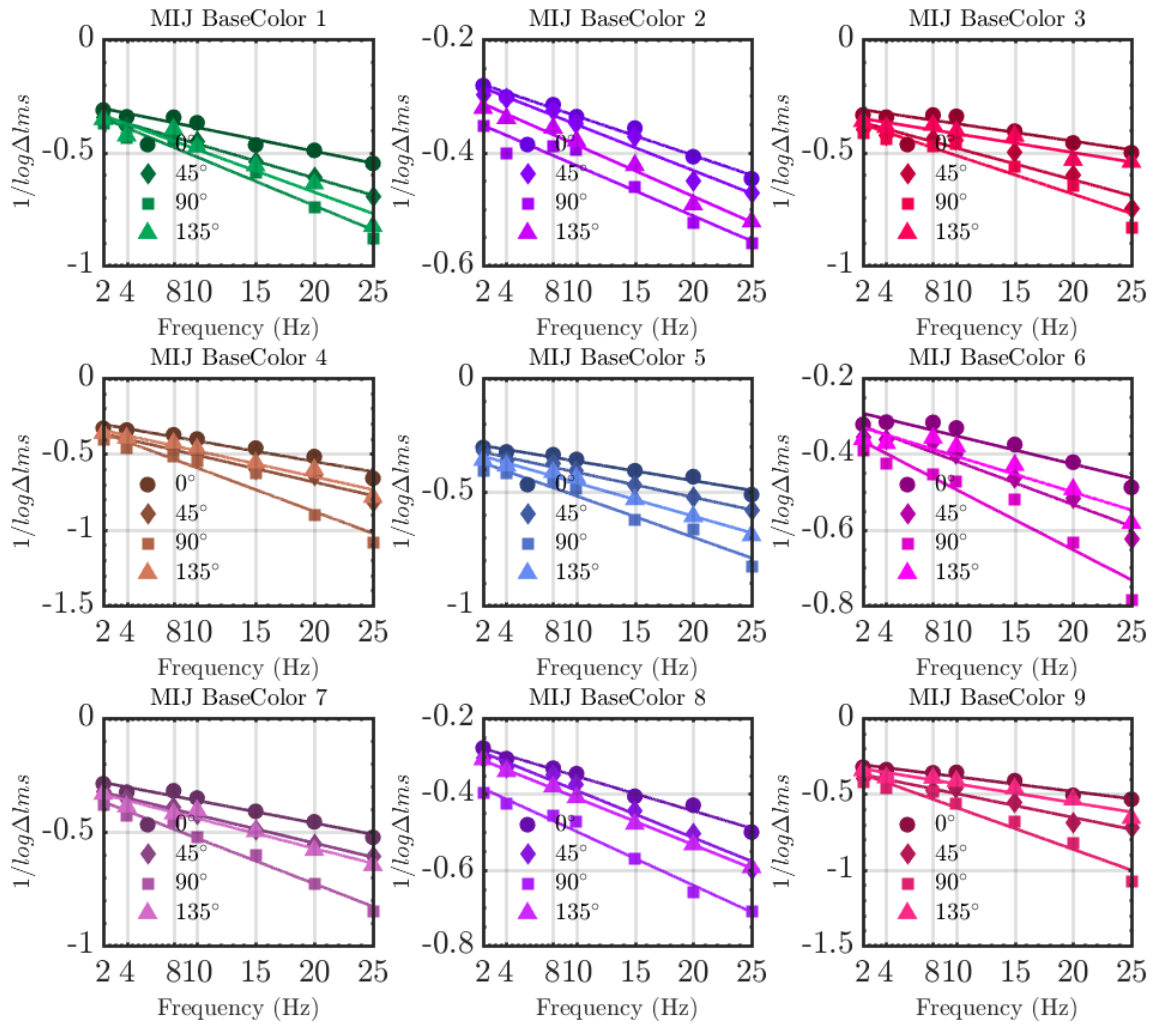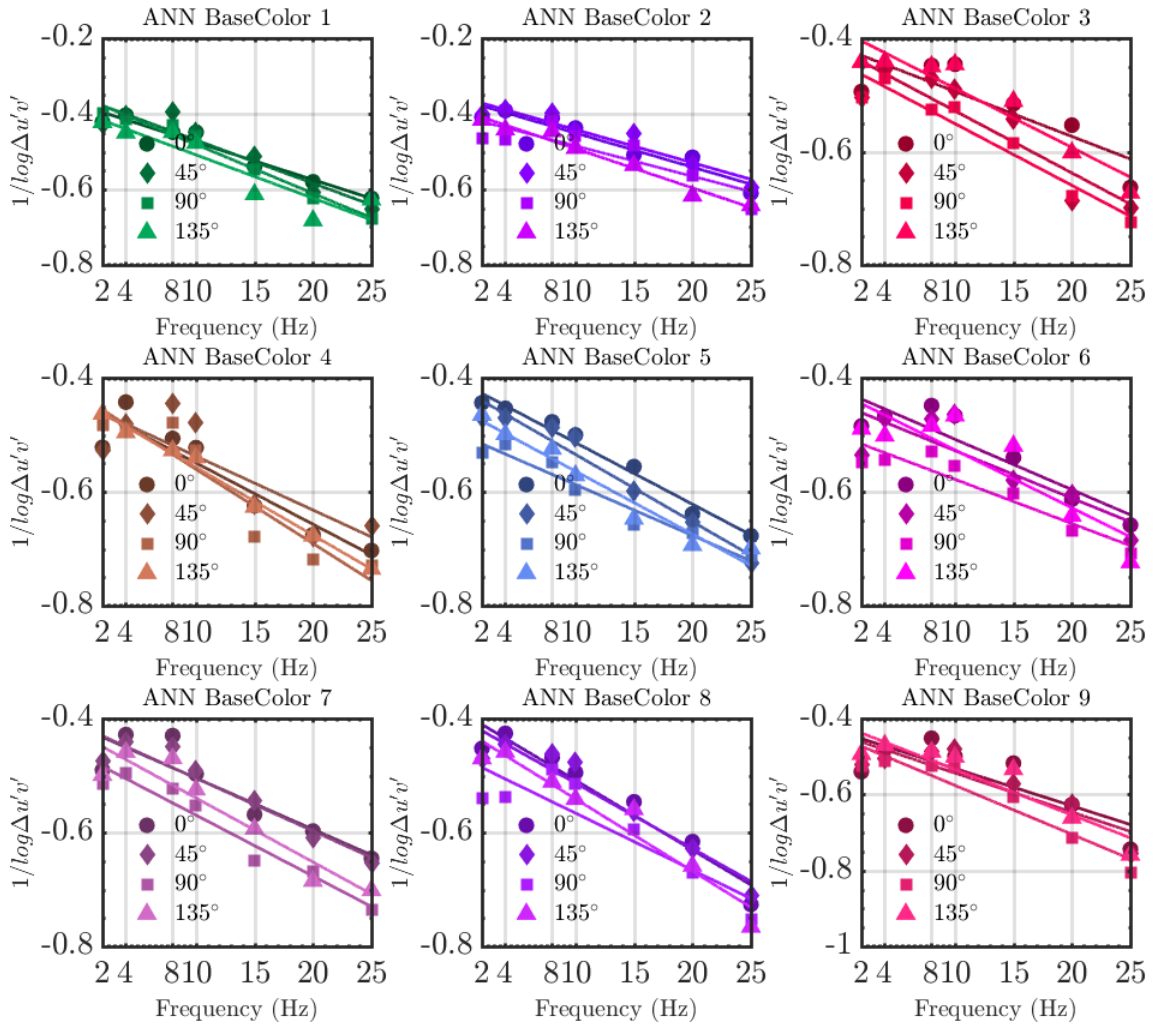
Figure D.9: tCSFs $(1/\log \Delta lms)$ & linear fits on a logarithmic scale for participant **KON**.
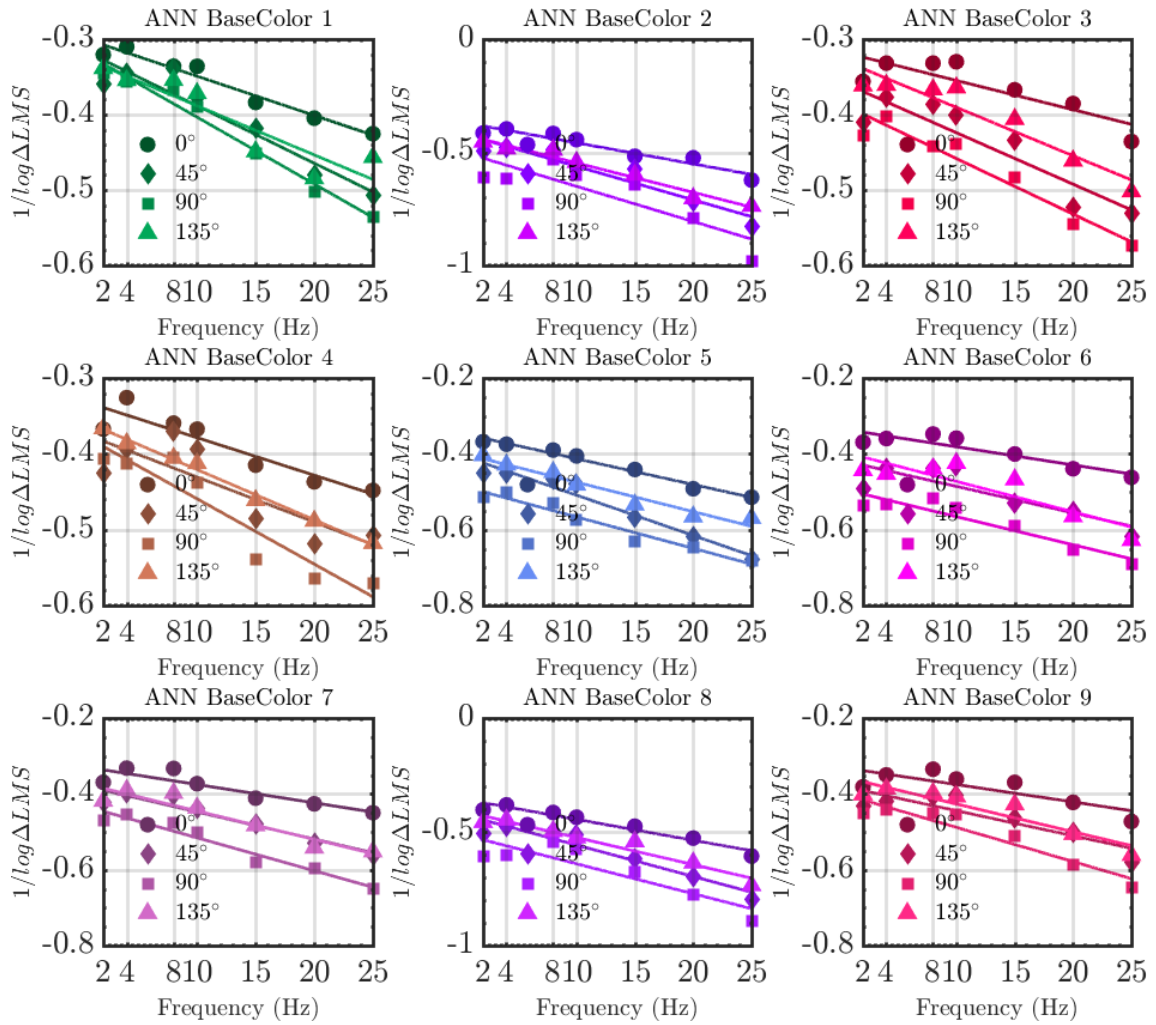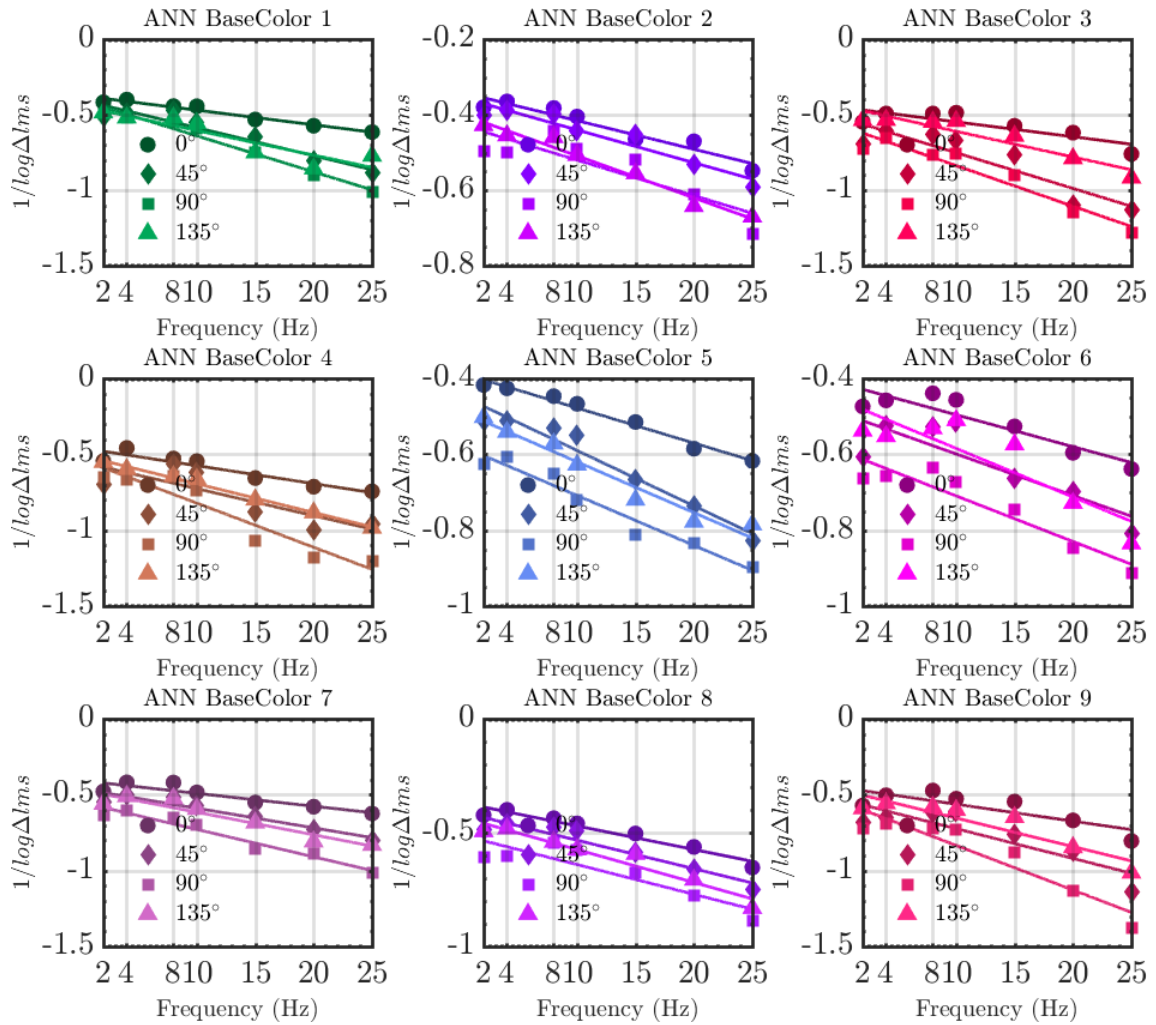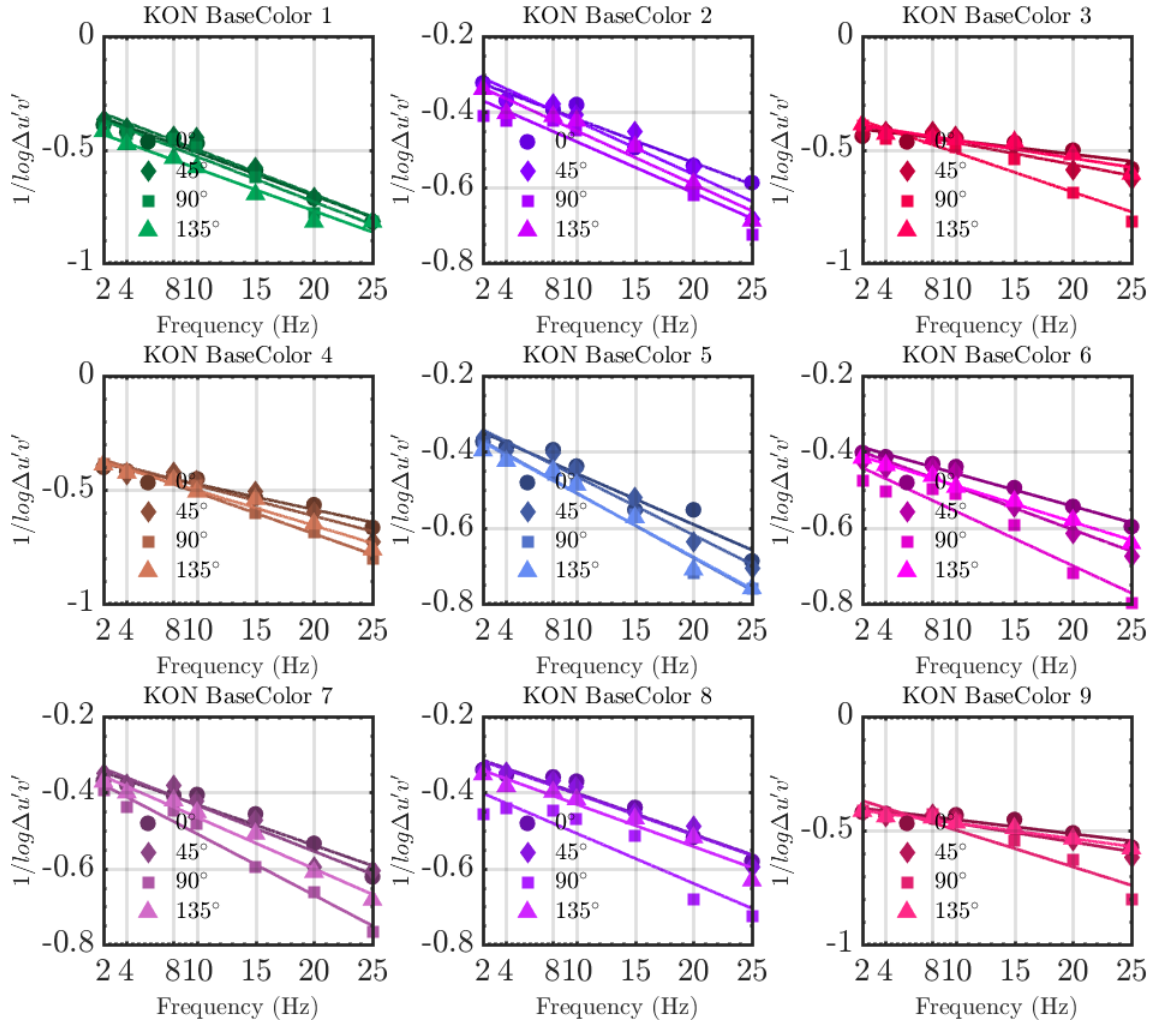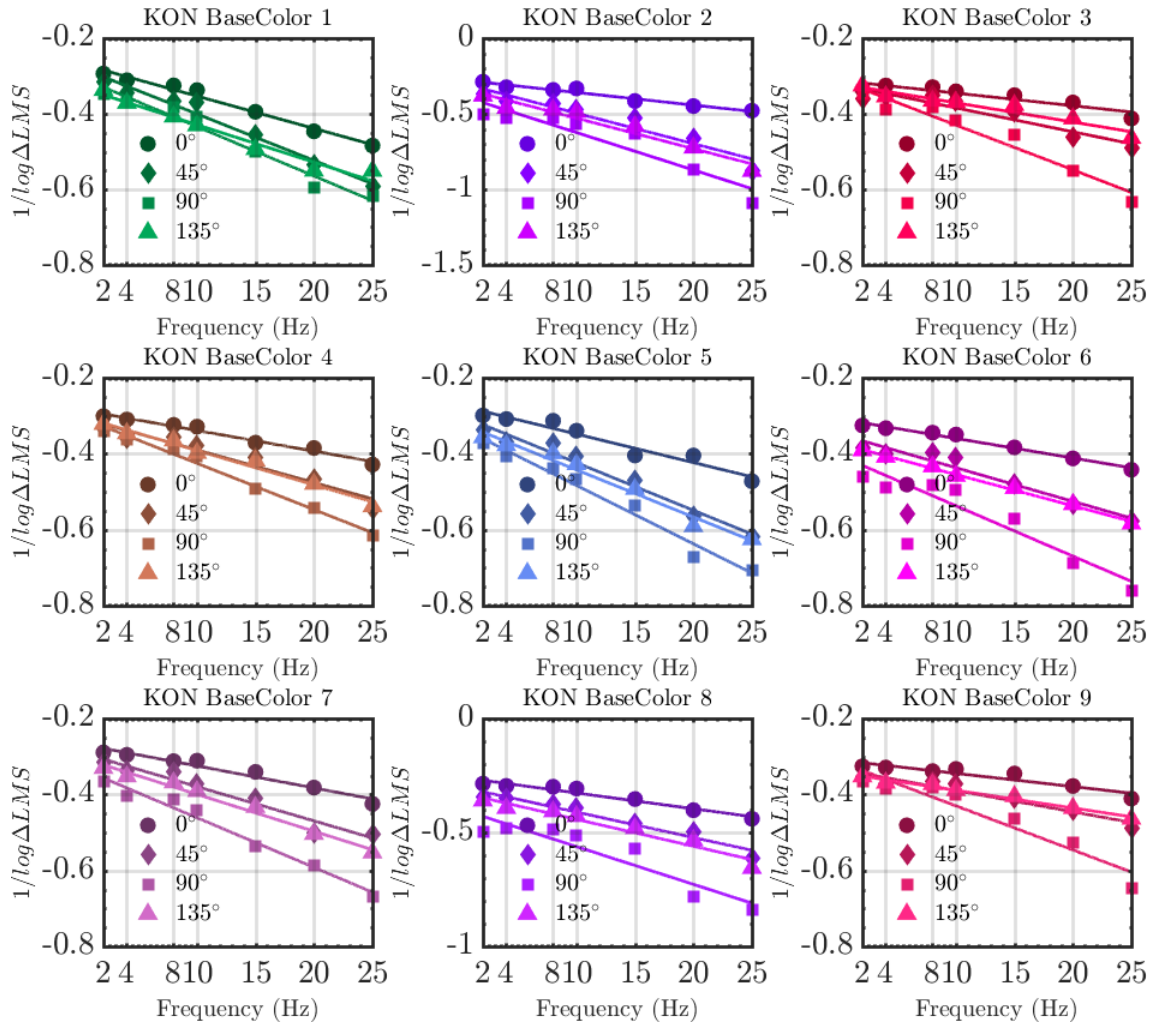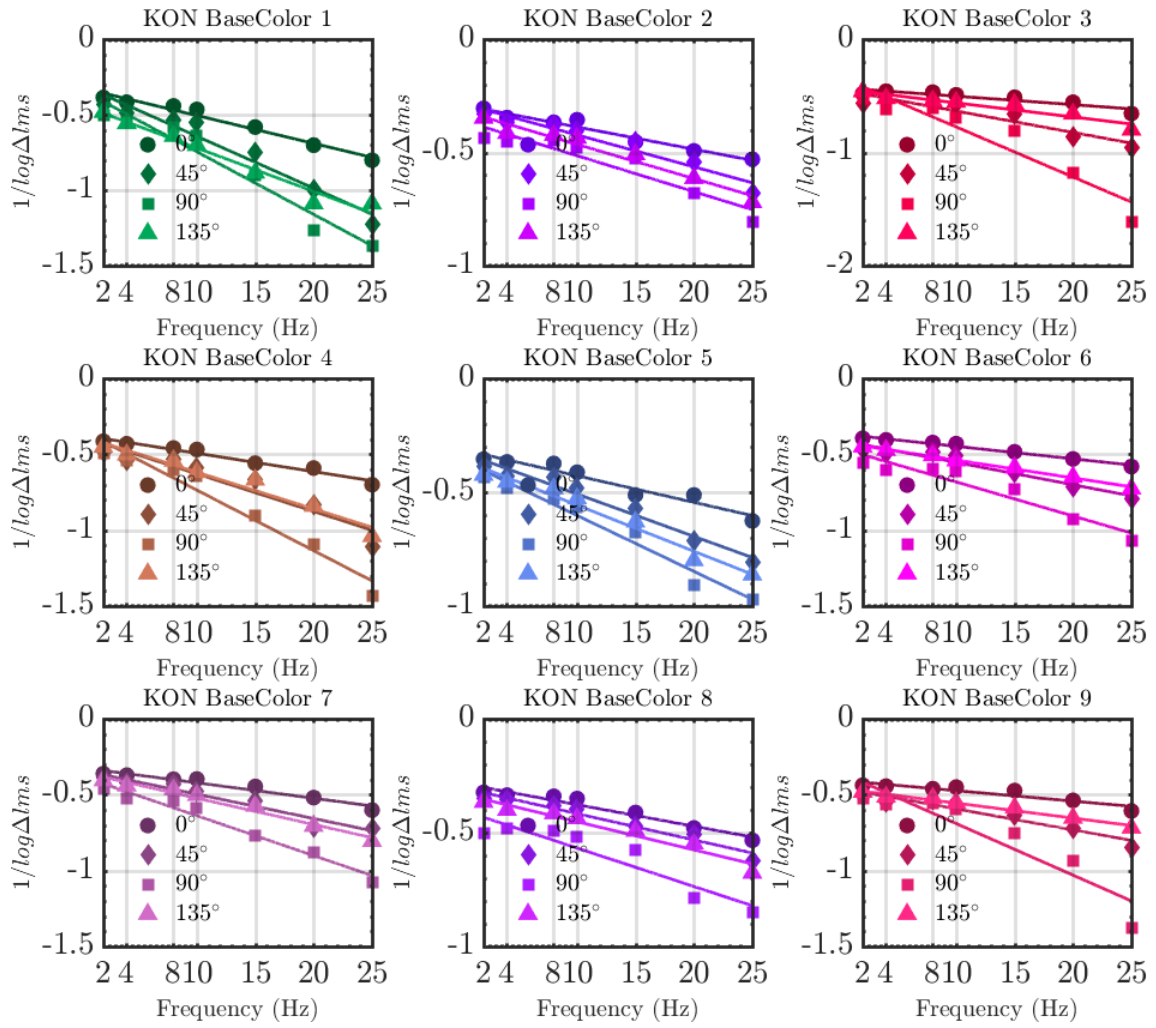
Appendix E.

Ellipse Fits Code & Plots

```matlab
1  function ellipse_t = EllipseFit( x,y,axis_handle, omit_axis, color)
2  %
3  % fit_ellipse − finds the best fit to an ellipse for the given set of points.
4  %
5  % Format:     ellipse_t = fit_ellipse( x,y,axis_handle )
6  %
7  % Input:      x,y            − a set of points in 2 column vectors. AT LEAST 5 points
        are needed !
8  %             axis_handle − optional. a handle to an axis, at which the estimated
        ellipse
9  %                              will be drawn along with it's axes
10 %
11 % Output:    ellipse_t − structure that defines the best fit to an ellipse
12 %                          a            − sub axis (radius) of the X axis of the non−
        tilt ellipse
13 %                          b            − sub axis (radius) of the Y axis of the non−
        tilt ellipse
14 %                          phi          − orientation in radians of the ellipse (tilt)
15 %                          X0           − center at the X axis of the non−tilt ellipse
16 %                          Y0           − center at the Y axis of the non−tilt ellipse
17 %                          X0_in        − center at the X axis of the tilted ellipse
18 %                          Y0_in        − center at the Y axis of the tilted ellipse
19 %                          long_axis   − size of the long axis of the ellipse
20 %                          short_axis  − size of the short axis of the ellipse
21 %                          status      − status of detection of an ellipse
22 %
23 % Note:       if an ellipse was not detected (but a parabola or hyperbola), then
24 %             an empty structure is returned
25
26 % ===================================================================================
27 %                   Ellipse Fit using Least Squares criterion
28 % ===================================================================================
29 % We will try to fit the best ellipse to the given measurements. the mathematical
30 % representation of use will be the CONIC Equation of the Ellipse which is:
31 %
32 %     Ellipse = a*x^2 + b*x*y + c*y^2 + d*x + e*y + f = 0
33 %
34 % The fit−estimation method of use is the Least Squares method (without any weights
        )
35 % The estimator is extracted from the following equations:
36 %
37 %     g(x,y;A) := a*x^2 + b*x*y + c*y^2 + d*x + e*y = f
38 %
39 %     where:
40 %        A   − is the vector of parameters to be estimated (a,b,c,d,e)
41 %        x,y − is a single measurement
42 %
43 % We will define the cost function to be:
44 %
45 %     Cost(A) := (g_c(x_c,y_c;A)−f_c)'*(g_c(x_c,y_c;A)−f_c)
```

```
46  %                  = (X*A+f_c) '*(X*A+f_c)
47  %                  = A'*X'*X*A + 2*f_c '*X*A + N*f^2
48  %
49  %      where:
50  %          g_c(x_c,y_c;A)  −  vector function of ALL the measurements
51  %                              each element of g_c() is g(x,y;A)
52  %          X               − a matrix of the form: [x_c.^2, x_c.*y_c, y_c.^2, x_c, y_c
           ]
53  %          f_c             − is actually defined as ones(length(f),1)*f
54  %
55  % Derivation of the Cost function with respect to the vector of parameters "A"
           yields:
56  %
57  %      A'*X'*X = −f_c '*X = −f*ones(1,length(f_c))*X = −f*sum(X)
58  %
59  % Which yields the estimator:
60  %
61  %
        ~~~~~~~~~~~~~~~~~~~~~~~~~~~~~~~~~~~~~~~~~~~~~~~~~~~~~~~~~~~~~~~~~~~~~~~~~~~~~~~~~
62  %          |   A_least_squares = −f*sum(X)/(X'*X)  −>(normalize by −f) = sum(X)/(X'*X)
           |
63  %
        ~~~~~~~~~~~~~~~~~~~~~~~~~~~~~~~~~~~~~~~~~~~~~~~~~~~~~~~~~~~~~~~~~~~~~~~~~~~~~~~~
64  %
65  % (We will normalize the variables by (−f) since "f" is unknown and can be
           accounted for later on)
66  %
67  % NOW, all that is left to do is to extract the parameters from the Conic Equation.
68  % We will deal the vector A into the variables: (A,B,C,D,E) and assume F = −1;
69  %
70  %      Recall the conic representation of an ellipse:
71  %
72  %          A*x^2 + B*x*y + C*y^2 + D*x + E*y + F = 0
73  %
74  % We will check if the ellipse has a tilt (=orientation). The orientation is
           present
75  % if the coefficient of the term "x*y" is not zero. If so, we first need to remove
           the
76  % tilt of the ellipse.
77  %
78  % If the parameter "B" is not equal to zero, then we have an orientation (tilt) to
           the ellipse.
79  % we will remove the tilt of the ellipse so as to remain with a conic
           representation of an
80  % ellipse without a tilt, for which the math is more simple:
81  %
82  % Non tilt conic rep.:  A'*x^2 + C'*y^2 + D'*x + E'*y + F' = 0
83  %
84  % We will remove the orientation using the following substitution:
85  %
86  %      Replace x with cx+sy and y with −sx+cy such that the conic representation is:
87  %
88  %      A(cx+sy)^2 + B(cx+sy)(−sx+cy) + C(−sx+cy)^2 + D(cx+sy) + E(−sx+cy) + F = 0
89  %
90  %      where:       c = cos(phi)     ,    s = sin(phi)
91  %
92  %      and simplify ...
93  %
94  %          x^2(A*c^2 − Bcs + Cs^2) + xy(2A*cs +(c^2−s^2)B −2Ccs) + ...
95  %              y^2(As^2 + Bcs + Cc^2) + x(Dc−Es) + y(Ds+Ec) + F = 0
96  %
97  %      The orientation is easily found by the condition of (B_new=0) which results in:
98  %
99  %      2A*cs +(c^2−s^2)B −2Ccs = 0  ==> phi = 1/2 * atan( b/(c−a) )
100 %
101 %      Now the constants    c=cos(phi)  and  s=sin(phi)  can be found, and from them
102 %      all the other constants A',C',D',E' can be found.
103 %
104 %      A' = A*c^2 − B*c*s + C*s^2                    D' = D*c−E*s
105 %      B' = 2*A*c*s +(c^2−s^2)*B −2*C*c*s = 0        E' = D*s+E*c
```

```
106 %     C' = A*s^2 + B*c*s + C*c^2
107 %
108 % Next, we want the representation of the non-tilted ellipse to be as:
109 %
110 %          Ellipse = ( (X-X0)/a )^2 + ( (Y-Y0)/b )^2 = 1
111 %
112 %          where:  (X0,Y0) is the center of the ellipse
113 %                  a,b     are the ellipse "radiuses" (or sub-axis)
114 %
115 % Using a square completion method will define:
116 %
117 %          F'' = -F' + (D'^2)/(4*A') + (E'^2)/(4*C')
118 %
119 %          Such that:    a'*(X-X0)^2 = A'(X^2 + X*D'/A' + (D'/(2*A'))^2 )
120 %                        c'*(Y-Y0)^2 = C'(Y^2 + Y*E'/C' + (E'/(2*C'))^2 )
121 %
122 %          which yields the transformations:
123 %
124 %              X0   =   -D'/(2*A')
125 %              Y0   =   -E'/(2*C')
126 %              a    =   sqrt( abs( F''/A' ) )
127 %              b    =   sqrt( abs( F''/C' ) )
128 %
129 % And finally we can define the remaining parameters:
130 %
131 %    long_axis   = 2 * max( a,b )
132 %    short_axis  = 2 * min( a,b )
133 %    Orientation = phi
134 %
135 %
136
137 % default color
138 if nargin < 5
139     color = 'r';
140 end
141
142 % initialize
143 orientation_tolerance = 1e-3;
144
145 % empty warning stack
146 warning( '' );
147
148 % prepare vectors, must be column vectors
149 x = x(:);
150 y = y(:);
151
152 % remove bias of the ellipse - to make matrix inversion more accurate. (will be
        added later on).
153 mean_x = mean(x);
154 mean_y = mean(y);
155 x = x-mean_x;
156 y = y-mean_y;
157
158 % the estimation for the conic equation of the ellipse
159 X = [x.^2, x.*y, y.^2, x, y ];
160 a = sum(X)/(X'*X);
161
162 % check for warnings
163 if ~isempty( lastwarn )
164     disp( 'stopped because of a warning regarding matrix inversion' );
165     ellipse_t = [];
166     return
167 end
168
169 % extract parameters from the conic equation
170 [a,b,c,d,e] = deal( a(1),a(2),a(3),a(4),a(5) );
171
172 % remove the orientation from the ellipse
173 if ( min(abs(b/a),abs(b/c)) > orientation_tolerance )
174
```

```matlab
175     orientation_rad = 1/2 * atan( b/(c-a) );
176     cos_phi = cos( orientation_rad );
177     sin_phi = sin( orientation_rad );
178     [a,b,c,d,e] = deal(...
179         a*cos_phi^2 - b*cos_phi*sin_phi + c*sin_phi^2 ,...
180         0 ,...
181         a*sin_phi^2 + b*cos_phi*sin_phi + c*cos_phi^2 ,...
182         d*cos_phi - e*sin_phi ,...
183         d*sin_phi + e*cos_phi );
184     [mean_x,mean_y] = deal( ...
185         cos_phi*mean_x - sin_phi*mean_y ,...
186         sin_phi*mean_x + cos_phi*mean_y );
187 else
188     orientation_rad = 0;
189     cos_phi = cos( orientation_rad );
190     sin_phi = sin( orientation_rad );
191 end
192
193 % check if conic equation represents an ellipse
194 test = a*c;
195 switch (1)
196 case (test>0),  status = '';
197 case (test==0), status = 'Parabola found';  warning( 'fit_ellipse: Did not locate
        an ellipse' );
198 case (test<0),  status = 'Hyperbola found'; warning( 'fit_ellipse: Did not locate
        an ellipse' );
199 end
200
201 % if we found an ellipse return it's data
202 if (test>0)
203
204     % make sure coefficients are positive as required
205     if (a<0), [a,c,d,e] = deal( -a,-c,-d,-e ); end
206
207     % final ellipse parameters
208     X0          = mean_x - d/2/a;
209     Y0          = mean_y - e/2/c;
210     F           = 1 + (d^2)/(4*a) + (e^2)/(4*c);
211     [a,b]       = deal( sqrt( F/a ),sqrt( F/c ) );
212     long_axis   = 2*max(a,b);
213     short_axis  = 2*min(a,b);
214
215     % rotate the axes backwards to find the center point of the original TILTED
        ellipse
216     R           = [ cos_phi sin_phi; -sin_phi cos_phi ];
217     P_in        = R * [X0;Y0];
218     X0_in       = P_in(1);
219     Y0_in       = P_in(2);
220
221     % pack ellipse into a structure
222     ellipse_t = struct( ...
223         'a',a ,...
224         'b',b ,...
225         'phi',orientation_rad ,...
226         'X0',X0 ,...
227         'Y0',Y0 ,...
228         'X0_in',X0_in ,...
229         'Y0_in',Y0_in ,...
230         'long_axis',long_axis ,...
231         'short_axis',short_axis ,...
232         'status','' );
233 else
234     % report an empty structure
235     ellipse_t = struct( ...
236         'a' ,[] ,...
237         'b' ,[] ,...
238         'phi' ,[] ,...
239         'X0' ,[] ,...
240         'Y0' ,[] ,...
241         'X0_in' ,[] ,...
```

```matlab
242             'Y0_in' ,[] ,...
243             'long_axis' ,[] ,...
244             'short_axis' ,[] ,...
245             'status',status  );
246 end
247
248 % check if we need to plot an ellipse with it's axes.
249 if (nargin >2) & ~isempty( axis_handle ) & (test >0)
250 %
251 %       % rotation matrix to rotate the axes with respect to an angle phi
252 %       R = [ cos_phi sin_phi; -sin_phi cos_phi ];
253 %
254 %       % the axes
255 %       ver_line        = [ [X0 X0]; Y0+b*[-1 1] ];
256 %       horz_line       = [ X0+a*[-1 1]; [Y0 Y0] ];
257 %       new_ver_line    = R*ver_line ;
258 %       new_horz_line   = R*horz_line ;
259 %
260 %       % the ellipse
261 %       theta_r         = linspace (0,2*pi );
262 %       ellipse_x_r     = X0 + a*cos( theta_r );
263 %       ellipse_y_r     = Y0 + b*sin( theta_r );
264 %       rotated_ellipse = R * [ellipse_x_r;ellipse_y_r];
265 %
266 %       % draw
267 %       hold_state = get( axis_handle,'NextPlot' );
268 %       set( axis_handle,'NextPlot','add' );
269 %       if ~omit_axis
270 %           plot( new_ver_line(1,:),new_ver_line(2,:),'r' );
271 %           plot( new_horz_line(1,:),new_horz_line(2,:),'r' );
272 %       end
273 %       p = plot( rotated_ellipse(1,:),rotated_ellipse(2,:),'r' );
274 %       p.LineWidth = 2;
275 %       set( axis_handle,'NextPlot',hold_state );
276
277       EllipsePlot(X0, Y0, a, b, orientation_rad , axis_handle , omit_axis , color);
278
279 end
```

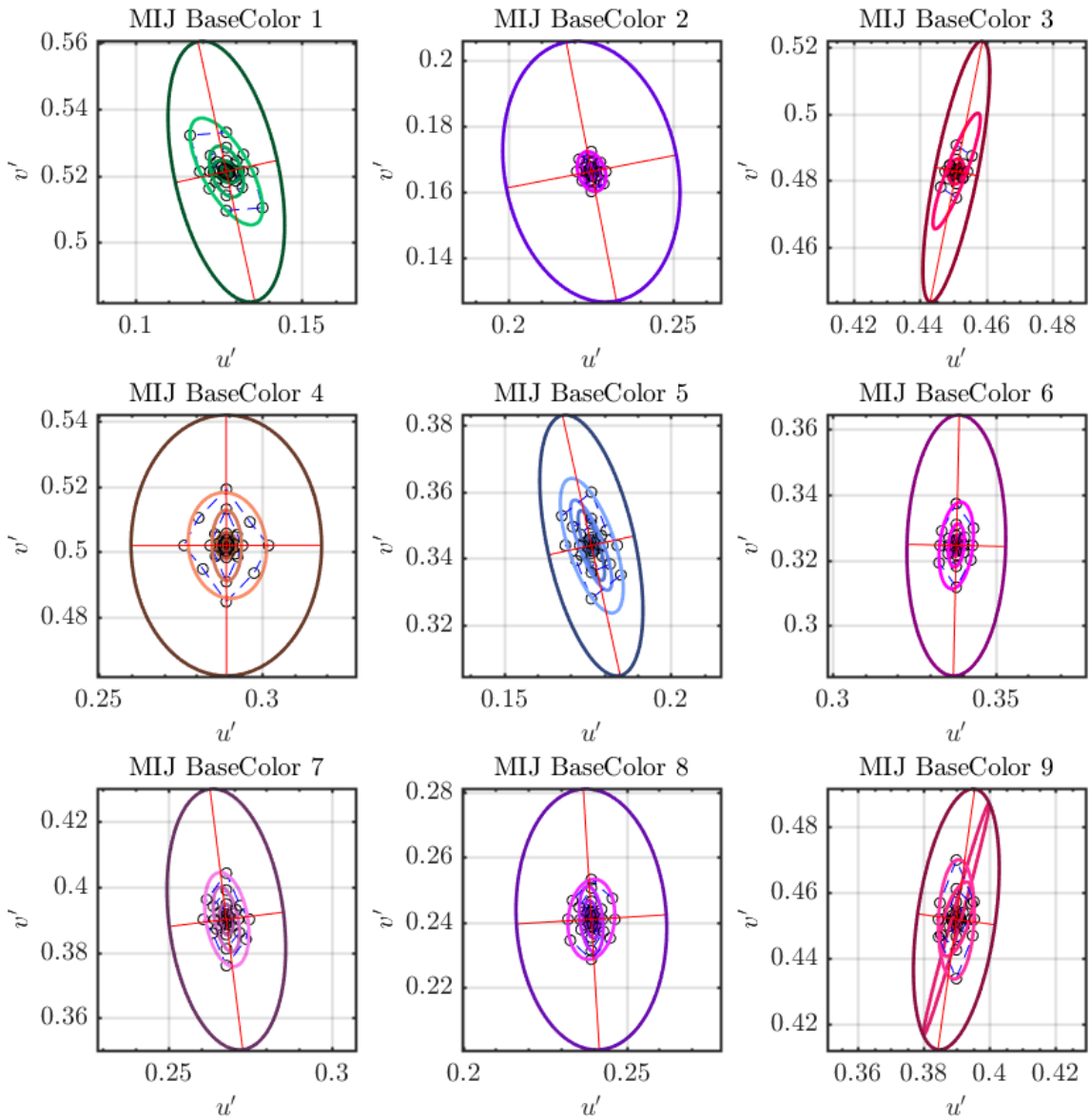**Listing E.1:** Ellipse Fit MATLAB code. Obtained from File Exchange, made by Ohad Gal.

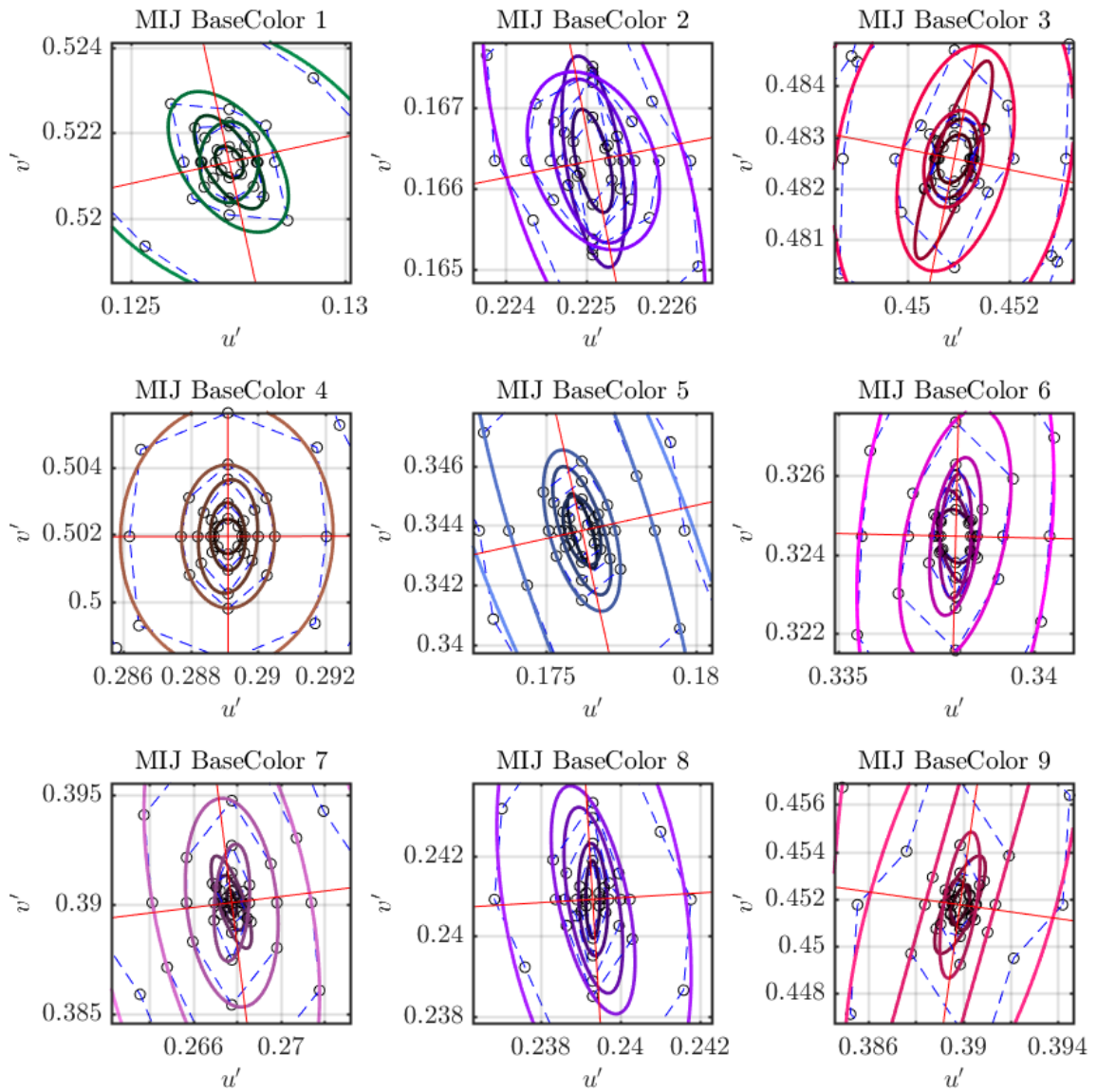**Figure E.1:** The ellipse fits (Zoomed out to high frequencies) of participant **MIJ**.

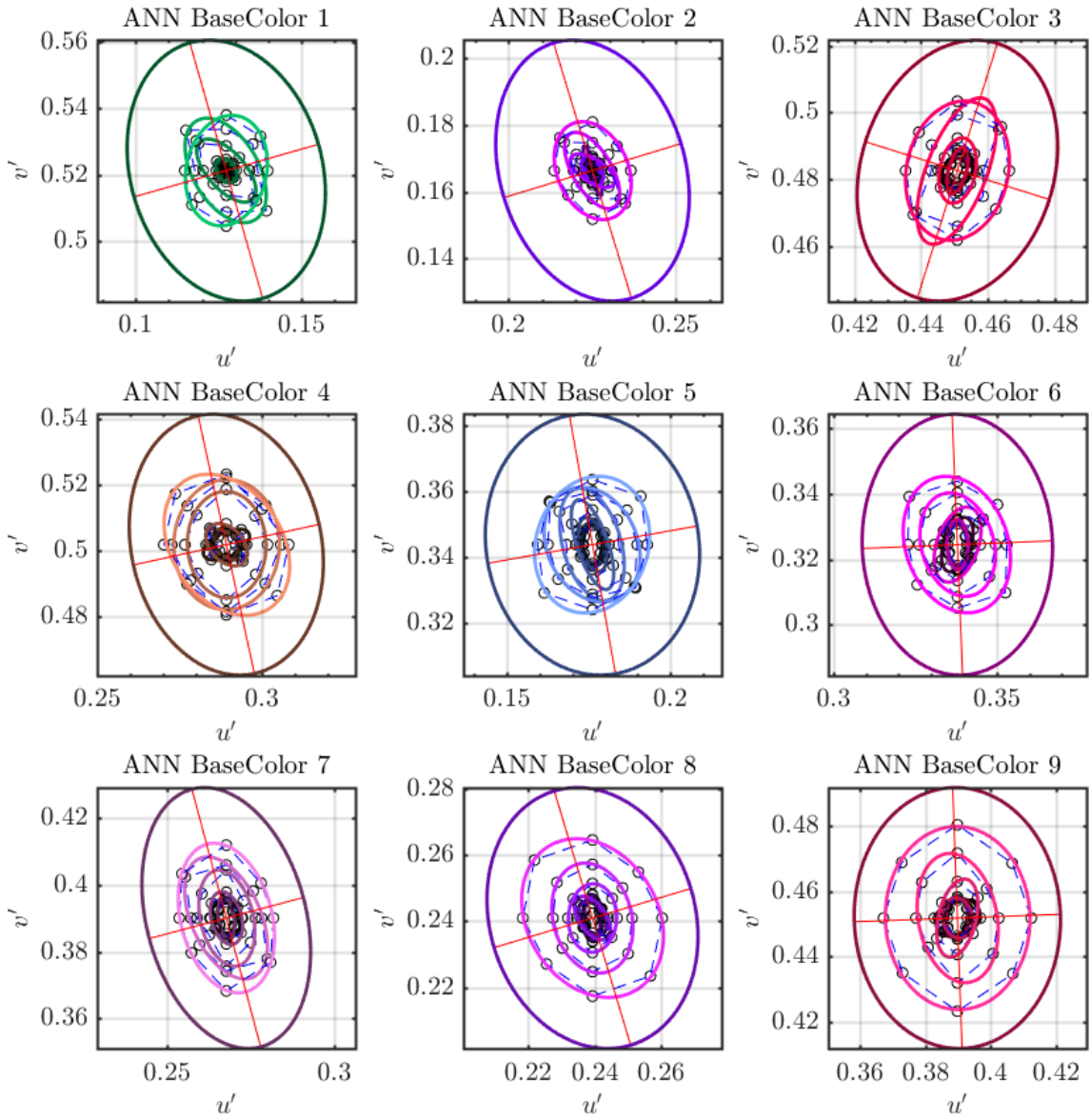**Figure E.2:** The ellipse fits (Zoomed in to low frequencies) of participant **MIJ**.

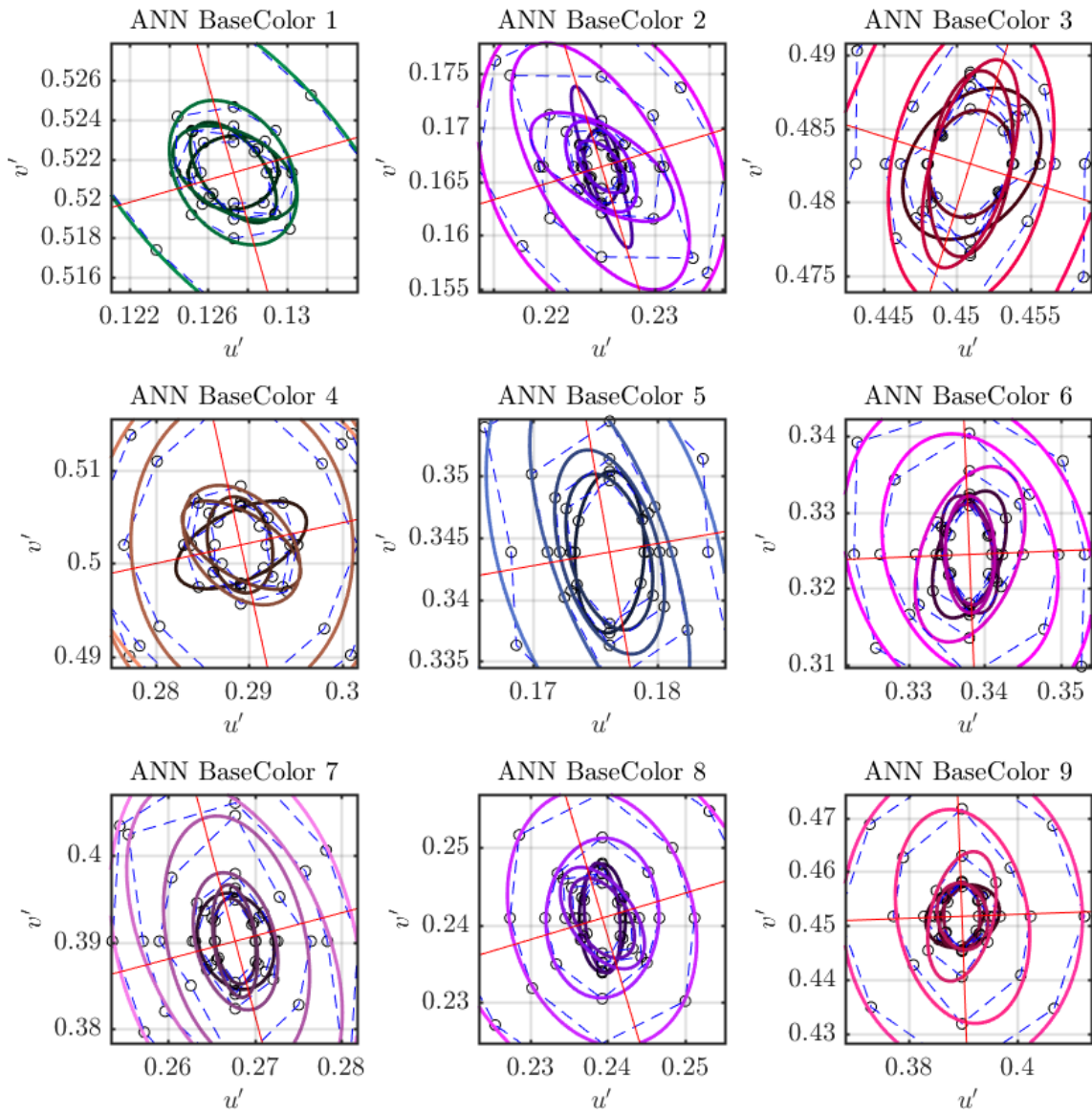**Figure E.3:** The ellipse fits (Zoomed out to high frequencies) of participant **ANN**.

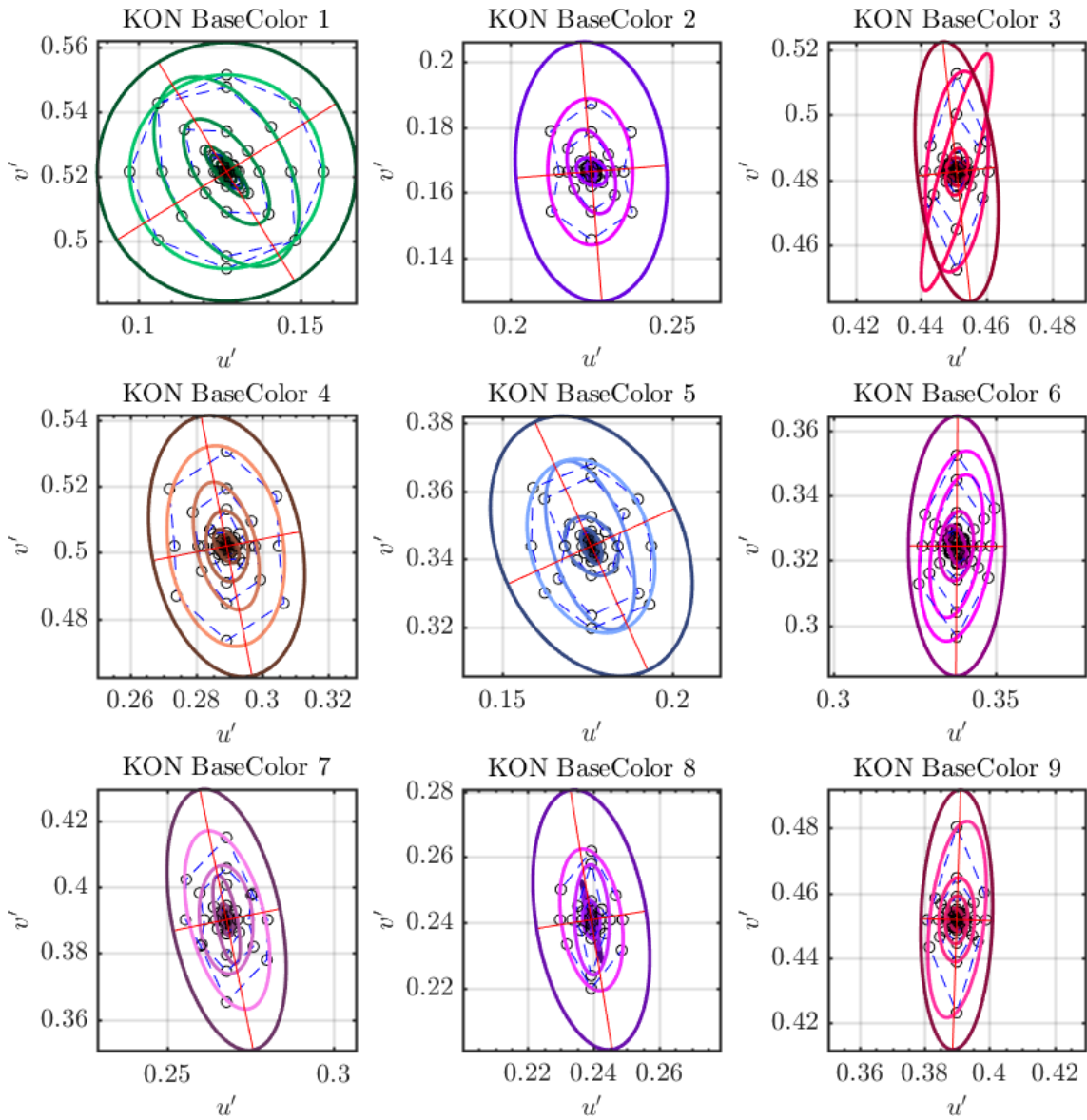**Figure E.4:** The ellipse fits (Zoomed in to low frequencies) of participant **ANN**.

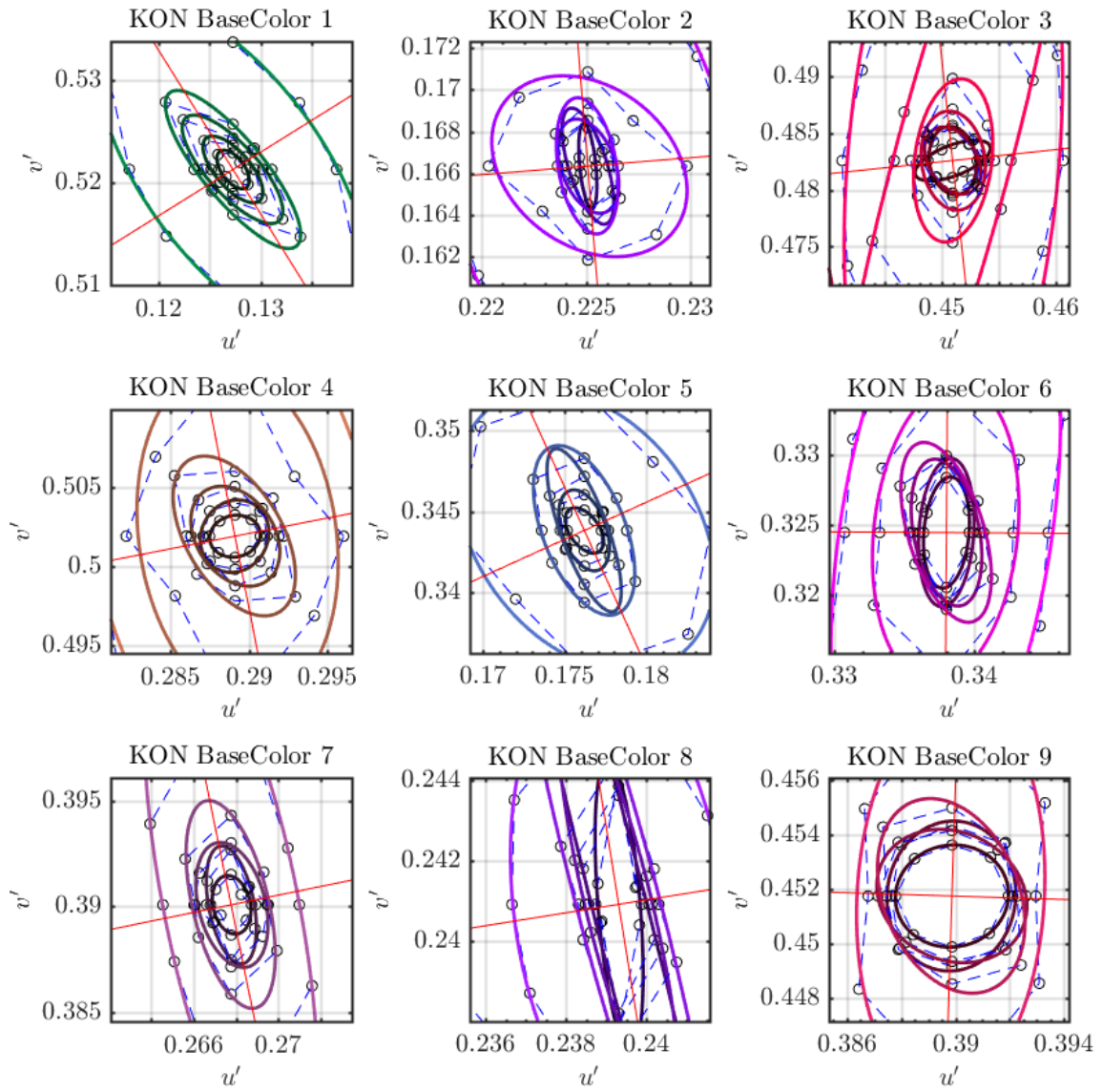**Figure E.5:** The ellipse fits (Zoomed out to high frequencies) of participant **KON**.

Figure E.6: The ellipse fits (Zoomed in to low frequencies) of participant **KON**.
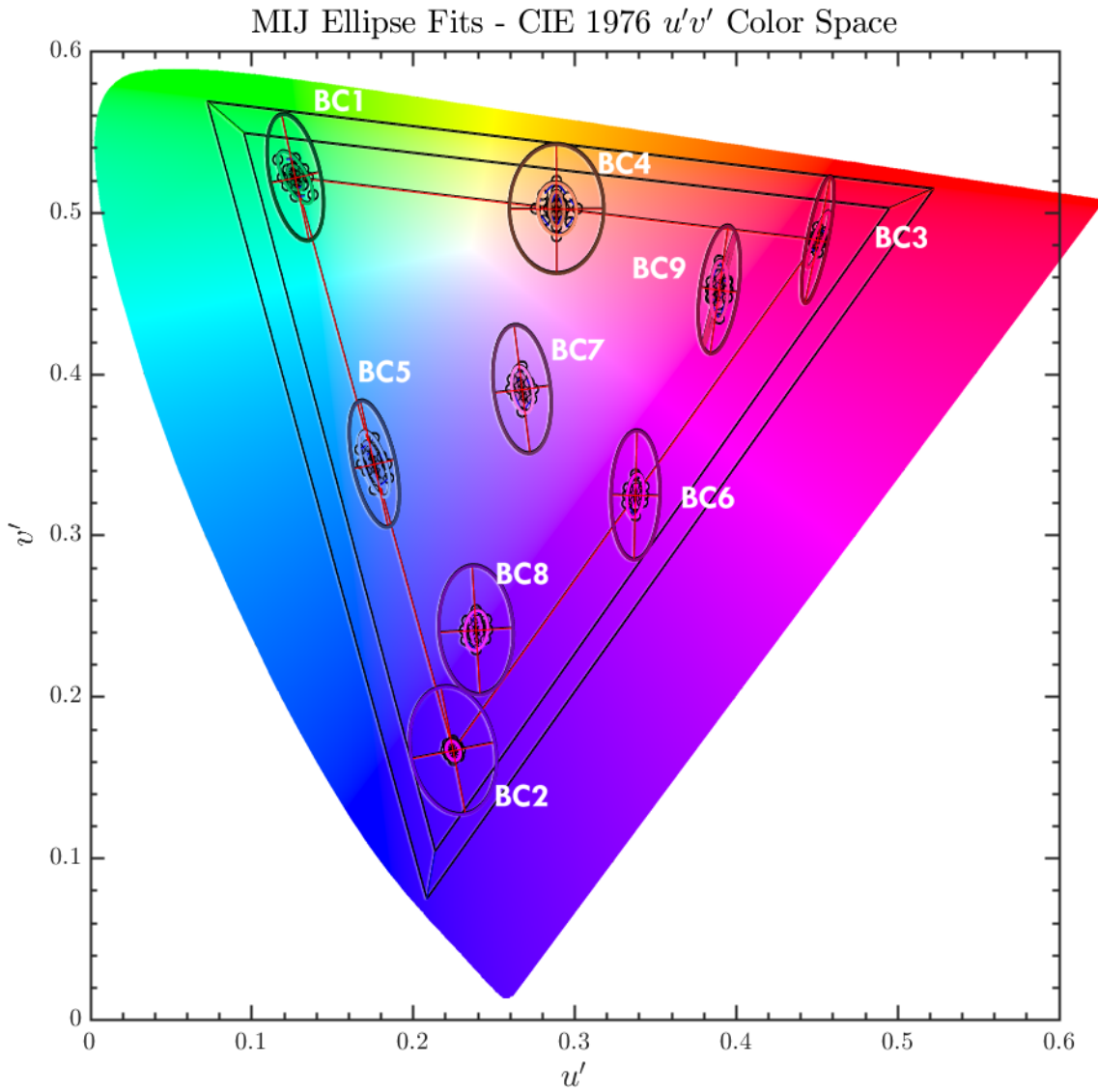
Figure E.7: The ellipse fits plotted on the $u'v'$ color space to illustrate the overall shapes and orientations of the ellipses of participant **MIJ**.
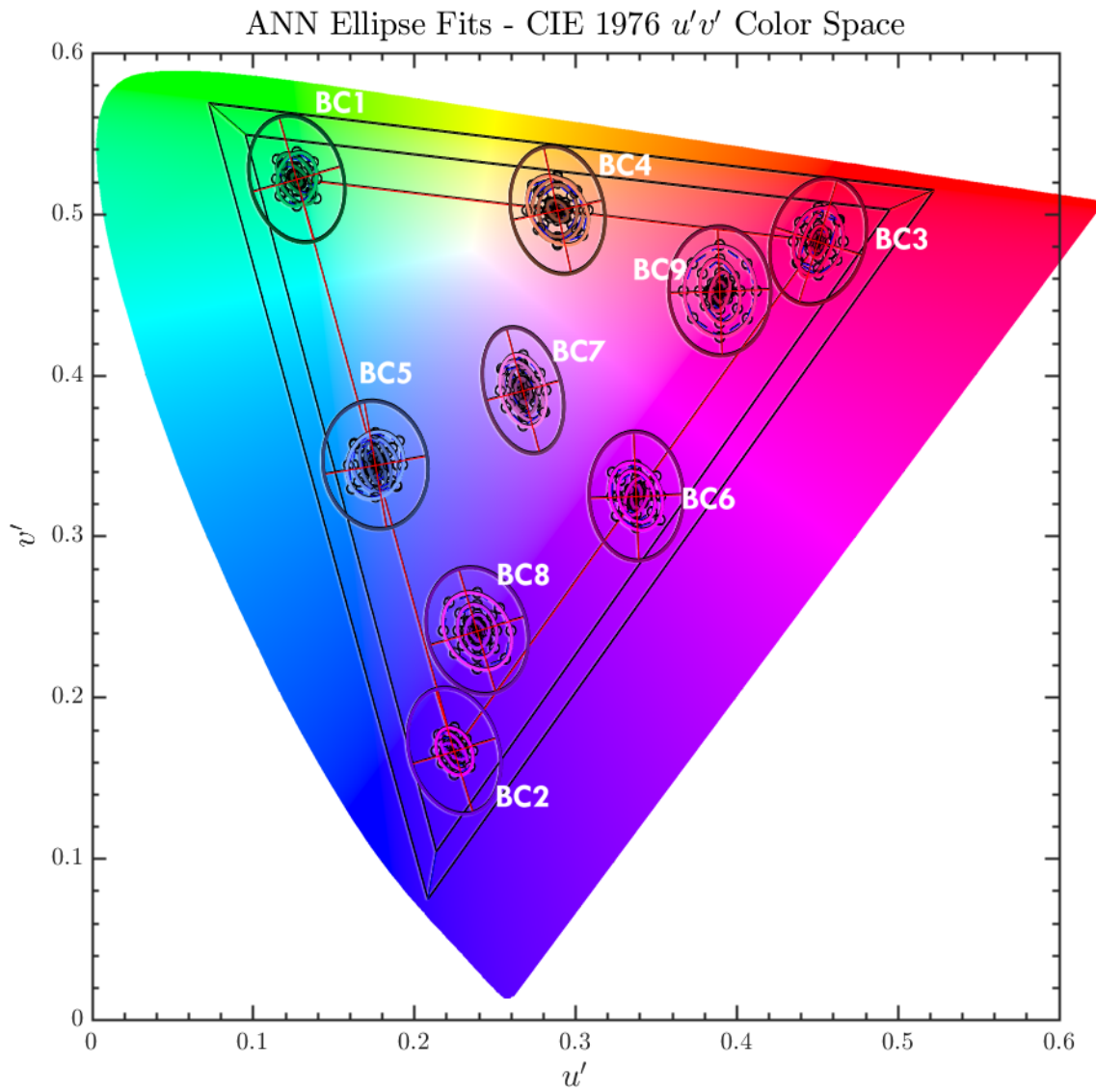
Figure E.8: The ellipse fits plotted on the $u'v'$ color space to illustrate the overall shapes and orientations of the ellipses of participant **ANN**.
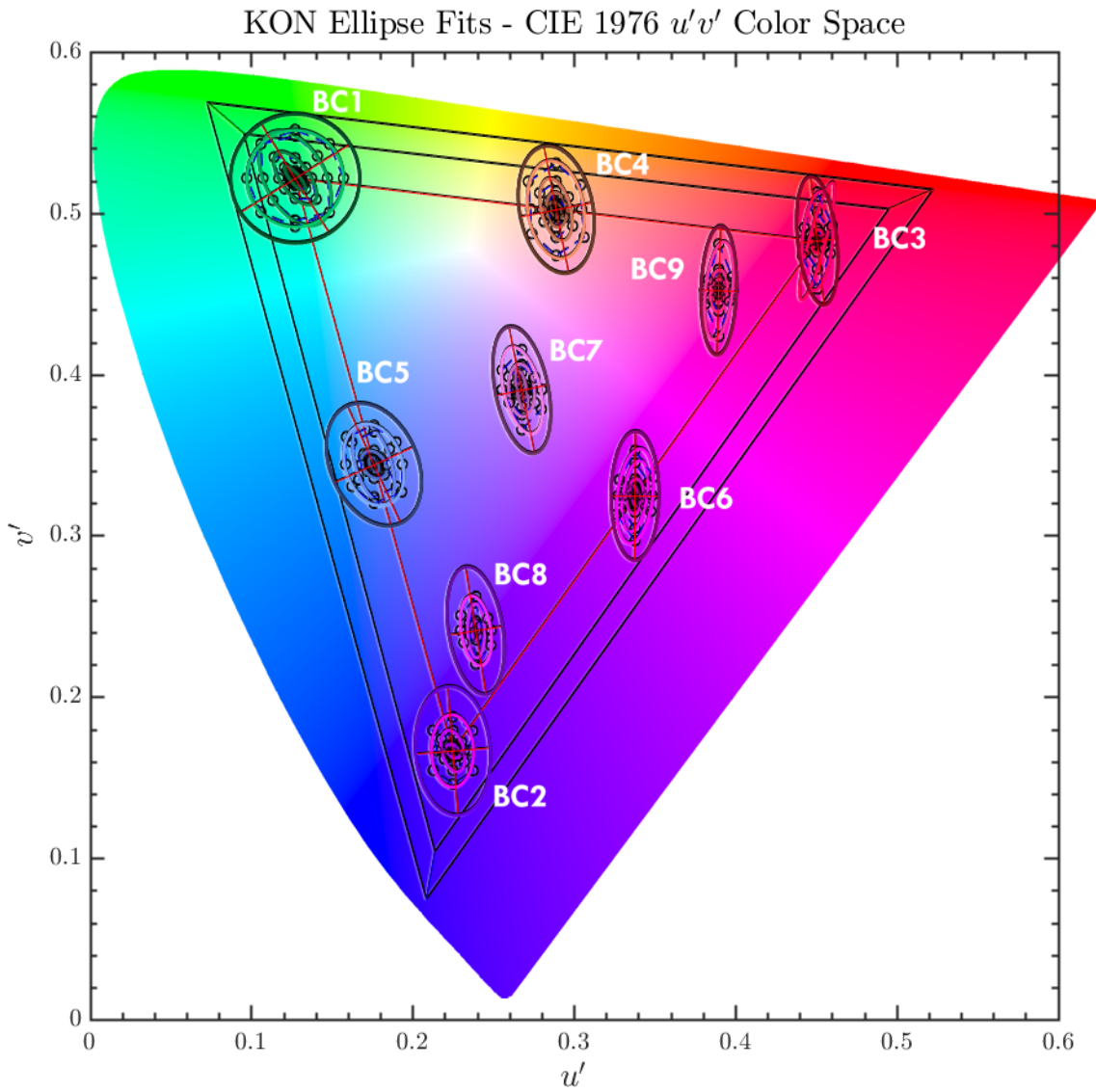
Figure E.9: The ellipse fits plotted on the $u'v'$ color space to illustrate the overall shapes and orientations of the ellipses of participant **KON**.